

UNIVERSITY OF MINNESOTA  
**ST. ANTHONY FALLS LABORATORY**  
Engineering, Environmental and Geophysical Fluid Dynamics

Project Report No. 415

**Physical and Numerical Model Study  
of the Little Falls Reservoir,  
Mississippi River at Little Falls, Minnesota**

by

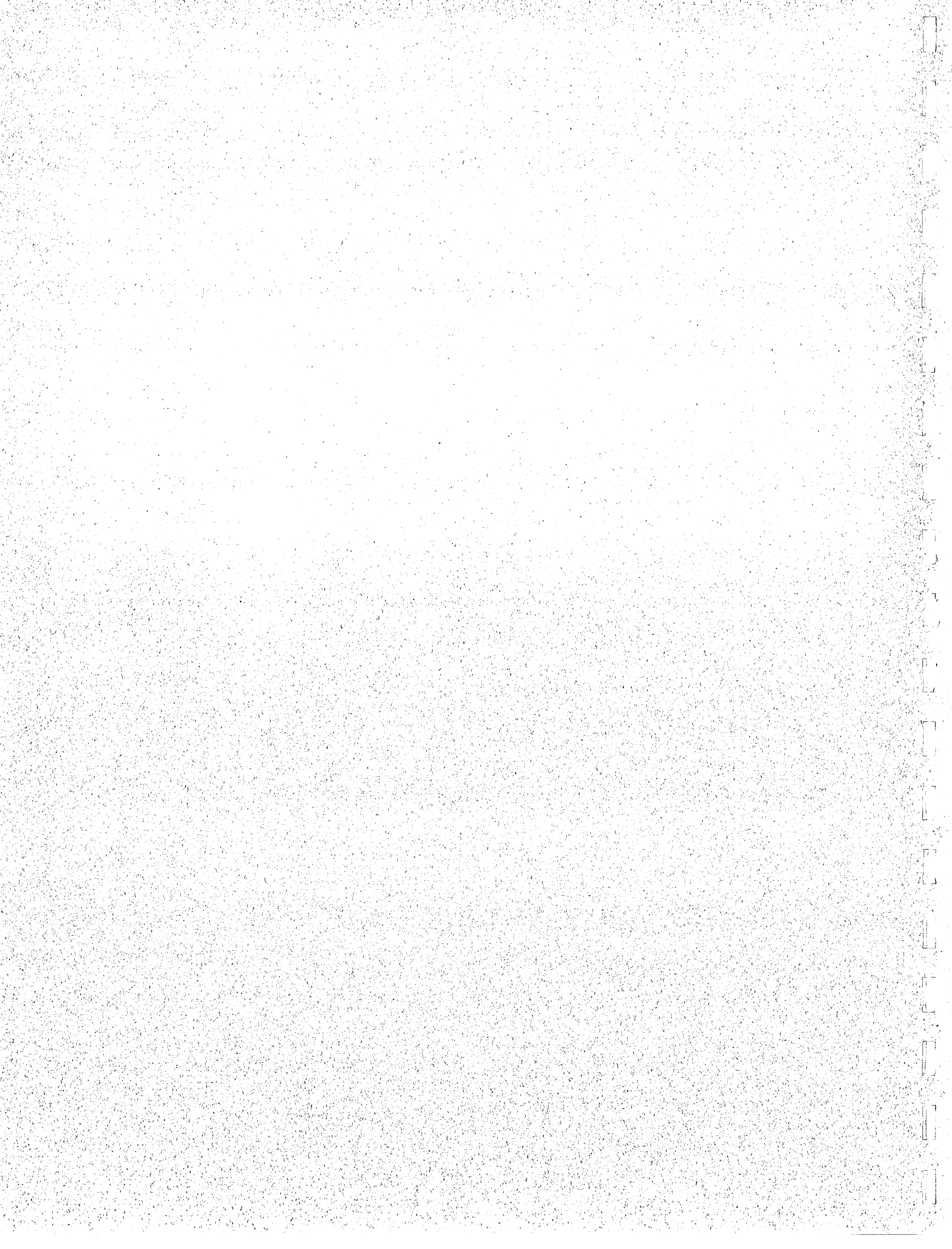
Tracy Winjum, Richard L. Voigt, Jr., and Gary Parker



Prepared for

Morrison County, Minnesota  
Little Falls, MN 56345

March 1998  
**Minneapolis, Minnesota**



UNIVERSITY OF MINNESOTA  
**ST. ANTHONY FALLS LABORATORY**  
Engineering, Environmental and Geophysical Fluid Dynamics

Project Report No. 415

**Physical and Numerical Model Study  
of the Little Falls Reservoir,  
Mississippi River at Little Falls, Minnesota**

by

Richard L. Voigt, Jr., Gary Parker, and Tracy Winjum

Prepared for

Morrison County, Minnesota  
Little Falls, MN 56345

March 1998  
**Minneapolis, Minnesota**



The University of Minnesota is committed to the policy that all persons shall have equal access to its programs, facilities, and employment without regard to race, religion, color, sex, national origin, handicap, age or veteran status.

Prepared for: Morrison County, MN

Last Revised: 4/7/98

Disk Locators: (Zip Disk #7/c:\winword\Morrison)

c:\winword\Morrison (Pat) - txt&figcaps

c:\tracy\Morrison (Tracy) - PSD & TIF

c:\tracy\tif\embankment, Fig.14-33, Figs3-6

c:\Pats\Embankments, Fig. 14-33, Fig. 3-6



## ABSTRACT

The St. Anthony Falls Laboratory (SAFL) conducted a physical and numerical model study of the Little Falls Reservoir. The Reservoir is located approximately 120 miles northwest of Minneapolis, Minnesota, on the Mississippi River. The testing portion of the study was begun in early 1997 and completed in December 1997. Problems related to decreased flow and increased sedimentation are being experienced in the small east channel and the eastern shore of the reservoir. Various agencies have conducted studies of the problems in an effort to determine the cause. SAFL's task was to determine whether the U.S. Highway 10 bypass and bridge constructed in 1975, as well as possible other factors, might be the cause, and provide recommendations for mitigation of the problem. The report presents SAFL's findings and results of its physical and numerical model analysis.

This report can be used by others to carry out Environmental Reviews and Permitting.



## ACKNOWLEDGMENTS

The cooperation of Morrison County officials and the opportunity to perform these modeling tests is greatly appreciated and acknowledged.

The authors/research leaders on this project would like to also thank and acknowledge the efforts and expertise of the following SAFL research team members: Ben Erickson for photo and video support; Jessica Collin for help with the model operation; Aaron Buesing, Scott Morgan, and Stacy Watters for their help with model design and construction; Chris Ellis for assistance with the data collection equipment; Jeff Marr and Peter Harff for lighting advice and support; and Pat Swanson for report preparation and production.



# TABLE OF CONTENTS

<b>ABSTRACT .....</b>	<b>i</b>
<b>ACKNOWLEDGMENTS .....</b>	<b>ii</b>
<b>TABLE OF CONTENTS .....</b>	<b>iii</b>
<b>LIST OF FIGURES.....</b>	<b>v</b>
<b>1. INTRODUCTION .....</b>	<b>1</b>
<b>2. SETTING AND PROBLEM HISTORY.....</b>	<b>3</b>
1992 U.S. ARMY CORPS OF ENGINEERS RECONNAISSANCE REPORT .....	5
1993 DNR INVESTIGATION OF SEDIMENT AND VEGETATION PROBLEMS .....	7
NOTES ON SEDIMENTATION IN THE LITTLE FALLS RESERVOIR BY DR. GARY PARKER.....	9
<b>3. STUDY OBJECTIVES.....</b>	<b>12</b>
<b>4. PHYSICAL MODEL DESIGN AND CALIBRATION.....</b>	<b>13</b>
DISTORTED FROUDE MODELING .....	13
APPLICATION TO THE LITTLE FALLS RESERVOIR .....	14
ISSUES CONCERNING SEDIMENT TRANSPORT.....	14
MODEL CALIBRATION .....	15
<b>5. NUMERICAL MODEL CREATION AND CALIBRATION .....</b>	<b>17</b>
NUMERICAL MODEL OVERVIEW .....	17
MODELING ISSUES AND DATA REQUIREMENTS.....	17
NUMERICAL MODEL CALIBRATION.....	18
NUMERICAL MODEL OUTPUT.....	19
<b>6. OVERVIEW OF EXPERIMENTS .....</b>	<b>21</b>
<b>7. PHYSICAL MODEL RESULTS.....</b>	<b>23</b>
FLOW RATE RESULTS.....	23
Case 1: No Embankment.....	23
Case 2: With Embankment.....	23
Case 3: Spurdike 500 ft in length.....	24
Case 4: Extended Spurdike 750 ft in length.....	24
Case 5: Dredging of the East Channel Region .....	24
Case 6: New Bridge Opening.....	25
VELOCITY AND FLOW PATTERN EXPERIMENTS.....	25
SEDIMENT TRACER RESULTS .....	26



<b>8. NUMERICAL MODEL RESULTS .....</b>	<b>28</b>
FLOW RATE RESULTS.....	28
Case 1: No Embankment.....	28
Case 2: With Embankment.....	28
Case 3: Spurdike 500 ft in length.....	29
Case 4: Extended Spurdike 750 ft in length .....	29
Case 5: Dredging of the East Channel Region .....	29
Case 6: New Bridge Opening.....	29
VELOCITY RESULTS .....	30
ADDITIONAL DREDGING SIMULATIONS.....	30
<b>9. CONCLUSIONS AND RECOMMENDATIONS .....</b>	<b>33</b>
<b>REFERENCES .....</b>	<b>36</b>

**FIGURES 1 through 67**



## LIST OF FIGURES

- Figure 1 Little Falls Reservoir showing location of main channel, east channel, small east channel and embankment and bridge structure.
- Figure 2 Map of Minnesota showing location of Little Falls, MN.
- Figure 3 Aerial photo of Little Falls Reservoir in 1963.
- Figure 4 Aerial photo of Little Falls Reservoir in 1980.
- Figure 5 Aerial photo of Little Falls Reservoir in 1986.
- Figure 6 Aerial photo of Little Falls Reservoir in 1991.
- Figure 7 Plot of island area in the Little Falls Reservoir versus years (from MN DNR Investigation).
- Figure 8 Location of sounding/boring holes in Little Falls Reservoir (from MN DNR Investigation).
- Figure 9 Water surface profiles in the Little Falls Reservoir (from U.S. Army Corps of Engineers).
- Figure 10 Physical and numerical model calibration results compared to expected water surface profiles.
- Figure 11 Numerical model Manning's  $n$  values.
- Figure 12 Example of water surface elevation contour plot for a flow of 25,850 cfs.
- Figure 13 Schematic showing potential mitigative options.
- Figure 14 Surface flow velocities exiting east channel opening for a flow of 5285 cfs with no embankment.
- Figure 15 Surface flow velocities along east shoreline for a flow of 5285 cfs with no embankment.
- Figure 16 Surface flow velocities exiting east channel opening for a flow of 10,200 cfs with no embankment.
- Figure 17 Surface flow velocities along east shoreline for a flow of 10,200 cfs with no embankment.
- Figure 18 Surface flow velocities exiting east channel opening for a flow of 25,850 cfs with no embankment.
- Figure 19 Surface flow velocities along east shoreline for a flow of 25,850 cfs with no embankment.
- Figure 20 Surface flow velocities along the east shoreline for a flow of 5285 cfs with the embankment in place.
- Figure 21 Surface flow velocities along the east shoreline for a flow of 10,200 cfs with the embankment in place.

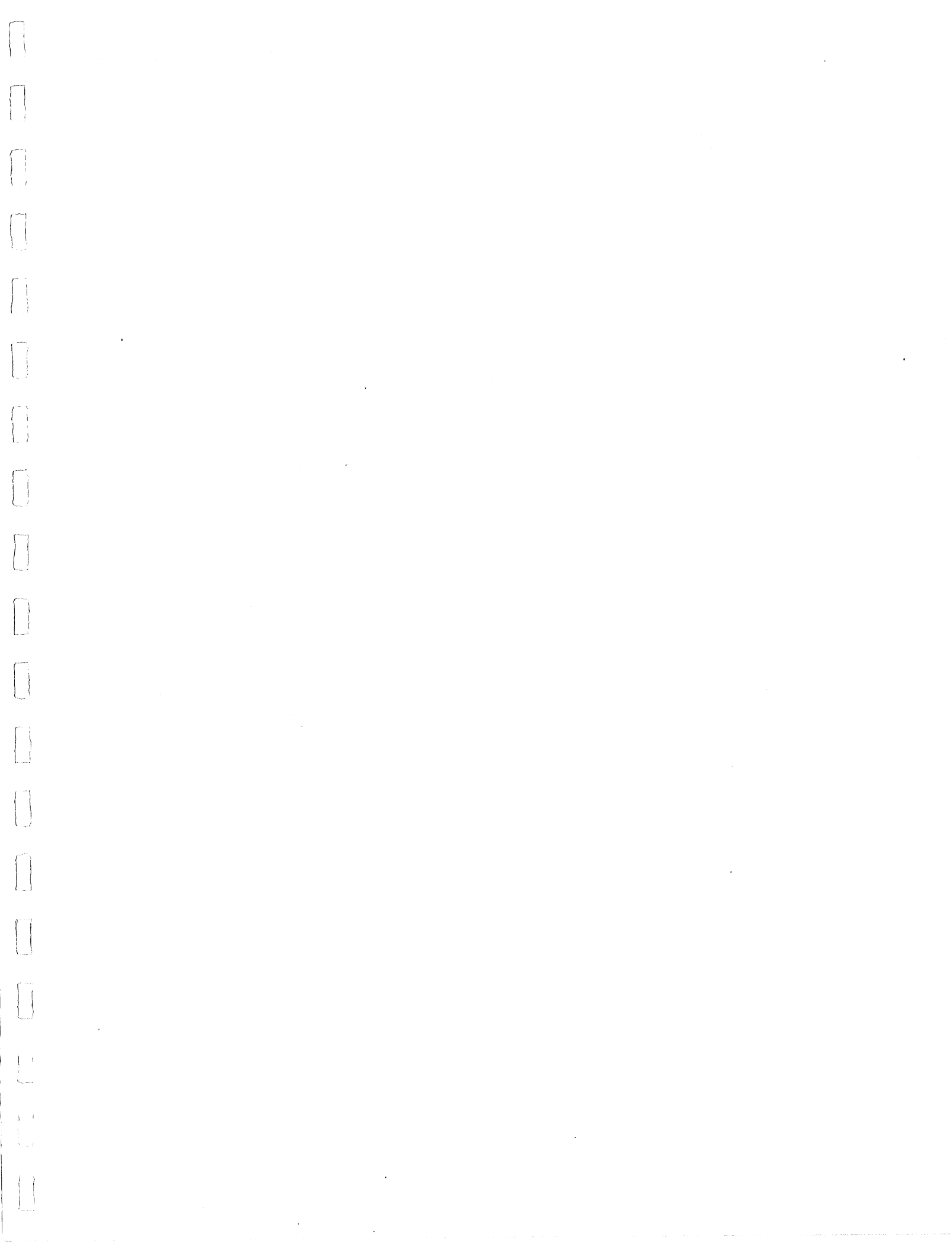


- Figure 22 Surface flow velocities along the east shoreline for a flow of 25,850 cfs with the embankment in place.
- Figure 23 Surface flow velocities along the east shoreline for a flow of 5285 cfs with spurdike in place.
- Figure 24 Surface flow velocities along the east shoreline for a flow of 10,200 cfs with spurdike in place.
- Figure 25 Surface flow velocities along the east shoreline for a flow of 25,850 cfs with spurdike in place.
- Figure 26 Surface flow velocities along the east shoreline for a flow of 10,200 cfs with dredging of east channel.
- Figure 27 Surface flow velocities along the east shoreline for a flow of 25,850 cfs with dredging of east channel.
- Figure 28 Surface flow velocities exiting new opening in embankment for a flow of 5285 cfs.
- Figure 29 Surface flow velocities along east shoreline for a flow of 5285 cfs with a new opening in the embankment.
- Figure 30 Surface flow velocities exiting new opening in the embankment for a flow of 10,200 cfs.
- Figure 31 Surface flow velocities along the east shoreline for a flow of 10,200 cfs with a new opening in the embankment.
- Figure 32 Surface flow velocities exiting the new opening in the embankment for a flow of 25,850 cfs.
- Figure 33 Surface flow velocities along the east shoreline for a flow of 25,850 cfs with a new opening in the embankment.
- Figure 34 Subsurface sediment tracer deposition without the embankment.
- Figure 35 Subsurface sediment tracer deposition with the embankment in place.
- Figure 36 Subsurface sediment tracer deposition with a new opening in the embankment.
- Figure 37 Surface flow patterns without the embankment
- Figure 38 Surface flow patterns with the embankment in place.
- Figure 39 Surface flow patterns with a new opening in the embankment.
- Figure 40 Velocity contour plot of entire reservoir showing area enlarged in velocity contour plots.
- Figure 41 Velocity contours for a flow of 5285 cfs without the embankment.
- Figure 42 Velocity contours for a flow of 10,200 cfs without the embankment.
- Figure 43 Velocity contours for a flow of 25,850 cfs without the embankment.
- Figure 44 Velocity contours for a flow of 5285 cfs with the embankment.
- Figure 45 Velocity contours for a flow of 10,200 cfs with the embankment.
- Figure 46 Velocity contours for a flow of 25,850 cfs with the embankment.



- Figure 47 Velocity contours for a flow of 5285 cfs with the spurdike option.
- Figure 48 Velocity contours for a flow of 10,200 cfs with the spurdike option.
- Figure 49 Velocity contours for a flow of 25,850 cfs with the spurdike option.
- Figure 50 Velocity contours for a flow of 5285 cfs with 5 ft of dredging in the east channel.
- Figure 51 Velocity contours for a flow of 10,200 cfs with 5 ft of dredging in the east channel.
- Figure 52 Velocity contours for a flow of 25,850 cfs with 5 ft of dredging in the east channel.
- Figure 53 Velocity contours for a flow of 5285 cfs with the new opening option.
- Figure 54 Velocity contours for a flow of 10,200 cfs with the new opening option.
- Figure 55 Velocity contours for a flow of 25,850 cfs with the new opening option.
- Figure 56 Additional dredging scenario #1 involving dredging along east shoreline downstream of small bridge.
- Figure 57 Additional dredging scenario #2 involving dredging of downstream two-thirds of east channel and along east shoreline downstream of small bridge.
- Figure 58 Additional dredging scenario #3 involving dredging of downstream two-thirds of east channel region.
- Figure 59 Velocity contours for a flow of 5285 cfs with additional dredging scenario #1.
- Figure 60 Velocity contours for a flow of 10,200 cfs with additional dredging scenario #1.
- Figure 61 Velocity contours for a flow of 25,850 cfs with additional dredging scenario #1.
- Figure 62 Velocity contours for a flow of 5285 cfs with additional dredging scenario #2.
- Figure 63 Velocity contours for a flow of 10,200 cfs with additional dredging scenario #2.
- Figure 64 Velocity contours for a flow of 25,850 cfs with additional dredging scenario #2.
- Figure 65 Velocity contours for a flow of 5285 cfs with additional dredging scenario #3.
- Figure 66 Velocity contours for a flow of 10,200 cfs with additional dredging scenario #3.
- Figure 67 Velocity contours for a flow of 25,850 cfs with additional dredging scenario #3.







## 1. INTRODUCTION

The Little Falls Reservoir is located on the Mississippi River, approximately 120 miles northwest of Minneapolis/St. Paul, Minnesota. The reservoir as it exists today was created in 1920 as a result of the construction of the Little Falls Dam. In 1975 construction was completed on the U.S. Highway 10 bypass at Little Falls. Part of the bypass included a combination bridge and embankment structure at the north end of the reservoir, as seen in Fig. 1. The structure consists of two flow openings: the main bridge section which is approximately 1000 ft wide and a smaller bridge of approximately 50 ft across the small east channel. The embankment portion of the structure closed a channel of approximately 250 feet in width.

Since construction was completed, problems related to a decrease in flow and an increase in sedimentation have been reported in the small east channel and the eastern shore of the reservoir downstream of the embankment and bridge structure. These problems include:

- a decrease in reservoir depth
- siltation in areas previously exhibiting sand deposition
- an increase in the growth of aquatic vegetation
- a decrease in the flow available to flush decaying aquatic vegetation from the reservoir
- stagnant water conditions
- odors due to decaying vegetation.

It has been speculated that the embankment and bridge structure may be the primary cause of the current problems in the reservoir.

The role of the embankment and bridge structure as the primary cause of the problems in the reservoir has been a major topic of investigation since about 1984. Various agencies have conducted studies of the problem in an effort to determine the structure's effect on the reservoir and to propose various mitigation techniques. The primary investigations of the reservoir previously conducted are listed below:

- 9/28/84 Russ Schultz, DNR Area Hydrologist summarized possible causes of the problems and recommended further detailed study.
- 10/12/85 U.S. Army Corps of Engineers letter report summarized possible causes of the problems.

- 3/1/92 U.S. Army Corps of Engineers Reconnaissance Report examined the environmental and hydraulic history of the site. The report also discussed possible causes of the problems and potential mitigation techniques.
- 1/28/93 Notes on Sedimentation in the Mississippi River Near Little Falls, MN by Gary Parker, Professor, St. Anthony Falls Laboratory, Department of Civil Engineering, University of Minnesota. Dr. Parker discussed the geomorphologic history of the site.
- 3/1/93 Minnesota Department of Natural Resources and Minnesota Department of Transportation Investigation of Sediment and Vegetation Problems. Summarized reservoir history, effects of the embankment on sediment and vegetation problems, and provided suggestions for mitigation techniques and further study.

One suggestion for further study that was common to several of these reports was to conduct a physical model study of the reservoir. Numerical simulation of the reservoir was discussed as an additional modeling possibility.

St. Anthony Falls Laboratory was contacted about conducting a physical and numerical study of the reservoir in early 1995. Preliminary planning and data consolidation for the study began at that time. Model construction was begun in the early part of 1997 and completed in April of 1997. The study was conducted between May 1997 and November 1997. This report summarizes the results obtained in the course of the physical and numerical study of the reservoir.

## 2. SETTING AND PROBLEM HISTORY

The Mississippi River above Little Falls, Minnesota drains a watershed of approximately 11,145 square miles. The terrain in the watershed is primarily rolling plains, with a mix of forest, agricultural, pasture, urban, and suburban land uses. The most common land uses are agricultural and pasture with extensive wooded areas common along the river. The soils in the watershed are primarily glacial drift material. Several tributaries enter the Mississippi River upstream of the Little Falls Reservoir, including the Little Elk River which enters approximately 0.5 miles upstream. The slope of the Mississippi River above Little Falls is typically on the order of 1.8 feet per mile.

The first recorded attempts to establish a dam on the Mississippi River at Little Falls occurred in 1850. Several of the early dams were destroyed by floods. The first permanent structure, built in 1886, maintained a pool elevation of 1103 feet in the reservoir. The reservoir as it exists today has remained virtually unchanged since construction of a new dam in 1920. A pool elevation of 1107 feet plus or minus 0.5 feet is maintained at the dam. During flood events exceeding a 10-year frequency interval this pool elevation cannot be maintained. The reservoir extends approximately 1.9 miles upstream from the dam. The upstream end of the reservoir is located just downstream of an easterly bend in the river, 0.5 miles downstream of the mouth of the Little Elk River. This area is in a constant state of transition due to the dynamics of sedimentation and channel migration in the deltaic zone at the upstream end of the reservoir. Island formation in the area is a constant and dynamic process and can be seen in the series of aerial photos shown in Figures 3 through 6.

It should be noted that the process of sedimentation in reservoirs is both natural and unstoppable. Rivers are major transporters of sediment. The creation of a reservoir pool decreases the velocities in a river dramatically. As water enters the reservoir it slows, losing the ability to carry its sediment load. Coarse material has a tendency to settle out first. Fine material takes a longer time to settle out. Depending on the size of the reservoir fine material can be carried all the way through the reservoir. Increased growth of aquatic vegetation is also a common occurrence in reservoirs. A gradual decrease in water depth and the deposition of nutrient-rich sediments can promote vegetation growth. As more plants grow, they act to slow the water more, promoting further sediment deposition.

Flood events can also play a significant role in the sedimentation of reservoirs. Floods have the capability to introduce large amounts of sediment into the reservoir over a short period of time. The Little Falls Reservoir is regularly subjected to flood events due to spring snowmelt and periodic rainfall events. The record flood recorded at the Little Falls dam, as of 1993, was a flow of 36,951 cfs on April 15, 1965. The record low

flow was 254 cfs on November 25, 1936. Another low flow period occurred in August of 1975. A flow of 271 cfs was recorded on August 29, 1975. One flood event of particular interest occurred over July 21 - 22, 1972. During this event 10 to 12 inches of rain fell over the Little Elk River watershed and other nearby tributaries. The resulting flood along the Little Elk River and nearby Fletcher Creek was estimated to be of approximately a 500-year frequency. Significant erosion took place along the Little Elk River and Fletcher Creek which enter the Mississippi a short distance upstream of the reservoir. While little hard data is available on the amount of sediment introduced into the Little Falls Reservoir due to this flood event the potential for substantial sediment introduction is very high. The 1984 letter report by Russ Schultz, DNR Area Hydrologist, stated that, "Inspection of aerial photos prior to and after the 1972 flood reveal a significant change in sediment deposits in the bypass area. The little islands grew in size and new ones were created. I believe a lot of the additional sediment came from other streams entering the Mississippi River. For example, the Fletcher Creek washout near Highway 371 during the 1972 flood contributed a lot of the stream bed sediment load, in addition to the Little Elk River. It is entirely possible that most of the sediment we see today may have been a result of the 1972 flood."

In 1975, construction was completed on the U.S. Highway 10 bypass of Little Falls, Minnesota. Part of the bypass included a combination bridge and embankment structure located near the upstream end of the reservoir as seen in Fig. 1. The structure is located approximately 0.5 miles downstream of the mouth of the Little Elk River and 1.9 miles upstream from the dam. Two flow openings make up the bridge portion of the structure. The main bridge section spans approximately 1000 feet on the western side of the river. A smaller bridge spans the approximate 50 foot width of the easternmost small channel. The embankment portion of the structure closed the approximately 250 foot wide secondary channel east of the primary channel. Since the construction of the bridge and embankment, concerns related to decreased flow and increased sedimentation in the reservoir have been raised. The concerns include an apparent decrease in water depth in the reservoir, an increase in aquatic vegetation, siltation in areas previously exhibiting sand deposits, a decrease in the flow necessary to flush decaying aquatic vegetation through the reservoir, and odors due to decaying vegetation and stagnant water conditions. Concern was expressed as to the role of the bridge and embankment structure as the cause of the problems.

Whether the bridge and embankment structure is the cause of the problems is a very complex issue. Surely the structure has altered the flow in the upper region of the reservoir. However, the temporal proximity of the construction of the structure to the 1972 flood event described earlier, the August 1975 low flow period, and the natural process of reservoir sedimentation cloud the issue. These issues were examined in reports by the Minnesota Department of Natural Resources, the U.S. Army Corps of Engineers, and Dr. Gary Parker of the St. Anthony Falls Laboratory and the University of Minnesota. Their observations and conclusions are summarized here.

## 1992 U.S. Army Corps of Engineers Reconnaissance Report

In its 1992 Reconnaissance report, the U.S. Army Corps of Engineers identified four major possible causes of the sediment and vegetation problems. These were: natural sediment filling of a reservoir, flood events, the bridge bypass embankment, or a combination of the three. Their analysis relied primarily on aerial photographs and a reconnaissance mission by boat to examine surface velocities in the problem region. Caution must be exercised when considering aerial photographs as small changes in water surface elevation can change the visible land area dramatically.

Reservoirs begin filling with sediment at their upstream boundary. Coarser bed material is deposited first, followed by fine bed material, silts, then clays. Large reservoirs have the ability to trap all incoming sediment where in smaller reservoirs fine particles may be carried as suspended load through the entire reservoir. The Corps considers the Little Falls Reservoir a small reservoir. The problem area is near the upstream boundary of the reservoir just downstream of the convex bank of a bend in the river. Sediment deposition would occur in this region, regardless of the presence of the embankment, because of the river's tendency to actively migrate. The growth of the islands in the region before construction of the embankment demonstrate this fact.

The process of reservoir filling is further described by "Sedimentation Engineering" ASCE Manual No. 54:

"If the stream enters a wide pool, the flow tends to enter the pool much as a jet, and a finite velocity of flow will continue along this line for an appreciable distance. Part of the sand in transport will be carried into the pool to be deposited along this flow line to form an underwater ridge subtending a submerged channel. As this procedure progresses, this channel will be built up to the surface, and will extend farther into the reservoir. Vegetative growth encourages additional deposition on the banks during high flows. Such a channel may extend for several miles into the reservoir, along the west or south banks in the northern hemisphere, until a bank is breached at indeterminate location (avulsion) during a high inflow, and a new channel starts to form. During this process, a large portion of the fine sediment transported beyond the lower end of the channel will be carried by a reverse eddy back into the head of the pool and will be deposited there. Avulsions cause a new sand channel to be built up over the previously deposited fine sediment. Succeeding avulsions result in a delta consisting of a matrix of fine sediment and sand fingers, frequently with a number of entrapped pools. This formation is usually an unattractive swamp but offers an excellent area for the development of a wild-fowl refuge. Since it would be extremely difficult to predict the proportions of fine sediment that might be involved, or the sequence of avulsions, prediction of the formation or extent of a delta of this type at any given future time would be hopeless."

The Corps report concluded that this description nearly matches what is seen in the Little Falls Reservoir, assuming that the avulsions represented the sediment buildup in the area downstream of the embankment. The only discrepancy between this description and what has been occurring in the reservoir is that deposition is not evident in the main channel. Long term records of bed elevations would be necessary to prove conclusively that reservoir filling is the problem.

Flood events also play a significant role in the depositional patterns of a reservoir. Higher suspended loads and an increase in bed load are generally seen during flood events. This is due to an increase in loading from feeding tributaries and an increase in the erosive power of the river itself. If more sediment is introduced to a stream section than it can transport, the excess sediment will deposit. The suspended material is generally carried by the flow until the velocity becomes low enough for the material to settle out.

In the Corps' analysis of aerial photographs of the bypass region, it was concluded that floods prior to 1972 did not appear to alter the topography greatly. Little change is evident in the amount of land visible in existing pictures. The apparent stability of the bypass region seems to indicate that flood events did not significantly affect the topography. A lack of aerial photographs from the period between 1972 and bridge and embankment construction in 1975 makes it difficult to determine the role of July 1972 flood event. It has been suggested that this event introduced an unusually large amount of material to the bypass region just before construction of the embankment. The Corps of Engineers hypothesized that the coarser material introduced to the Mississippi by the 1972 flood may not have moved immediately into the problem region. They felt it was possible that this material may have taken several years to be transported downstream from the tributaries. The embankment may have already been in place when this material reached the bypass area. This material then proceeded to deposit at the site over a period of several years.

The Army Corps' report documented the difficulty in determining the role of the embankment as a cause of the problems experienced in the area. Extensive data including soundings, aerial photographs, and sediment samples before, during, and after construction would be necessary. Available data, however, was limited to a few aerial photographs, borings and soundings of the pre-construction area, local opinion, and a site visit. That notwithstanding, they were able to make several observations and conclusions with what data was available.

The existing aerial photographs did seem to show a decrease in water depths and an increase in aquatic vegetation. New islands can be seen and shallow areas show vegetation growth. Also, water velocities immediately downstream of the eastern portion of the embankment are almost non-existent. A site visit during fairly high water conditions showed negligible surface velocities from the embankment to about 2500 feet downstream compared to the velocities upstream of the embankment and through the small east channel. Low velocity shallow water will encourage vegetation growth.

Vegetation will further decrease water velocity causing more deposition. Finally, the Corps noted that the embankment appears to have influenced sediment depositional patterns. Aerial photographs from 1975 show deposition immediately downstream of the main bridge span's eastern abutment and the small bridge span's western abutment.

The Corps report concluded that the cause of the sediment and vegetation problems is still indefinite. Aerial photographs seem to indicate that the embankment has played a significant role. There is not, however, enough evidence to conclusively prove it is the cause of the problems. Further complicating the issue are the similarities between the natural process of reservoir filling and what is occurring in the bypass region. Finally, the possibility of the introduction of a larger than normal sediment load to the reservoir due to the July 1972 flood event must be considered. The combination of these three possibilities and a lack of adequate information regarding each did not allow for a definite conclusion.

### **1993 DNR Investigation of Sediment and Vegetation Problems**

In 1993 the Minnesota Department of Natural Resources in conjunction with the Minnesota Department of Transportation conducted an investigation into the sediment and vegetation problems in the Little Falls Reservoir. They also identified the potential causes of the problems to be flood events brought on by severe rainstorms, effects of the reservoir on natural river processes, and the bridge and embankment structure.

The DNR report points out that erosion resulting from severe rain events is a known source of reservoir sedimentation. The sediment load resulting from these storms can shorten the useful life of a reservoir. The July 1972 flood on the Little Elk River and Fletcher Creek, tributaries that enter the Mississippi a short distance upstream of the Little Falls Reservoir, was estimated to be greater than a 500 year frequency event. A Morrison County Flood Insurance Study indicates that the storm produced the greatest 24 hour rainfall in recorded Minnesota history at that time. The DNR reiterates the opinion of Russ Schultz, DNR Area Hydrologist, that, "It is entirely possible that most of the sediment we see today is a result of the 1972 flood."

The report also briefly discusses the effects of the reservoir on the natural processes of deposition and scour in rivers. Sediment deposition and scour in rivers are natural, dynamic, and continuous processes. The construction of a reservoir severely upsets the balance of these processes. Velocities in a reservoir pool are reduced to the point that sediment once carried through the river reach is now able to settle out of the flow. The reduction in velocities further affects the ability of the river to scour sediment within the pool during high flow events. Deposition will occur in the reservoir pool during high flow events until the flow area is restricted sufficiently. At this point, velocities high enough to restore the balance between scour and deposition will occur.

Vegetation growth in reservoirs is also discussed as an effect of the reservoir on natural river processes. Increased vegetation growth in reservoirs is a problem witnessed by the DNR throughout the state and can be a result of natural and unnatural conditions. Deposition of sands and fine silts can decrease water depths in reservoirs to levels that enable vegetation growth. Water clarity and nutrient level issues also can affect vegetation growth. Higher levels of nutrients may or may not be related to sediment deposition. In the Little Falls Reservoir, the increase in vegetation growth has been significant enough to restrict use of parts of the reservoir for certain recreational activities. Decaying vegetation has caused odor and cleanup problems.

The possible effects of the embankment on the deposition in the reservoir were considered by the DNR. The location of the problem area, downstream of the embankment on the eastern side of the river, was critical to the examination. This area is located on the inside of a natural bend in the river. It is natural for sediment deposition to occur on the inside and downstream of a bend. As water flows around the bend, centrifugal forces move the water toward the outside of the bend. There is a tendency for a secondary current to develop that pushes flow toward the inside of the bend, approximately perpendicular to the main current. Sediment is pushed with this secondary flow to the inside of the bend. The DNR concluded that the embankment likely strengthened this secondary flow by effectively increasing the sharpness of the original natural bend. This effect would cause sand and larger sediment particles to deposit more immediately downstream of the embankment and carry fine particles further toward the east shoreline.

The DNR makes the point that the embankment has not affected the amount of sediment that enters the reservoir. Furthermore, the embankment has not increased the amount of sediment that settles out in the reservoir. However, the embankment does appear to have changed the pattern of sediment distribution within the reservoir. In regard to the growth of aquatic vegetation, the DNR concludes that increased growth would likely have occurred with or without the embankment due to the ongoing process of sediment deposition within the reservoir.

The DNR also examined the increase in island area in the reservoir. Aerial photographs between 1940 and 1992 were digitized and plotted to scale. The photographs show that island growth did occur before construction of the embankment. A plot of total island area, in acres, versus years can be seen in Fig. 7. There appears to be a change in the rate of increase of visible island area between the time of the 1972 flood and the embankment construction.

Depth sounding data taken downstream of the embankment also indicate a change in the rate of deposition of sediment. Cores were taken in 1993 in locations where cores had previously been taken in 1968/1973 and in 1985. The rate of sediment deposition between 1985 and 1993 decreased compared to the rate between 1968 and 1985. The rates were 0.029 feet/year and 0.070 feet/year respectively. The location of test holes can be seen in Fig.8.

The DNR report concluded that flow through the small eastern channel and bridge opening has been adequate to maintain a channel navigable by small craft. Certain portions of the reservoir, however, can no longer be used by larger watercraft. They also concluded that sediment and vegetation problems are not unique to this site. Construction of the bridge and embankment has affected rather than created these problems. A permanent resolution of the problems through a one-time project or projects does not exist. Concern was also expressed over the environmental effects of any remedial actions taken in the reservoir. The recommendations of the DNR were for maintenance of the small bridge channel through periodic clearing, snagging and dredging. This would have the effect of minimizing odor problems and help prevent silt from depositing along the east shore. Periodic measurement of water depths and channel geometry should also be made to document future changes in the reservoir.

### **Notes on Sedimentation in the Little Falls Reservoir by Dr. Gary Parker**

The issue of sedimentation in the Little Falls Reservoir was examined in early 1993 by Dr. Gary Parker, a professor at the St. Anthony Falls Laboratory and the University of Minnesota. Dr. Parker's analysis was conducted using aerial photographs from between 1940 and 1992. Overlays created by reducing the photos to a common scale were also used. The author was also given a diagram showing total island area as a function of time from 1955 to 1990.

The aerial photos and overlays showed a steady increase in island area over the time period from 1940 to 1975. Dr. Parker estimated that by the 1975 the island area just downstream of the bridge site had increased by a factor of six. He concluded that the region has been an active area of deltaic sedimentation since at least 1940 with the location of maximum sedimentation located just downstream of the bridge site between the main channel and the now closed east channel. The analysis also showed the zone of sedimentation progressing downstream at a rate of approximately 20 feet per year. Less deposition was evident between the east channel and the far east bank of the reservoir. The branched delta forming at the mouth of the east channel was progressing downstream at a slower rate than the delta between the main and east channels.

Analysis of aerial photographs from 1975 and 1990, after the construction of the embankment, led to the conclusion that the progression of the delta forming at the mouth of the east channel was halted by the closure of the east channel. While the region between the main channel and the closed east channel showed a general increase in island area, the area between the east channel and the far east bank showed practically no increase. Also, the aerial photographs did not obviously suggest that the rate of delta formation had increased greatly over the same period. According to Dr. Parker's analysis, the zone of deposition seems to have continued to progress downstream at a rate of 20 feet per year.

The diagram showing total island area versus time seemed to indicate an increase in the rate of deposition in the deltaic zone since 1975. Dr. Parker is quick to point out that visible island areas are only truly comparable if every photograph were taken at the same reservoir stage. A strict comparison would involve normalization for varied reservoir stage and flood hydrology. Dr. Parker hypothesized that recalculation of island area taking these factors into account, and using only the island area downstream of the embankment, would likely display very little increase in the rate of island formation in the delta area compared to the pre-embankment period.

In terms of river behavior, Dr. Parker states that the aerial photographs should be viewed in the context of two natural processes. The first process to consider is the deltaic sedimentation of reservoirs. The second process of importance in this analysis is the behavior of rivers when bends are present.

In terms of the deltaic sedimentation of reservoirs, it is the natural fate of any reservoir to fill with sediment over time. In the upper midwest, siltation times of 50 to 100 years are common. As the reservoir silts in, braided island bars emerge. These bars progress downstream, grow, coalesce, and vegetate. Downstream of the deltaic zone is generally a deeper zone subject to a slower deposition of silt, clay and organic material. Dr. Parker states that the Little Falls Reservoir fits this framework. He suggests that the depth of the reservoir over its one mile reach causes most of the sand entering the reservoir to deposit in it. The point is made that there is no obvious physical mechanism by which the closure of the east channel could have increased the rate of sand deposition in the reservoir. The embankment could only alter the location of deposition. The aerial photographs reinforce this conclusion by indicating a reduction in the rate of sand deposition between the closed east channel and the east bank of the reservoir. This is due to the fact that the source of the sand, the east channel, has been cut off.

The second important thing to consider is the bend in the river at the upstream end of the reservoir. Dr. Parker states that the effect of the bend should generate an eastward bottom secondary flow at its downstream end. The downstream end of the bend in this case is adjacent to the zone of maximum sedimentation. This should generate a downstream and eastward migrating lobe of sand which would eventually form islands in this region. The closure of the east channel should accelerate this process at the expense of sedimentation at the mouth of now closed east channel. He cites the aerial photos as strong evidence of this effect.

Dr. Parker was able to draw the following conclusion in terms of sand deposition and island formation with some degree of confidence. He concluded that the closure of the east channel has likely reduced the rate of sand deposition downstream of the embankment between the east channel and the east bank of the river. This also resulted in a likely increase in the rate of sand deposition between the main channel and the closed east channel. This conclusion was further supported by bathymetric maps of the region. The maps showed the greatest increase in bed elevation downstream of the embankment occurred between the main channel and the mouth of the closed east channel.

The above conclusion suggests that the closure of the east channel acted to reduce the deposition of sand between the closed east channel and the east bank. Dr. Parker states that the same is not necessarily true of finer material. Fine material tends to be transported across the delta front into deeper, wider slack water before settling out. Dr. Parker states that the closure of the east channel may have modified the depositional patterns of this sediment. The jet from the mouth of the delta before closure of the east channel may have prohibited the deposition of fines along the east bank. Closure of the east channel created a zone of slower flowing water between the east channel and the east bank, promoting the deposition of fines. However, Dr. Parker makes the point that the eventual complete siltation of the region is a forgone conclusion, embankment or no embankment.

Dr. Parker suggests several proposals to alleviate the sedimentation problems in the reservoir. One possibility he suggests is a spur dike at the head of the east channel to draw more flow into the region. However, he cautions that as long as the shallow region contains aquatic vegetation, even substantially increased flow is unlikely to result in removal of existing sediment deposits. The increase in flow may actually bring more sediment into the region. Existing vegetation will retard the bottom flow and possibly cause more deposition. This leads Dr. Parker to conclude that it makes little sense to augment the flow without dredging the region near the east bank of the reservoir. This may, but is not guaranteed to, slow the rate of sedimentation. It will not, however, halt the natural process by which the reservoir is filling.

Another possibility suggested would be to widen the existing small bridge span. This may also necessitate dredging of the small channel. Dr. Parker cautions that dredging, however, invites more deposition within the channel. Some control structure would likely be necessary to reduce the supply of sand to the east channel.

Dr. Parker recommended that the situation could be studied through the use of a physical model. He recommends the use of a fixed bed model in which plastic tracer particles could be used to visualize the effect the closure of the east channel on sediment deposition.

Dr. Parker concludes by cautioning that the natural processes occurring in the Little Falls Reservoir cannot be easily reversed or stopped. Deposition will occur in the reservoir regardless of the presence of the embankment. All that can be done is to rearrange the zones of maximum deposition, slowing an otherwise inevitable process.

### **3. STUDY OBJECTIVES**

The physical and numerical model study of the Little Falls Reservoir had several objectives. The primary objective of the study was to examine the effectiveness of potential mitigation techniques on the sediment and vegetation problems in the reservoir. The secondary objectives of the study were to evaluate the effect of the bridge and embankment structure on reservoir behavior and attempt to identify its role regarding the problems in the reservoir.

The focus of the mitigation techniques involved structural changes to increase flow rates and velocities through the problem region. The intended effect of these measures would be to reduce sediment deposition in, prevent the growth of aquatic vegetation in, and provide sufficient flow to flush decaying vegetation from the affected area of the reservoir.

The examination of the role of the embankment focused on the flow rates and velocities in the reservoir prior to and after the embankment was constructed. Surface flow patterns and sediment tracer depositional patterns were also observed in an effort to visualize the effects of the structure on sedimentation.

## 4. PHYSICAL MODEL DESIGN AND CALIBRATION

### Distorted Froude Modeling

The design of physical river models is based on the principle of Froude similarity. The Froude number is defined as:

$$Fr = \frac{V}{\sqrt{gH}}$$

where: V is velocity, g is gravitational acceleration, and H is flow depth.

Models are scaled so that  $[Fr]_{\text{model}}$  is equal to  $[Fr]_{\text{prototype}}$ , or model Froude number equals prototype Froude number.

The horizontal dimensions of the area to be modeled and the size of the model basin generally determine the scale of the model. However, this scaling ratio usually results in vertical water surface elevation differences and model bed elevation differences that are too small to measure or set accurately. Introduction of a distortion factor between the vertical and horizontal scales is one way to overcome these difficulties. This is known as distorted Froude modeling.

When distorted Froude modeling is used the following relations result; where x is horizontal distance, H is vertical distance,  $\lambda$  denotes the vertical or horizontal scaling factor, S is slope, V is velocity, and Q is flow rate,

$$(x)_m = \lambda_h (x)_p$$

$$(H)_m = \lambda_v (H)_p$$

$$(S)_m = \lambda_v / \lambda_h (S)_p$$

$$(V)_m = \lambda_v^{1/2} (V)_p$$

$$(Q)_m = \lambda_h \lambda_v^{3/2} (Q)_p$$

These relations then allow for accurate design of the model dimensions and proper sizing of the water supply components of the model.

## Application to the Little Falls Reservoir

The reach of the Mississippi River upstream of Little Falls that was to be modeled is approximately 1.5 miles in length. Due to the shape of the bend in the river at the upstream end of the reservoir, a horizontal scale of  $\lambda_h = 1:135$  was chosen. This allowed the model to be fitted in a model basin with maximum width of approximately 28 ft. In order to adequately represent bed contours and water surface elevation changes a distortion factor of 5 was chosen. That is, model elevations are five times greater with respect to horizontal dimensions. The distortion factor led to a vertical scale ratio of  $\lambda_v = 1:27$ .

The corresponding distorted Froude modeling relationships for the Little Falls Reservoir model are given below. Unless specifically stated otherwise, all results from the model are reported in prototype units.

$$(x)_m = 1/135 (x)_p$$

$$(H)_m = 1/27 (H)_p$$

$$(S)_m = 5 (S)_p$$

$$(V)_m = 1/(27)^{1/2} (V)_p$$

$$(Q)_m = 1/(135(27)^{3/2}) (Q)_p$$

Templates were cut to match cross-sectional profiles from topographic and bathymetric maps of the reservoir. The river bed and bank areas were the molded in concrete. Certain areas of the bed were formed by placing a layer of pea-gravel dusted with cement on top of the concrete base. This had the dual purpose of providing model roughness and allowing for the potential simulation of dredging in areas of the reservoir.

## Issues Concerning Sediment Transport

Movable-bed models are often used to model patterns of deposition for sand and other larger sediment particles. Movable-bed models are models in which the banks and floodplain areas are molded in an immobile material such as concrete, but the rest of the model basement is filled with an erodible material that simulates the sediment present in the river. Similar sediment is then fed into the river upstream. The flow and sediment transport are given time to reach a steady-state condition. At this point, bed topography for that particular flow and sediment loading can be measured.

In movable-bed models, however, patterns of circulation and fine material deposition cannot be adequately studied. Fixed-bed models are recommended for this case, for which plastic tracer particles can be used to simulate fine deposition. The physical model of the Little Falls Reservoir was therefore constructed as a fixed-bed

model. The bed contours and topographic features were molded in concrete. Polystyrene beads with a specific gravity of 1.017 were used to examine the effect of the embankment on sediment deposition patterns.

## Model Calibration

The calibration of physical models is essentially a trial and error process. The position of the tailgate necessary to achieve the desired water surface profile in the reservoir must be determined. Frequently the bed roughness of the model must also be modified in order to achieve this desired slope. Modifying model roughness is accomplished by adding or removing roughness tabs from the model. The procedure is as follows:

1. The model flow rate is set for the desired flood event.
2. The model is operated unchanged until steady state conditions are reached.
3. The tailgate is set to achieve the correct tailwater elevation for the flow rate in question.
4. Water surface elevations are measured at the upstream and downstream ends of the reservoir and at key points in between.
5. The water surface profile is calculated and compared to field measurements for the flow rate in question.
6. If the model slope is too flat, roughness is increased through the addition of metal roughness tabs.
7. Steps 1 - 6 are repeated until the model water surface profile matches the field measurements.

The Little Falls reservoir was calibrated for the following return periods and flow rates.

Return Period ( years )	Prototype Flow ( cfs )	Model Flow ( cfs )
10	25,850	1.365
50	33,485	1.768
100	38,900	2.054

The water surface profiles measured in the model at these flow rates were then compared to the field measurements obtained by the U.S. Army Corps of Engineers and seen in Fig. 9. In addition, the water surface profile values were compared to results from a numerical model described in more detail later in this report. Numerical model calibration was achieved sooner than the physical model. Numerical model values agreed well with the

field data, which allowed for the numerical model to be used fairly confidently as an aide in the calibration of the physical model. Examining the effect of bed roughness in the physical model provided insight into the behavior of the physical model. Initially, the model water surface slope was too shallow. Roughness tabs were distributed throughout the upstream portion of the model. This region of the model was expected to be hydraulically too smooth due to the relative smoothness of the concrete. After several trials and additional roughness tabs, an acceptable match of water surface profiles was obtained. The prototype water surface profiles are compared to model water surface profiles in Fig. 10

Additional checks were performed to verify that the proper flow split between the main channel and the east channel was being achieved. Flow rates were measured in the eastern channel and compared to field data for several flow rates. Numerical model values were also used as a comparison for the channel flow rates. Adjustments were made to the east channel region in order to obtain a better match with the field data. Exact matches between the numerical, physical, and measured flow rates were not obtained. However, the range of the values obtained gave confidence that the model was performing satisfactorily.

## **5. NUMERICAL MODEL CREATION AND CALIBRATION**

### **Numerical Model Overview**

The numerical model of the Little Falls Reservoir was created using a program called Surface Water Modeling System (SMS). SMS was developed by the Engineering Computer Graphics Laboratory at Brigham Young University in cooperation with the U.S. Army Corps of Engineers Waterways Experiment Station (WES) and the U.S. Federal Highway Administration. The numerical analysis of the model is performed by RMA-2, a hydrodynamic modeling program maintained by the U.S. Army Corps of Engineers.

SMS is a comprehensive environment created to aid in hydrodynamic modeling. It serves as a pre- and post-processor for two-dimensional finite element, two-dimensional finite difference, and one-dimensional backwater modeling programs. The interfaces within SMS have been specifically designed to interact with the Corps' TABS-MD suite of programs. These programs can calculate water surface elevations and flow velocities and support steady-state or dynamic conditions. They also have the capability of modeling contaminant migration and sediment transport. SMS allows for the creation of a finite element mesh representing the site. Boundary conditions and site specific data necessary for analysis can be saved to model specific files. The mesh and boundary conditions are then exported to RMA-2 where the hydrodynamic analysis is performed. Resulting solutions files are then imported back into SMS for data visualization purposes. SMS has the ability to generate water surface elevation plots, cross-sectional plots, two-dimensional vector plots, color-shaded contour plots, time-variant curve plots, and dynamic animation sequences to aid in the visualization of the solutions.

RMA-2 is a two-dimensional depth averaged finite element hydrodynamic numerical model. It uses a finite element solution to the Reynolds form of the Navier-Stokes equations for turbulent flows. It is capable of computing water surface elevations and horizontal velocity components for subcritical, free-surface flow in two dimensional flow fields. RMA-2 is designed for farfield problems in which vertical accelerations are negligible and velocity vectors generally point in the same direction over the entire depth of the water column at any instant of time. RMA-2 is not intended for problems where vortices, vibrations, or vertical accelerations are of primary interest.

### **Modeling Issues and Data Requirements**

In order to create a properly functioning numerical model, all aspects of the model geometry and input data must be in harmony. The geometry and boundary condition files

must contain the information necessary to simulate the case of interest. Guidelines for creating a good mesh as outlined in the RMA-2 users guide should be followed as much as the situation allows. Input data should be estimated as accurately as possible if not known exactly.

The most important requirement for a successful numerical model is the preparation of a good finite element mesh. Maintaining good element properties is the first step in developing a good mesh. Good element properties include: length to width ratios of less than one to ten; restricting element shapes to undistorted triangles or rectangles; elements with corner angles of greater than ten degrees; bathymetric elevations that all lie in one plane; longitudinal element depth changes of less than 20%. Maintaining good overall mesh properties is also important. These include: good element properties as discussed previously; smooth bathymetric contours; wetting and drying elements lying on bathymetric contours; boundary break angles not exceeding ten degrees; maximum size differences of 50% between neighboring elements; adequate resolution to model the features of the prototype. Adequate mesh resolution should also consider the purpose of the study.

The other requirement for a successful numerical model is input data. The primary input data needs of RMA-2 are related to the hydraulic behavior of the model. They include: flow rate through the model reach; starting or ending water surface elevations; bed and bank area material types; Manning's n (roughness parameter) values for each material type; eddy diffusivity values for each material type. It is also necessary to specify the number of iterations for the simulation, the units to be used during the analysis, whether the solution is steady state or dynamic, and how often the effect of wetting and drying of elements is to be examined.

## **Numerical Model Calibration**

The calibration of numerical models is also a trial and error process. Once the finite element mesh is created, trial runs must be performed to confirm that the solutions generated by the model are representative of the area to be simulated. Bed roughness parameters are varied within the model to generate the desired water surface elevation. Often, necessary minor changes to the mesh geometry become apparent during calibration. Eddy diffusivity values are also varied in order to improve the stability of the numerical solution.

The Little Falls Reservoir was calibrated for return periods and flow rates similar to the physical model. The return period, flow rate, and tailwater elevation are shown below:

Return Period ( years )	Prototype Flow ( cfs )	Tailwater Elevation ( ft )
10	25,850	1107.9
50	33,485	1109.3
100	38,900	1110.3

Different Manning's n roughness values were assigned to different areas of the reservoir and river. A starting range for these values was obtained from a Minnesota Department of Natural Resources Flood Insurance Survey of the region. This document suggested a range of channel roughness values from 0.032 to 0.050. Starting values for each region of the mesh were then estimated taking into account regions of the reservoir that are more heavily vegetated and keeping in mind typical values for various bed materials. Since RMA-2 does not allow for the input of sidewall roughness, the bed roughness of elements forming the edges of the waterway and in the side channel region were exaggerated to compensate. Simulations were then performed at the above flow rates. The water surface profiles were compared to the measurements obtained by the U.S. Army Corps of Engineers as seen in Fig. 10. Roughness values were then adjusted and the simulations repeated. This process was repeated until the water surface profiles obtained in the numerical model matched the field data. The final roughness values and the regions they were assigned to in the model can be seen in Fig. 11.

Numerical models also require some form of stabilization. In RMA-2, the Galerkin method of weighted residuals is employed. This method does not include any form of stabilization other than the eddy viscosity terms. The Galerkin method requires a certain amount of turbulence to achieve stability and not impair the solution. The turbulent exchange coefficient, E, is used to control the freedom of the velocity vectors to change directions in the iterative solution. Values of E that are too low allow the velocity vectors too much freedom to change direction, causing a numerically unstable problem. The program will diverge rather than converge to a solution. The solution is to increase E until a stable solution is reached. The eddy viscosity terms were adjusted by trial and error using recommendations in the RMA-2 users guide in order to obtain stable model solutions. A value of 40 lb-sec/ft<sup>2</sup> for E was found to give stable model solutions.

The numerical model was also checked against data on the side channel flow rates from the MN-DNR. The flow rates through the east channel region were examined at various total flow rates by the DNR. Minor changes to the model mesh were made in order to achieve similar east channel flows.

## Numerical Model Output

SMS allows the user to generate several useful forms of output from an RMA-2 solution file. These include bathymetric contour maps of the model mesh, water surface elevation contour plots, velocity contour plots, velocity vector plots, and dynamic animation sequences. The water surface elevation contour plots were useful in the calibration process; an example can be seen in Fig. 12. The velocity contour plots were

useful in examining the results of different mitigative options and comparing them to the existing conditions in the reservoir. Numerous examples of these plots can be seen in Figures 41 through 55.

## 6. OVERVIEW OF EXPERIMENTS

As stated earlier, the objectives of the study were to examine the effect of several mitigative options on the flow, sedimentation, and vegetation problems in the reservoir. As the study progressed, visits with representatives from Little Falls and the various agencies involved in previous studies of the problem made it clear that the major concern in the reservoir was the insufficient flow through the east channel region. The flow rates and velocities on the east side of the reservoir downstream of the embankment were not sufficient to flush decaying vegetation from the region, or to prevent further vegetation from taking root. In addition, the decrease in velocities was believed to be responsible for an increased amount of sedimentation in this region. It also became apparent that the dynamic nature of the bend in the river had caused sedimentation in the region regardless of the presence of the embankment. Lack of data related to the amount of sediment load in the river made it difficult to accurately model the amount of sediment deposition in the problem region. The change in flow rate and velocities in the problem region provided by each option therefore became the focus of the experiments. The sediment transport issues in the reservoir were then examined in a more qualitative fashion drawing conclusions from the flow rate and velocity results, and by using sediment tracers and surface flow patterns to visualize the effect of the embankment.

Each mitigative option was examined using both the physical and the numerical models. The physical model results were used as the primary results and the numerical model results were used to augment what was seen in the physical model. The first experiments were run in both models in order to determine the pre-embankment flow rates in the east channel. The flow rates for the case with the embankment in place were then measured. The various options examined in the experiments were: 1) a spurdiike at the upstream entrance to the east channel region; 2) reopening the larger closed east channel; and 3) dredging of the east channel. Fig. 13 shows each option. In each case, the pre-embankment flow rates were used as a target line while the flow rates with the embankment in place were used to show the increase provided by each option.

Velocities and flow patterns were examined in both models following a similar procedure. The pre-embankment velocities were again used as target values. The increase in velocities provided by each option can be seen by comparing each to the velocities from the case with the embankment in place.

Sediment tracers were used to visualize the effects of the bridge embankment on the location of sediment deposition. The location of the areas where sedimentation would be expected to occur were estimated for each option based on the sediment tracer video footage, flow patterns, flow rates, and velocities generated by each option.

The mitigative options were examined at overall river flow rates of 5,285 cfs, 10,200 cfs, and 25,850 cfs. The flow rate of 25,850 cfs represents a flood event with a return period of ten years. The other two flow rates represent floods with return periods of less than two years. These flows were chosen in order to represent more commonly occurring flow rates. It was felt that since one of the major concerns was the continual flushing effect of flow through the reservoir, more frequently occurring flows should be examined as well as flood flows.

## 7. PHYSICAL MODEL RESULTS

### Flow Rate Results

As stated previously, the flow rates for the case with no embankment were examined first. These flow rates were used as target values for each of the mitigative options examined. The idea was to try to re-establish the flow rates as close to the original pre-embankment values as possible. It should be noted that the numerical values for the flow rates have some variability associated with them. Exact calculation of flow rates in a physical model with irregular bathymetry is not possible. The values given here are approximations and hence have some variability. However, the procedure used to measure and calculate the flow rates was consistent throughout the study, and the trends seen in the results are representative of the change due to each option. Table 1 compares the flow rate values of all the options.

**Table 1: Physical Model East Channel Flow Rates at Experimental Total Flow Rates**

	5285 cfs	% of target value	10,200 cfs	% of target value	25,850 cfs	% of target value
No Embankment	225 cfs	100	1000 cfs	100	2560 cfs	100
With Embankment	45 cfs	20	285 cfs	28	1485 cfs	58
Spurdike	30 cfs	13	300 cfs	30	1940 cfs	76
Extended Spurdike	80 cfs	36	410 cfs	41	2060 cfs	80
5 ft Dredging	450 cfs	200**	930 cfs	93	2175 cfs	85
New Bridge Opening	203 cfs	90	763 cfs	76	3470 cfs	136**

\*\* see physical model results section

#### *Case 1: No Embankment*

At a total flow rate in the reservoir of 5285 cfs the flow rate through the east channel region was 225 cfs. At 10,200 cfs the flow rate in the east channel region was 1000 cfs. At a total flow rate of 25,850 cfs in the reservoir the flow rate in the east channel region was 2560 cfs. These physical model flow rates were used as target values for each of the mitigative options examined in the physical model.

#### *Case 2: With Embankment*

With the embankment structure in place, the flow rates were measured to get an idea of the current behavior of the reservoir. The values also give another point of

reference with which to compare the flow rates for each solution option. At a total flow of 5285 cfs, the flow rate in the east channel was found to be 45 cfs. This value is only 20% of the flow rate that was seen in the east channel without the embankment. At 10,200 cfs the east channel flow rate was 285 cfs, or only 28% of the flow rate seen without the embankment for the same conditions. At a total flow rate of 25,850 cfs the east channel flow rate was found to be 1485 cfs, or 58% of the pre-embankment flow rate.

#### *Case 3: Spurdike 500 ft in length*

Several spurdike orientations were explored before the orientation seen in Fig. 13 was studied in detail. At a total river flow rate of 5285 cfs with the spurdike in place the flow rate seen in the east channel was 30 cfs. This lower value is probably due to the approximation of the flow rate. This value is approximately 13% of the pre-embankment flow rate. At 10,200 cfs the east channel flow rate in the model was found to be 300 cfs, or 30% of the flow rate without the embankment or spurdike. At 25,850 cfs the east channel flow rate was 1940 cfs or 76% of the pre-embankment flow rate.

#### *Case 4: Extended Spurdike 750 ft in length*

The relatively small increases seen in the 500 ft spurdike experiments were less than expected. It was originally thought that a longer spurdike would be more effective in drawing more water into the east channel region. A longer spurdike with similar orientation was then tested to see if it had any greater effect. At a flow rate of 5285 cfs the east channel flow with the extended spurdike in place was 80 cfs. This is approximately 36% of the pre-embankment flow rate. At 10,200 cfs the east channel region had a flow rate of 410 cfs, or 41% of the target flow rate. At 25,850 cfs the east channel flow rate was calculated at 2060 cfs which is 80% of the target flow rate. The values showed the extended spurdike to be somewhat more effective at drawing flow through the east channel region. The size of the structure, however, was deemed to be somewhat unrealistic for application.

#### *Case 5: Dredging of the East Channel Region*

The case examined the effect of dredging several feet of material throughout the east channel region. The average width of the region dredged was approximately 100 ft and an average dredging depth of 5 ft was simulated. The region considered for dredging can be seen in Fig. 13. It should be noted that the dredged depth of 5 ft was determined using the numerical model. Various dredging depths were simulated in the numerical model to determine what reasonable dredging depth could achieve flow rates close to the target values. The physical model results in this case were used to confirm that result.

At a flow rate of 5285 cfs in the reservoir the east channel flow rate after dredging was found to be 450 cfs. This value is 200% of the target value. This high value is likely an exaggeration. The result however, could be due to the approximate measurements of the flow rate, and the fact that in order to simulate the dredging of the east channel, the gravel bed was removed. This left a channel bottom of smooth concrete. The resulting lack of bed roughness, coupled with the approximate calculation of flow rate, might have

contributed to the very high value. At a total flow rate of 10,200 cfs the east channel flow rate was 930 cfs, or 93% of the pre-embankment value. At 25,850 cfs the east channel flow rate was calculated to be 2175 cfs, which is 85% of the target value.

#### *Case 6: New Bridge Opening*

This option considered reopening the channel that was closed by the embankment structure. A new bridge opening of approximately 150 ft was examined. At a total flow rate of 5285 cfs the east channel flow rate was calculated to be 203 cfs. This value is 90% of the target value. At 10,200 cfs the east channel flow rate was 763 cfs, or 76% of the target value. At a total flow rate of 25,850 cfs the east channel carried 3470 cfs. This value was 136% of the target value. Once again we must consider that this value may be an exaggeration, perhaps due to the effect of model roughness and the approximate nature of the flow rate measurements. However, it is possible that more flow passes through the east channel region with the new opening. During this flood event, much of the island area is submerged. Water that previously flowed over the islands may not be able to do so now due to the presence of the embankment. This may have the effect of forcing more water through the new bridge opening and the far east bridge opening.

### **Velocity and Flow Pattern Experiments**

Figures 14 through 33 show the surface velocities and flow patterns for each of the mitigative options examined. The area shown in the photos is immediately downstream of the embankment structure. Most of the photos concentrate on the east channel bridge opening and downstream. There are also several photos of the area immediately downstream of the channel closed by the construction of the embankment.

Overall, the trends seen in the flow rate analysis are also exhibited in the velocity and flow pattern experiments. The presence of the embankment causes a significant decrease in flow velocities downstream of it compared to the case with no embankment. This contrast can be seen in Figures 14 through 22. With the embankment in place, most of the region between the east channel and the east bank of the river show very low velocities. Other than in the deeper channel immediately adjacent to the east bank, the area is essentially covered by slack water. There are also significant changes visible in the flow pattern behavior. The area downstream of the embankment between the closed east channel and the east bank of the river tends to exhibit a circulating behavior. Water exits the mouth of the small east channel, travels downstream and then is recirculated through the region of interest, as seen in Figures 19, 20, and 22. The recirculating effect has the potential to allow more sediment to deposit in this region.

The spurdiike orientation described earlier shows the ability to increase velocities downstream of the embankment. It cannot, however, restore flow patterns similar to the case with no embankment. The flow still exhibits a tendency to circulate through the region immediately downstream of the embankment between the closed channel and the east bank. Figures 23 through 25 show the spurdiike flow patterns and surface velocities.

Dredging of the east channel region shows the ability to increase velocities a little more than the spurdiike option. This can be seen in Figures 26 and 27. Still, the issue of circulation in the region of interest is a concern. Dredging of the east channel region does not alleviate this problem.

A new opening in the embankment at the mouth of the closed east channel shows the ability to increase the surface flow velocities significantly. It also is the option that shows a flow pattern most similar to the pre-embankment scenario, since they are the most physically similar to each other. These results can be seen in Figures 28 through 33. However, the new opening option does exhibit a slight tendency to induce circulation downstream of the embankment as seen in Figure 33. This is most likely due to the difference in water velocity exiting each bridge opening. Also, the new opening is somewhat narrower than the unaltered channel present before embankment construction. This may have the effect of creating more of a jet-like stream exiting the mouth of the east channel than previously existed. Finally, surface velocities through the small bridge opening and along the east bank downstream of the embankment are decreased due to the flow now passing through the new opening.

## **Sediment Tracer Results**

Figures 34 through 36 show subsurface sediment deposits with the embankment present, without the embankment, and with a new opening in the embankment. The deposits formed due to the input of polystyrene beads in the upper region of the east channel. The idea was to observe the location of the particles as they settled out and moved along the bottom of the reservoir. The tracers were examined at the 25,850 cfs flow rate, which is a flood flow expected to input and move sediment within the reservoir. For the cases with the spurdiike in place, and with the east channel dredged, similar depositional patterns as the case with the embankment in place would occur. The additional flow would most likely carry more sediment into the east channel and downstream. The increase in velocity would, however, aid in moving this additional load through the region. The differences between these cases and the case with the embankment in place would be difficult to see. Since the results of the tracer experiments are qualitative in nature, and were primarily to help visualize the effect of the embankment, these cases were not photographed.

Without the embankment present, as seen in Figure 34, the majority of the suspended sediment in the east channel passes through the opening that was closed by the embankment. As it enters the region of slower moving water downstream of the opening it begins to settle out and form the delta seen in the photographs. Over time the delta progresses downstream and spreads laterally. The zones of heaviest deposition are located along the sides and appear as bright white in the photographs. With continued sediment loading the delta would continue to expand both downstream and laterally, eventually spilling over into the deeper channel along the east bank. With time it appears that this channel would have been filled by the sediment depositing in the delta.

With the embankment in place the supply of sediment to the delta is cut off. Now the majority of the sediment passes through the small east bridge opening. However the flow through the east channel region as a whole is reduced, decreasing the overall sediment load drawn into the region. The sediment carried through the east channel exits the small bridge opening and deposits as seen in Figure 35. The heaviest deposition occurs along the edge of the channel following the east bank. With the embankment in place, the flow exhibits a tendency to maintain this channel. Limited deposition did occur within the channel, but most of the sediment was moved downstream by the flow, or deposited along the edge of the channel.

The case with a new opening in the embankment is seen in Figure 36. Similar to the case with no embankment, the majority of the sediment passes through the new opening. It then settles out and forms a delta downstream of the opening. However, the lateral expansion of the delta occurs farther downstream of the opening than in the case with no embankment. Also, the delta formed is not as wide as that formed in the case with no embankment. This is due to the fact that the new opening is not as wide as the channel closed by the embankment. The constriction of the channel increases the velocities through the opening and causes sediment to be carried farther downstream before settling out. With continued sediment loading the delta would continue to progress downstream and laterally. However, it does not appear that the delta would spill over into the channel along the east bank until much farther downstream.

The surface flow patterns seen in Figures 37 through 39 help to illustrate the effect of the embankment on the flow patterns in the reservoir. With no embankment in place the flow exits through the larger east channel opening more rapidly than through the far east opening. As it flows into the wider region downstream, it slows. The more rapidly moving water behind pushes the flow outward laterally, toward the center of the reservoir and the east bank. The slower moving flow exiting the small opening joins this flow and moves downstream. This effect is seen in Figure 37.

The surface flow patterns with the embankment in place are shown in Figure 38. The flow passes through the small bridge opening and travels along the east shoreline. As the flow progresses downstream some of it is pulled into the region of "low velocity" water downstream of the closed east channel. Farther downstream, the flow along the east shoreline shows a tendency to be recirculated back into the slack water region.

The surface flow patterns with a new opening in the embankment can be seen in Figure 39. The flow exits the new opening more rapidly than it exits the small bridge opening, similar to the case with no embankment. As it enters the region downstream of the new opening, it slows and is spread laterally by the flow pushing from behind. The slower moving flow from the small bridge opening joins this laterally spreading flow. There is a slight tendency for circulation as these flows meet.

## 8. NUMERICAL MODEL RESULTS

### Flow Rate Results

In correspondence with the methodology of the physical model, the flow rates with no embankment present were examined first in the numerical model. These values were used as the target flow rates for each of the following cases. Once again, the idea was to see which option was able to come closest to reestablishing pre-embankment flow rates. Table 2 shows the east channel flow rates for each of the following cases.

**Table 2: Numerical Model East Channel Flow Rates at Experimental Total Flow Rates**

	5285 cfs	% of target value	10,200 cfs	% of target value	25,850 cfs	% of target value
No Embankment	330 cfs	100	840 cfs	100	3600 cfs	100
With Embankment	90 cfs	27	320 cfs	38	1100 cfs	31
Spurdike	147 cfs	45	500 cfs	60	1360 cfs	37
Extended Spurdike	190 cfs	58	650 cfs	77	1385 cfs	38
5 ft Dredging	215 cfs	65	645 cfs	77	2000 cfs	56
New Bridge Opening	290 cfs	88	725 cfs	86	2350 cfs	65

\*\* see numerical model results section

#### *Case 1: No Embankment*

At a total flow rate in the reservoir of 5285 cfs the numerical model predicted a flow rate of 330 cfs through the east channel region. At 10,200 cfs the flow rate in the east channel region was 840 cfs. At a flow rate of 25,850 cfs the numerical model predicted a flow rate of 3600 cfs in the east channel. These values were used as the target flow rates for each of the following cases, similar to the physical model results.

#### *Case 2: With Embankment*

With the embankment structure in place, the flow rates through the east channel were again examined to see the effect of the structure. At a total flow of 5285 cfs the east channel flow rate was 90 cfs. This value is 27 % of the flow that is seen in the east channel without the embankment. At 10,200 cfs the east channel flow rate was found to be 320 cfs, or 38 % of the pre-embankment flow. At 25,850 cfs the east channel flow rate was 1100 cfs, or 31 % of the target value.

### *Case 3: Spurdike 500 ft in length*

The spurdike was examined in the numerical model at the same length and orientation as in the physical model. At a total river flow rate of 5285 cfs the east channel flow rate with the spurdike in place was 147 cfs. This value is 45 % of the flow rate seen in the east channel without the spurdike or the embankment. At 10,200 cfs the east channel flow rate is 500 cfs, or 60 % of the target value. At 25,850 cfs the east channel carried a flow of 1360 cfs which is 38 % of the pre-embankment value.

### *Case 4: Extended Spurdike 750 ft in length*

The 500 ft spurdike showed the ability to create only a small increase in the east channel flow rate in the numerical model as well as the physical model. Once again a longer version of the spurdike was examined to verify this effect. At a total flow rate of 5285 cfs the east channel flow rate with the extended spurdike was found to be 190 cfs. This value represents 58 % of the target value. At 10,200 cfs the east channel carried a flow of 650 cfs, or 77 % of the pre-embankment value. At a total flow rate of 25,850 cfs the east channel flow rate was 1385 cfs, or 38 % of the target value. These results also showed that the longer spurdike was somewhat more effective at drawing more flow into the east channel at the two lower flows. However, at the 10-year flood flow rate the extended spurdike showed no significant increase over the first spurdike.

### *Case 5: Dredging of the East Channel Region*

Dredging of the east channel region shown in Fig. 13 was examined in the numerical model. Dredging depths ranging from 1 ft to 5 ft were examined to see whether they could generate flow rates approaching the target values. Dredging depths greater than 5 ft were not examined as the amount of material needed to be removed was considered excessive. The results reported here are for an average dredging depth of 5 ft throughout the region shown. At a total flow of 5285 cfs the east channel flow rate was 215 cfs. This value is 65 % of the target flow rate. At a total flow of 10,200 cfs the east channel flow rate was 645 cfs, or 77 % of the pre-embankment value. At the high flow rate of 25,850 cfs the east channel carried 2000 cfs, or 56 % of the target flow rate.

### *Case 6: New Bridge Opening*

Reopening the channel that was closed due to the embankment construction was also examined in the numerical model. Similar to the physical model a new opening of about 150 ft was examined. At the low flow rate of 5285 cfs the east channel region carried a flow of 290 cfs which is 88 % of the target value. At 10,200 cfs the east channel region flow rate was 725 cfs, 86 % of the pre-embankment value. At the high flow rate of 25,850 cfs the east channel region flow rate was 2350 cfs, or 65 % of the target value.

The flow rate data shows a progressive increase in flow through the east channel due to each option. A new bridge opening exhibited the greatest ability to increase the flow through the region. This would be expected since this option is physically closest to the original setting of the area. The next highest increases were created by the dredging option, followed by the extended spurdike and the shorter spurdike.

## **Velocity Results**

Figures 41 through 55 show velocity contour plots generated by the numerical model for each of the mitigative options. The region focused on in the plots is outlined in Figure 40. It is similar to the region focused on in the physical model photographs. In general, the trends exhibited in the plots are also similar to the trends seen in the physical model. The presence of the embankment causes a significant decrease in the velocities compared to the case with no embankment. This effect can be seen in Figures 41 through 46. The eastern portion of the reservoir immediately downstream of the embankment is largely “low velocity” water. The only significant velocities in the region are in the channel that follows the eastern bank of the river.

The spurdiike velocity plots seen in Figures 47 through 49 show its ability to increase the velocities downstream of the embankment to some degree. The increase is most evident along the eastern bank of the reservoir. There is still a large region of low velocities downstream of the closed channel opening. This is the same region shown in the physical model to be circulating with low velocities.

The east channel dredging option also shows the ability to increase the velocities downstream of the embankment. The velocity plots for the dredging scenario can be seen in Figures 50 through 52. Once again the increase is most pronounced along the east bank of the reservoir, as more flow passes through the small opening. There is still a region of lower velocities downstream of the closed channel.

The velocity contour plots for a new opening in the embankment can be seen in Figures 53 through 55. The new opening produces velocities most similar to the pre-embankment velocities. The contours exhibit a very similar pattern as well, with only slight differences between the pre-embankment contours and the contours for the new opening. These are likely due to the fact that the new opening is narrower than the channel that was closed. Another factor affecting the patterns is that the embankment is still present. With no embankment in place, water flowed over some of the island areas. With the embankment prohibiting this in the case of a new opening, we would expect slight differences.

## **Additional Dredging Simulations**

As the study progressed it became clear that some form of dredging would be able to increase the flow rates and velocities through the east channel region and downstream. Dredging also has the potential to be a much more financially feasible option than construction of a new bridge span or spurdiike. However dredging of the entire east channel is not a perfect solution. This is due to the fact that dredged channels often act like magnets for more sediment, filling rather quickly. Therefore several different dredging options were further examined within the numerical model.

The areas considered for dredging in the additional scenarios can be seen in Figures 56 through 58. Two of the three scenarios included dredging of the channel along the east bank downstream of the small bridge opening. Dredging of this region would eliminate the immediate vegetation problems and improve navigational access for the residents along this shoreline. Dredging only the downstream two-thirds of the east channel was also examined. This would provide some increase in the flow rates and velocity through the east channel and downstream while also helping to prevent the drawing in of more sediment from the main channel.

The velocity contour plots for the additional dredging scenarios can be seen in Figures 59 through 67. The differences in predicted velocities between the scenarios is relatively minor. All of the scenarios show a zone of higher velocity flow along the east shoreline with a zone of very low velocity water downstream of the closed channel. Although minor, the velocity plots do show a slight difference along the east shoreline between scenarios. Dredging of only the region along the east shore downstream of the small bridge opening causes the velocities seen in Figures 59 through 61. Dredging of the downstream two-thirds of the east channel and along the east bank downstream of the small bridge shows a slight increase in velocities along the east shoreline as seen in Figures 62 through 64. Dredging of only the downstream two-thirds of the east channel also shows a slight increase in velocity in the channel along the east bank, seen in Figures 65 through 67. The velocity contours for the original dredging scenario, which involved the dredging of five feet of material throughout the entire east channel, are shown in Figures 50 through 52. This scenario caused the highest velocities to occur along the east bank. That is expected since the additional dredging scenarios were examined for dredging depths of approximately four feet compared to five feet in the original. Also, in the original scenario the dredging extended throughout the entire east channel, allowing more water to be drawn into the region at the upstream end.

The additional dredging simulations were also examined as to their effect on the flow rates through the east channel and region downstream. Table 3 lists the flow rates for each additional scenario as well as the original dredging scenario and the existing condition with the embankment in place. The differences in predicted east channel flow rates between scenarios are also relatively minor. All of the scenarios increase the flow rates in the east channel relative to the case with the embankment in place. Relative to each other, the scenario including dredging of two-thirds of the east channel and downstream along the east bank provides the highest flow rate in the east channel. These flow rates were 1600 cfs at a total river flow of 25,850 cfs, 520 cfs at a total flow of 10,200 cfs, and 170 cfs at a total flow of 5285 cfs. Next highest was the scenario in which only the downstream two-thirds of the east channel were dredged. The flow rates for this scenario were 1460 cfs at a total flow of 25,850 cfs, 460 cfs at a total flow of 10,200 cfs, and 152 cfs at 5285 cfs. Dredging of only the region along the east bank downstream from the small bridge opening provided only a minor increase in flow rate. The flow rates were 1450 cfs at a total flow of 25,850 cfs, 360 cfs at a total flow rate of 10,200 cfs, and 100 cfs at a total flow rate of 5285 cfs.

**Table 3: Numerical Model East Channel Flow Rates for Additional Dredging Scenarios**

Total Flow Rate	5285 cfs	10,200 cfs	25,850 cfs
Scenario #1	100 cfs	360 cfs	1450 cfs
Scenario #2	170 cfs	520 cfs	1600 cfs
Scenario #3	152 cfs	460 cfs	1460 cfs
Original Dredging	215 cfs	645 cfs	2000 cfs
With Embankment	90 cfs	320 cfs	1100 cfs

Note:

**Scenario #1** represents dredging of region downstream of the small bridge opening, parallel to the east bank of the reservoir.

**Scenario #2** represents dredging of the downstream two-thirds of the east channel region and along east bank of reservoir downstream of the small bridge opening.

**Scenario #3** represents dredging of the downstream two-thirds of the east channel region only.

## 9. CONCLUSIONS AND RECOMMENDATIONS

Based on the information obtained in the physical model, the numerical model, and previous examinations of the problems in the Little Falls Reservoir, several conclusions can be made. The conclusions relate to the effect of the embankment on flow, sedimentation, and vegetation growth in the reservoir, particularly in the region downstream of the embankment between the closed east channel and the east shoreline. The conclusions also relate to the effectiveness of the various mitigative techniques examined.

In terms of the flow in the reservoir, the embankment has caused a reduction in flow rate and velocity through the east channel region and the region downstream of the embankment between the closed east channel and the east shoreline. The embankment has also changed the pattern of the flow in the reservoir, specifically in the region downstream of the embankment between the closed east channel and the east shoreline. The only significant flow velocities in this region occur in the deeper channel along the east shoreline. The presence of the embankment does not appear to have significantly affected the velocities in this channel.

In terms of sedimentation, the embankment has changed the sediment deposition patterns in the reservoir. The exact nature of the changes, however, are difficult to determine. It does appear that the closure of the east channel has reduced the amount of coarse sediment depositing in the region between the closed east channel and the east shoreline. The closure of the east channel has cut off the supply of material to the delta forming in this region prior to embankment construction. Closure of the east channel also forced the locus of deposition of the coarser material farther west. The deposition of coarse material (sand) is responsible for island formation and channel shifting. Without the closure of the east channel, such a process could have completely silted in the east shoreline by now. With the locus of coarse material deposition now located farther west, in the island region west of the closed east channel and downstream of the embankment, the east shoreline is now receiving mostly fine-grained sediment.

The effect of the embankment on vegetation growth is difficult to determine. Aerial photographs of the reservoir do show an apparent increase in vegetation downstream of the embankment between the closed east channel and east shoreline. It is likely that deposition of fine material in the region of interest has aided the growth of aquatic vegetation. However, increased vegetation growth is a problem commonly encountered in reservoirs and is not unique to this site. As island bars grow, the natural progression is to grow, coalesce, and vegetate. Growth of aquatic vegetation in the region of interest would likely have eventually occurred, regardless of the embankment.

It must be noted that the difficulty in determining the precise role of the embankment is due to the dynamic nature of the processes involved. The construction of the embankment has not caused the siltation in the reservoir. It is the natural fate of reservoirs to fill with time. The age of the Little Falls Reservoir falls within the range of expected life for reservoirs in the upper midwest. The deposition of sediment along the inside bank of river bends, leading to the formation of island bars, is also a natural and inevitable process. The construction of the embankment has not increased the amount of sediment depositing in the reservoir. It has only served to alter the location of the zones of maximum deposition. Deposition would occur in the region of interest regardless of the presence of the embankment.

In terms of the effectiveness of mitigative techniques, both dredging and the reopening of the east channel exhibit the potential to improve the situation in the reservoir. Both exhibit the ability to increase the flow rates and velocities in the east channel region and downstream of the embankment. A new opening also exhibits the ability to create flow patterns most similar to pre-embankment patterns. Reopening the closed channel, however, would involve considerable cost due to the construction of new bridge spans and excavation of the current embankment. It would also be more than likely necessary to dredge the region downstream of the new opening. The vegetation in this region is likely so firmly entrenched that simply reopening the east channel would not remove it. Therefore, an option involving dredging of the east channel and an area immediately downstream of the small bridge opening shows the most potential in terms of a combination of problem mitigation and cost.

With these conclusions in mind, several recommendations and conclusions for the mitigation of the problems in the reservoir can be made.

1. Dredging of the downstream two-thirds of the east channel region and along the east shoreline downstream of the embankment, as shown in Figure 57, appears to be the best option for mitigation of the problems in the reservoir.
2. The dredging would begin approximately 850 feet downstream of the entrance to the east channel region. The dredging would follow the east channel and the east shoreline. It would continue approximately 2200 feet downstream of the small bridge opening. The area dredged would be approximately 70 feet wide in the portion upstream of the small bridge and approximately 200 feet wide downstream of the small bridge opening.
3. This option will help minimize the existing vegetation problems along the east shoreline and improve navigational access for the residents.
4. Beginning the dredged region downstream of the entrance to the east channel could help prevent the drawing in of sediment from the main channel.

5. An approximate dredging depth of four feet throughout this region shows the potential to increase the flow rates through the east channel region to 43% - 50% of pre-embankment flow rates. The existing flow rates are approximately 27% - 38% of the pre-embankment flow rates. Flow velocities in the region will also be increased relative to the existing conditions.
6. Increases in velocities along the east shoreline should help reduce the deposition of fine material in this region.
7. The approximate volume of material to be removed would be between 75,000 and 100,000 cubic yards. This assumes a width of 70 to 100 feet upstream of the small bridge and 200 to 250 feet downstream. At an estimated cost of \$8.00 per cubic yard, assuming on site disposal, the potential costs would range between \$600,000 and \$800,000. This cost needs to be balanced against the severity of the existing problem and the relative need for correcting it.
8. Periodical clearing and snagging should be used throughout the region of interest to help clear any decaying vegetation and obstructions to the flow.
9. Periodic checks of bed elevation should be used to monitor the filling of the dredged region.
10. The dredging of the east channel region and the area along the east shoreline downstream of the embankment will not provide a permanent solution. However, based on the estimated depositional rate of 0.029 ft/yr between 1985 and 1993, this option should minimize the problems experienced along the east shoreline for approximately 10 to 30 years.
11. A spur dike is not recommended at this time because a) it creates a potential navigation hazard, b) the environmental impact during construction could be significant, and c) construction of a spur dike has the potential to change local river dynamics in an undesirable manner such as the creation of higher flow velocities and the formation of a scour hole near the tip of the dike.

## REFERENCES

Parker, Gary, Marcelo Carcia, Helgi Johannesson, and Kazunori Okabe. Model Study of the Minnesota River Near Wilmarth Power Plant, Minnesota, University of Minnesota, St. Anthony Falls Laboratory Project Report No. 284, December 1988.

U.S. Army Corps of Engineers. Mississippi River Upstream of Minneapolis at Little Falls, Minnesota--Morrison County, Reconnaissance Report, March 1992.

Parker, Gary. Some Notes on Sedimentation in the Mississippi River Near Little Falls, Minnesota, January 28, 1993.

Minnesota Department of Natural Resources and Minnesota Department of Transportation. Investigation of Sediment & Vegetation Problems, Little Falls Reservoir - Little Falls, Minnesota, March 1993.

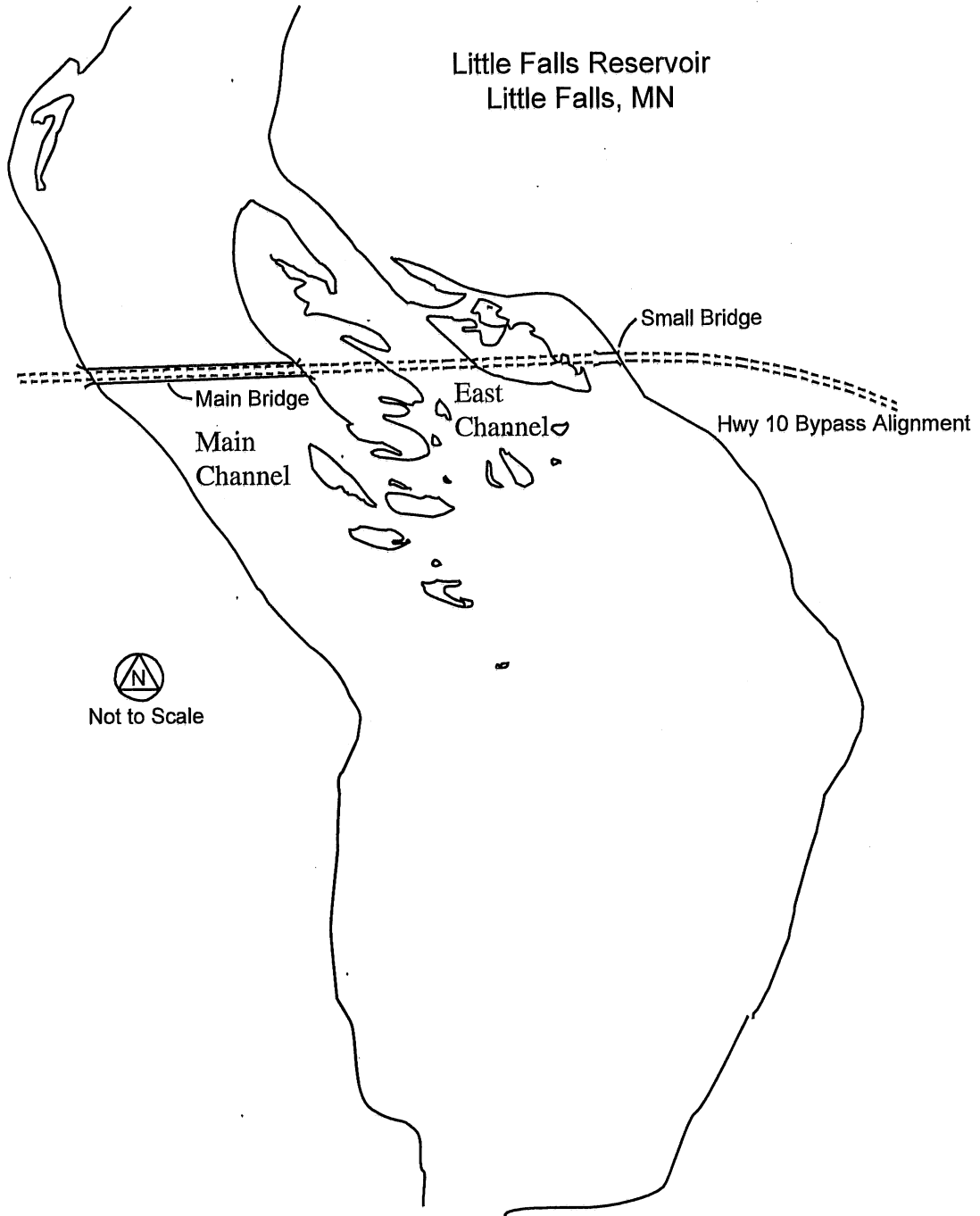


**Figure 1** Little Falls Reservoir showing location of main channel, east channel, small east channel and embankment and bridge structure.



**Figure 2** Map of Minnesota showing location of Little Falls, MN.



**Fig. 3. Aerial photo of Little Falls Reservoir in 1963.**



**Fig. 4. Aerial photo of Little Falls Reservoir in 1980.**



**Fig. 5. Aerial photo of Little Falls Reservoir in 1986.**



**Fig. 6. Aerial photo of Little Falls Reservoir in 1991.**

# Island Area Mississippi R. @ Little Falls

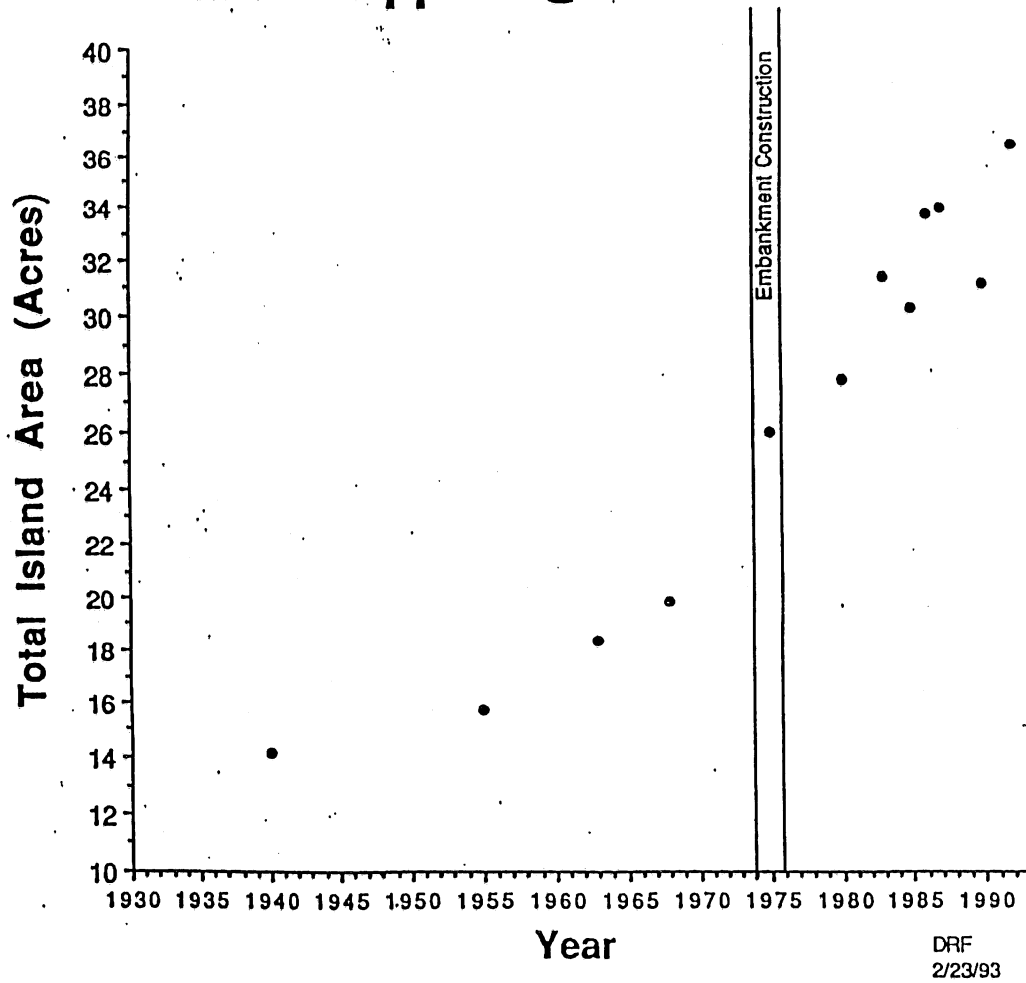


**Figure 7** Plot of island area in the Little Falls Reservoir versus years (from MN DNR Investigation).

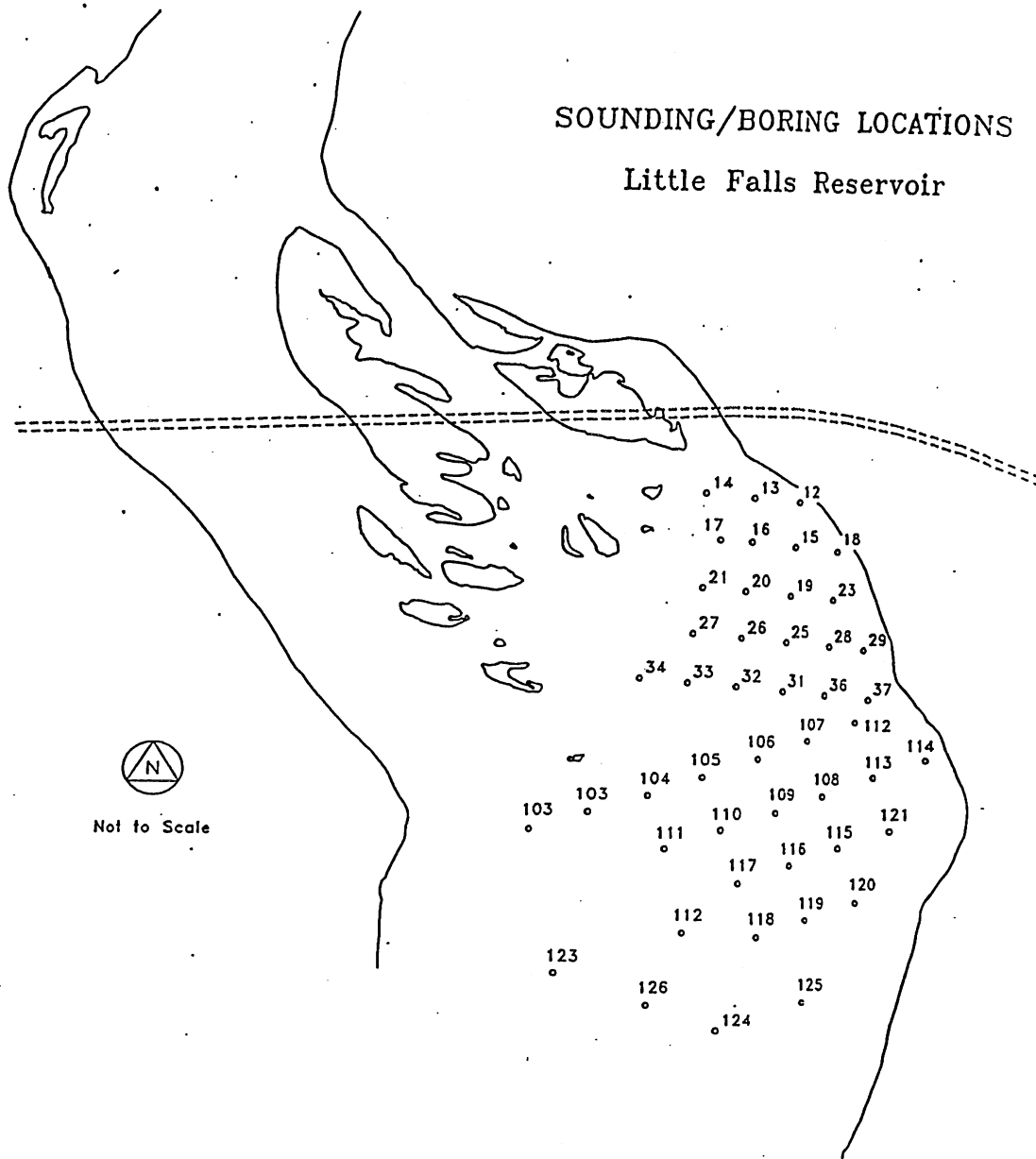


**Figure 8** Location of sounding/boring holes in Little Falls Reservoir (from MN DNR Investigation).

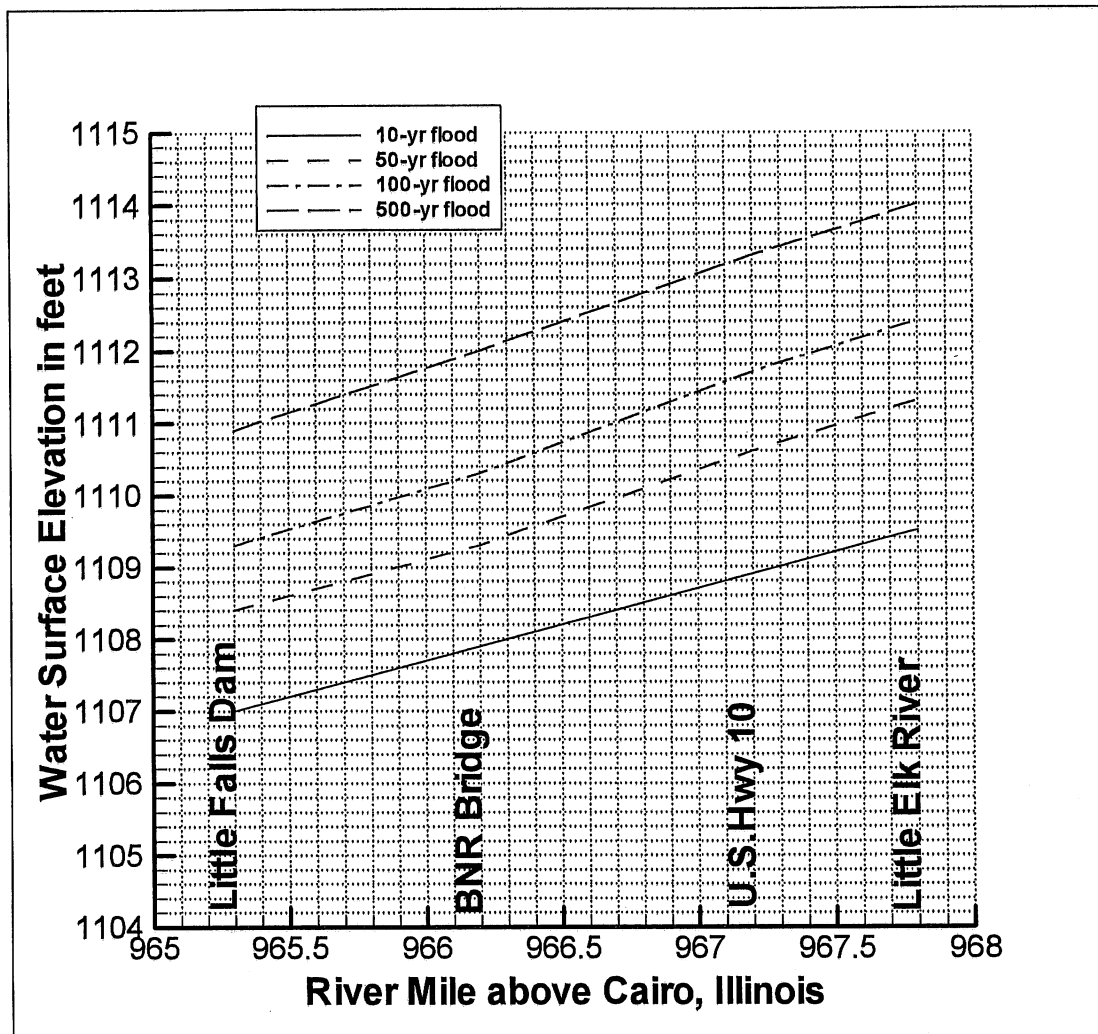


**Figure 9** Water surface profiles in the Little Falls Reservoir (from U.S. Army Corps of Engineers).

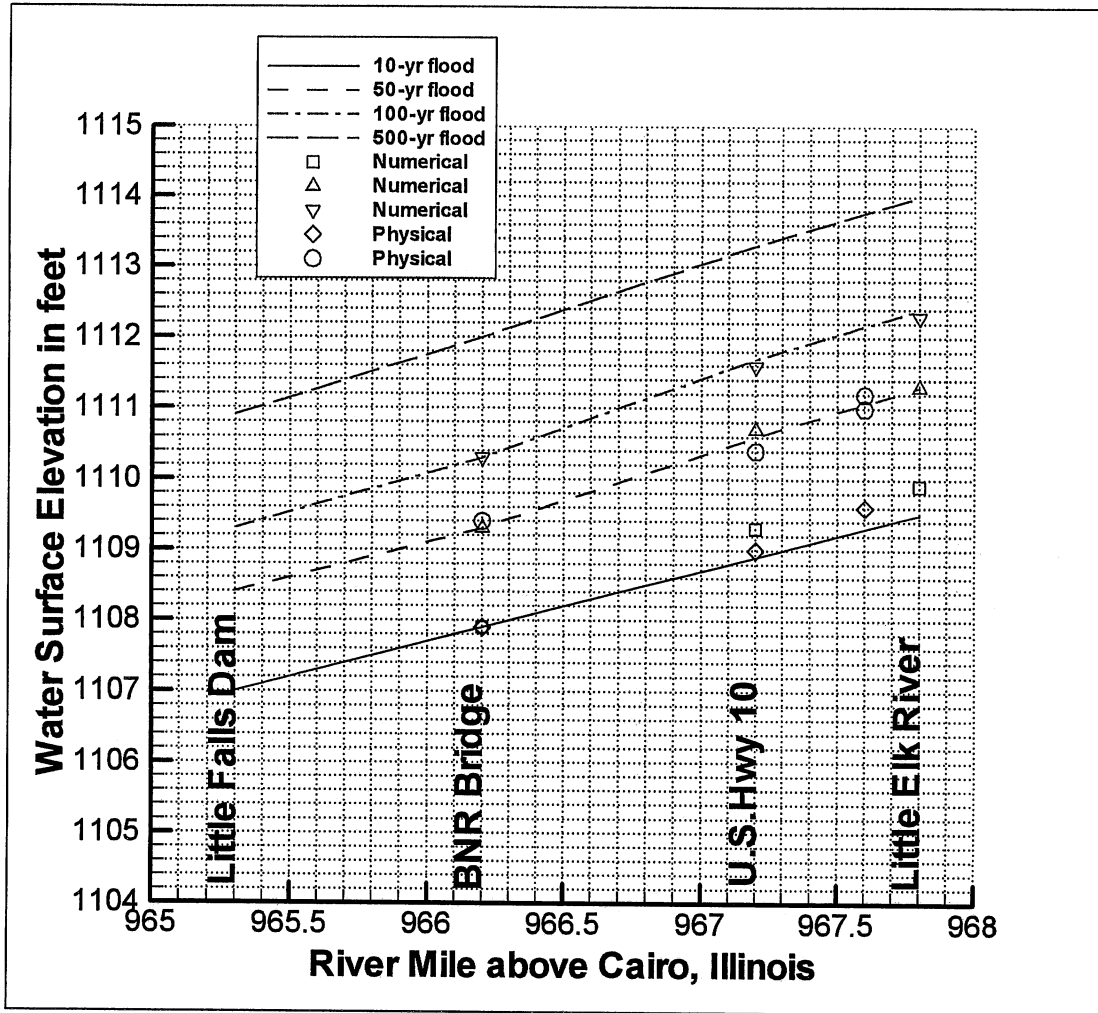


**Figure 10** Physical and numerical model calibration results compared to expected water surface profiles.



**Figure 11** Numerical model Manning's n values.

Water Surface Elevations for 25850 cfs

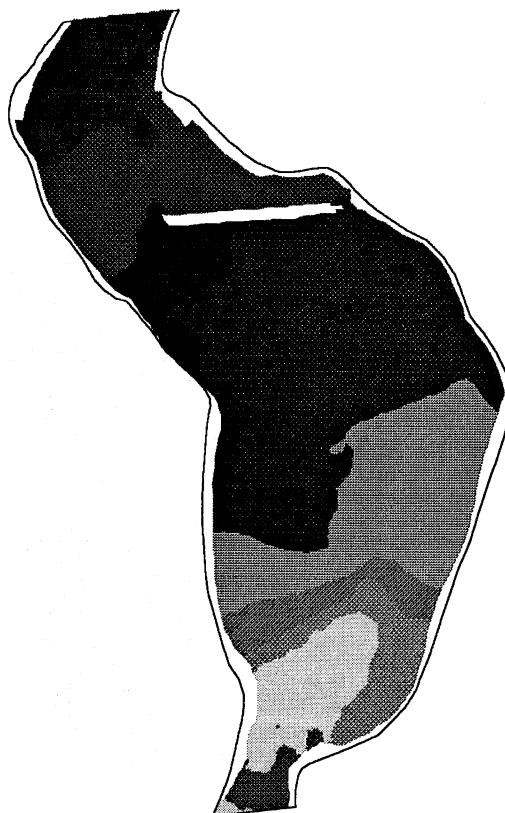
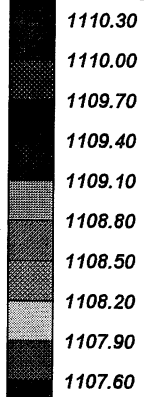


**Figure 12** Example of water surface elevation contour plot for a flow of 25,850 cfs.

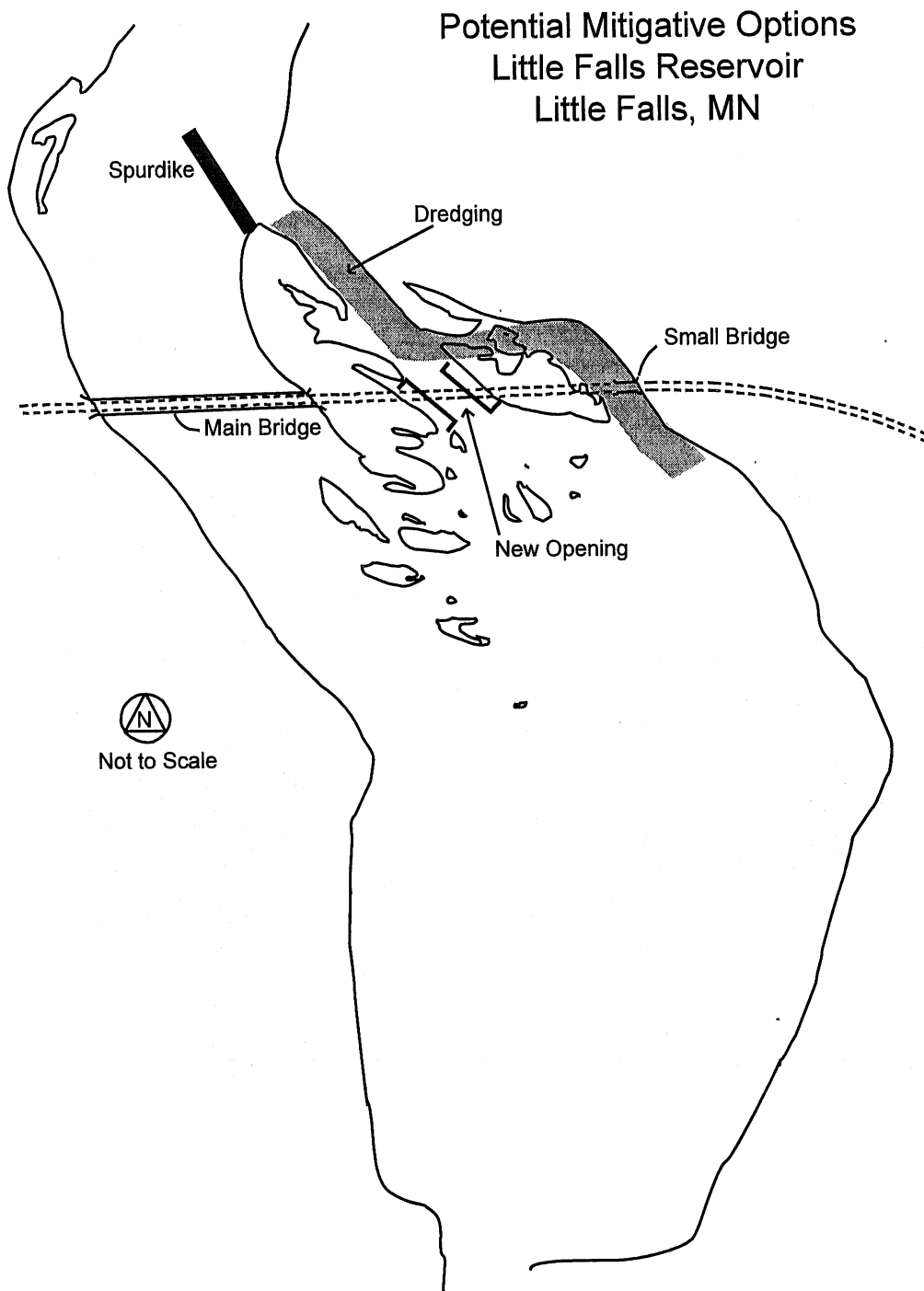


**Figure 13** Schematic showing potential mitigative options.

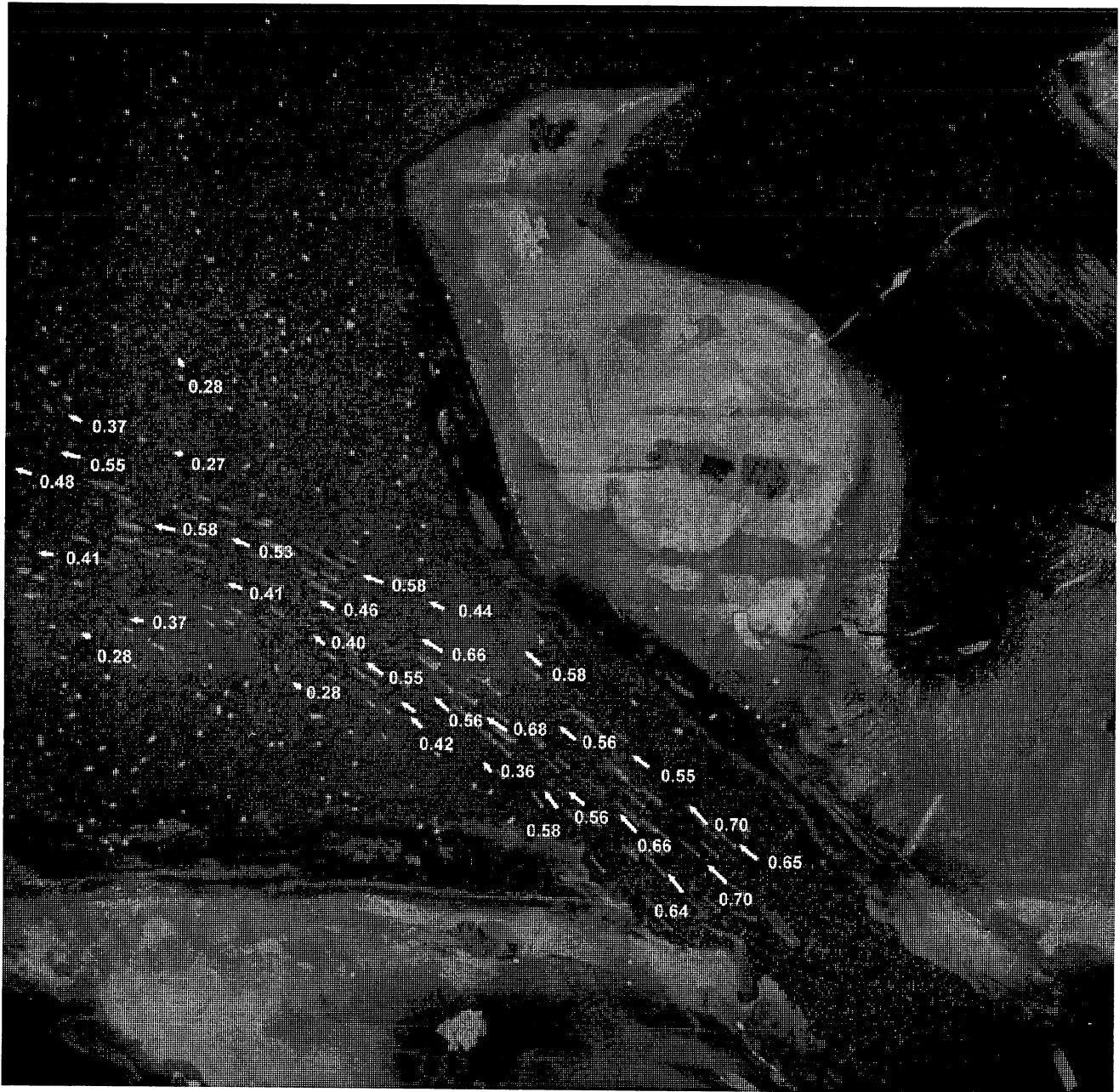


**Figure 14** Surface flow velocities exiting east channel opening for a flow of 5285 cfs with no embankment.

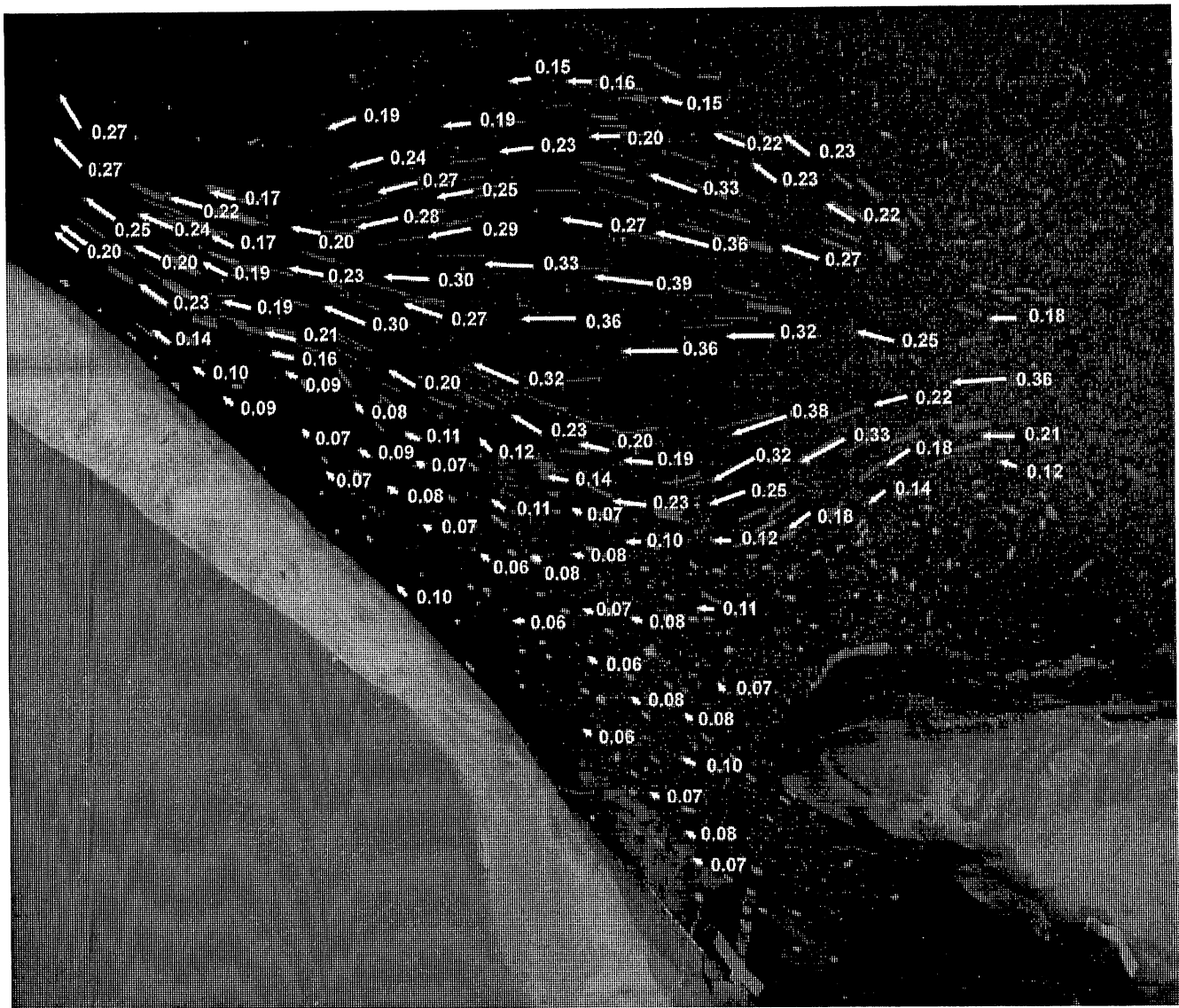


**Figure 15** Surface flow velocities along east shoreline for a flow of 5285 cfs with no embankment.

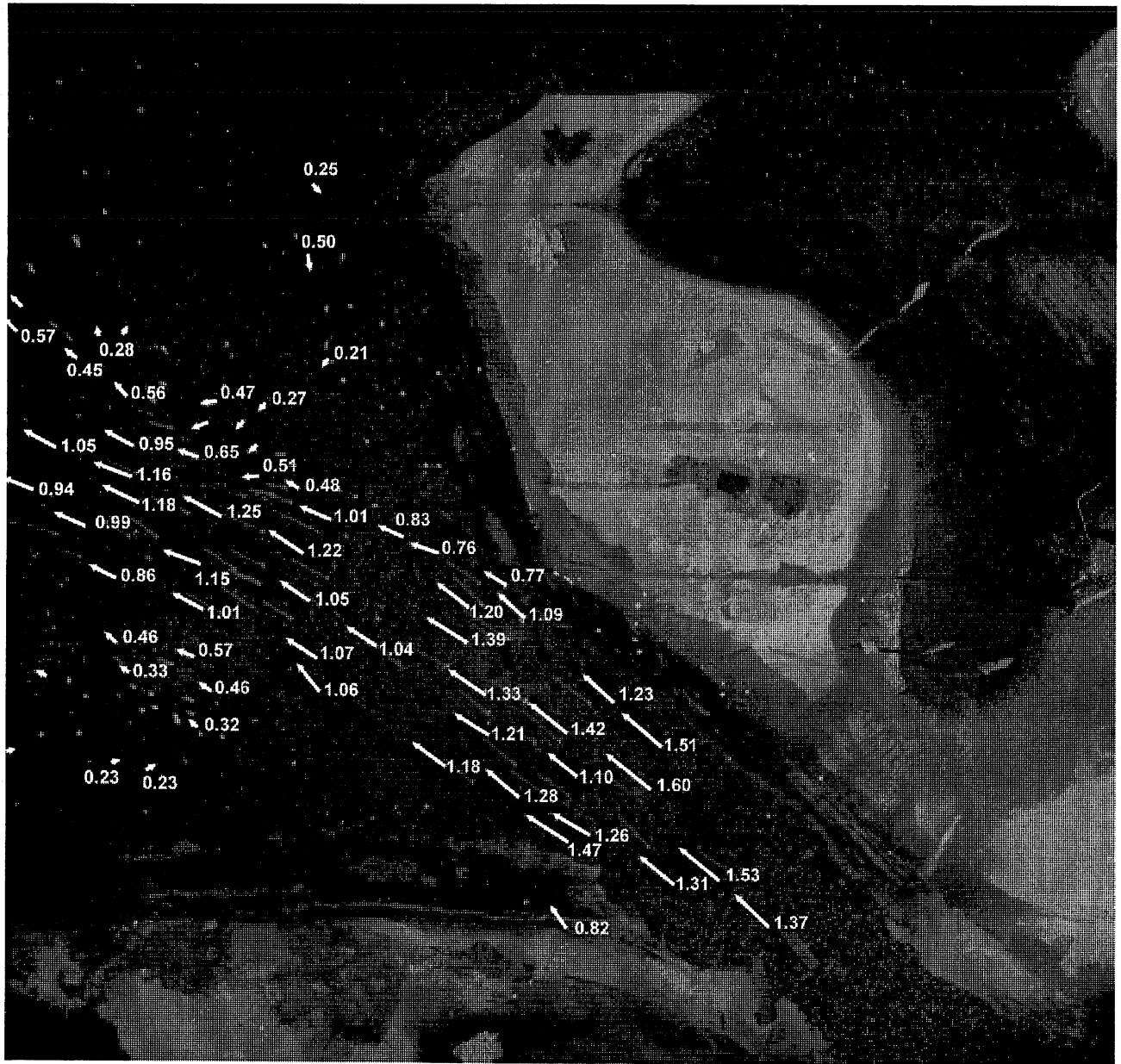


**Figure 16** Surface flow velocities exiting east channel opening for a flow of 10,200 cfs with no embankment.



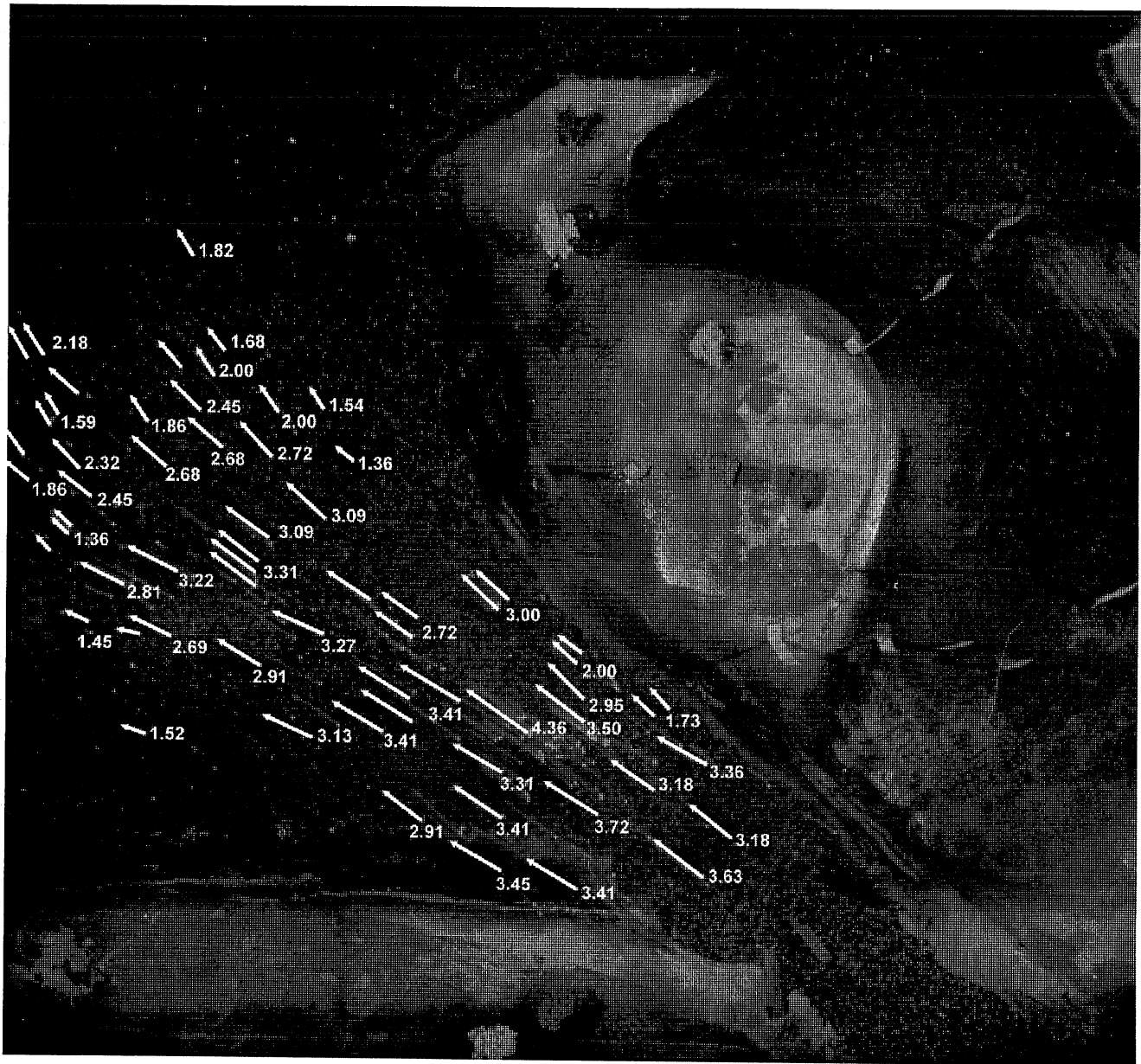


**Figure 18** Surface flow velocities exiting east channel opening for a flow of 25,850 cfs with no embankment.

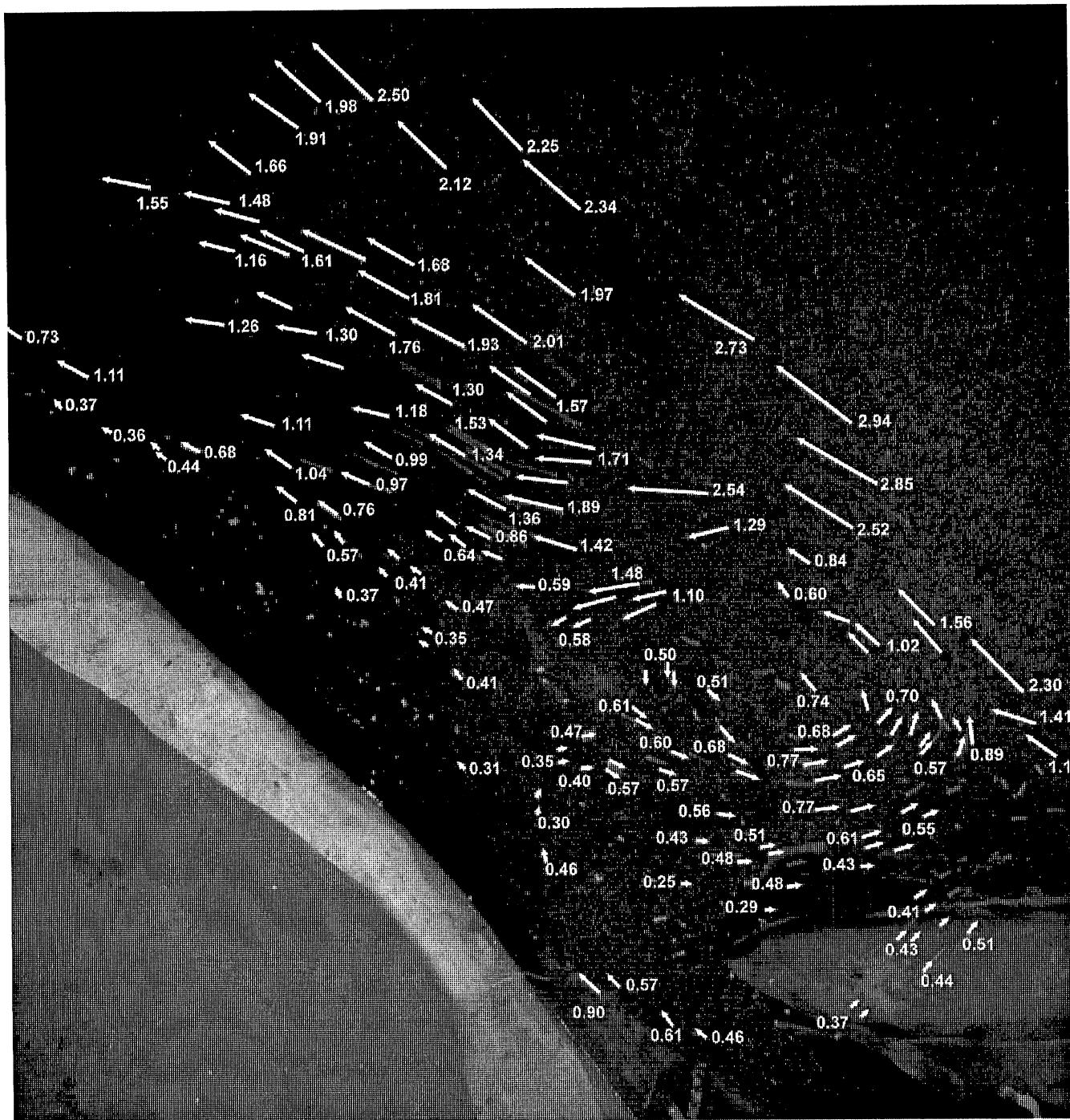


**Figure 19** Surface flow velocities along east shoreline for a flow of 25,850 cfs with no embankment.

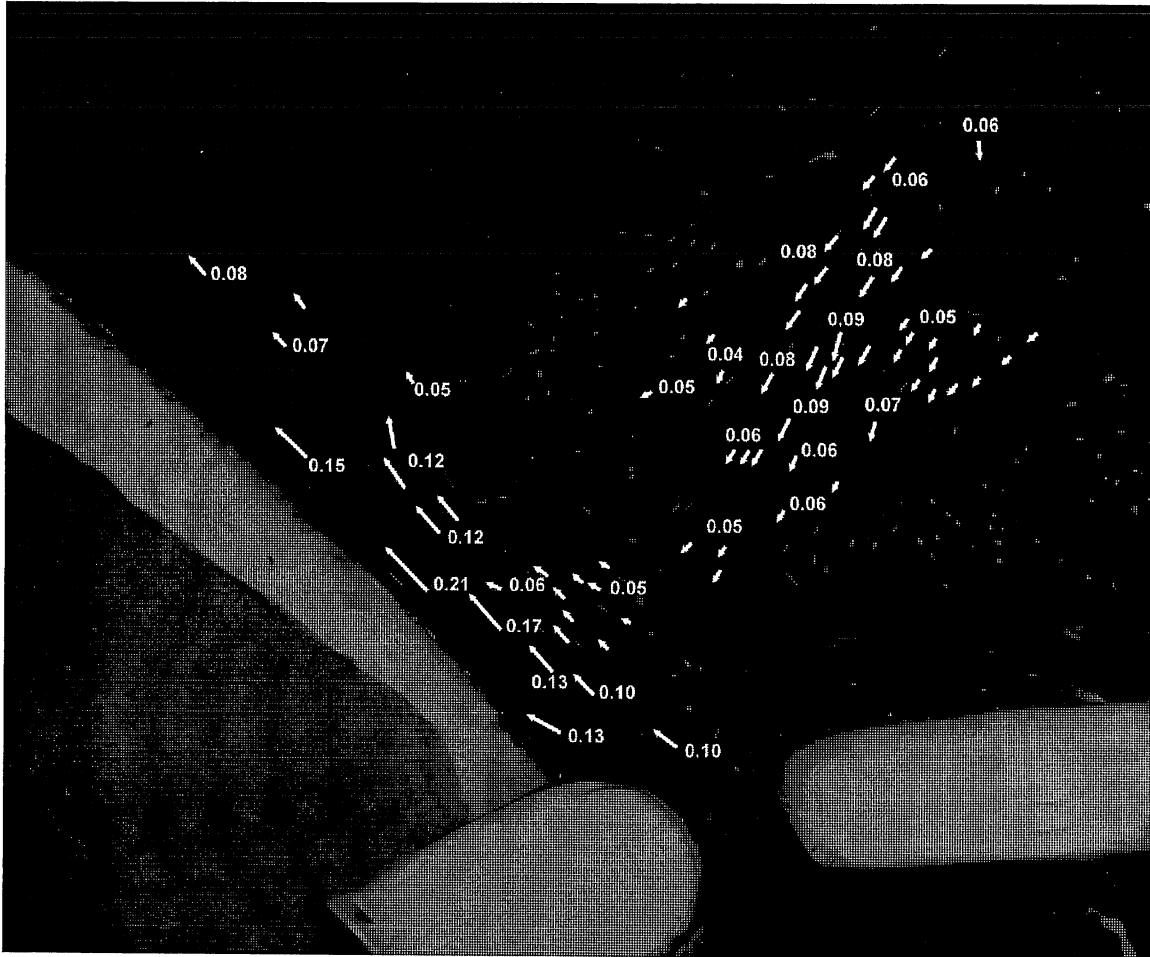


**Figure 20** Surface flow velocities along the east shoreline for a flow of 5285 cfs with the embankment in place.

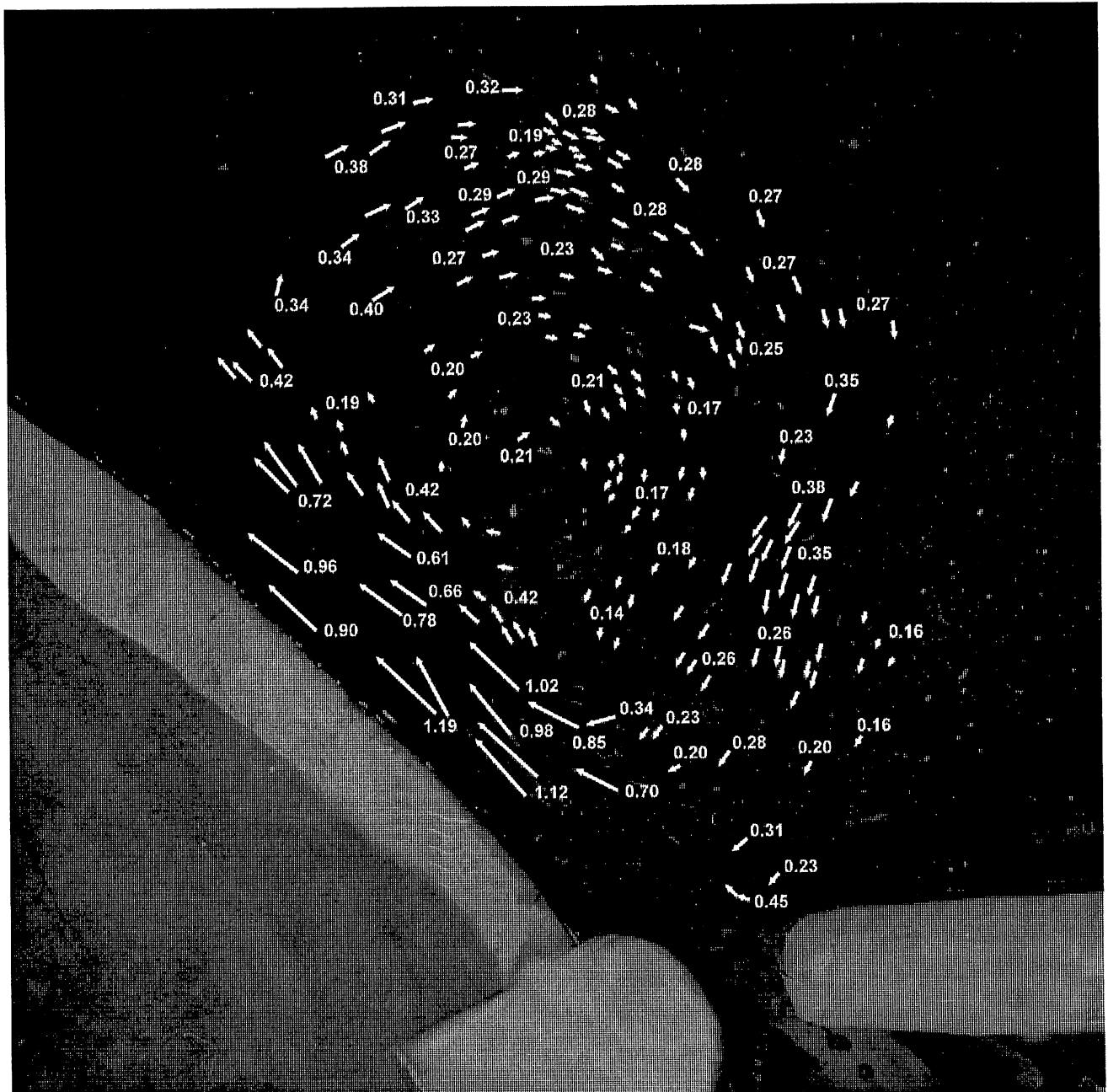


**Figure 21** Surface flow velocities along the east shoreline for a flow of 10,200 cfs with the embankment in place.



**Figure 22** Surface flow velocities along the east shoreline for a flow of 25,850 cfs with the embankment in place.

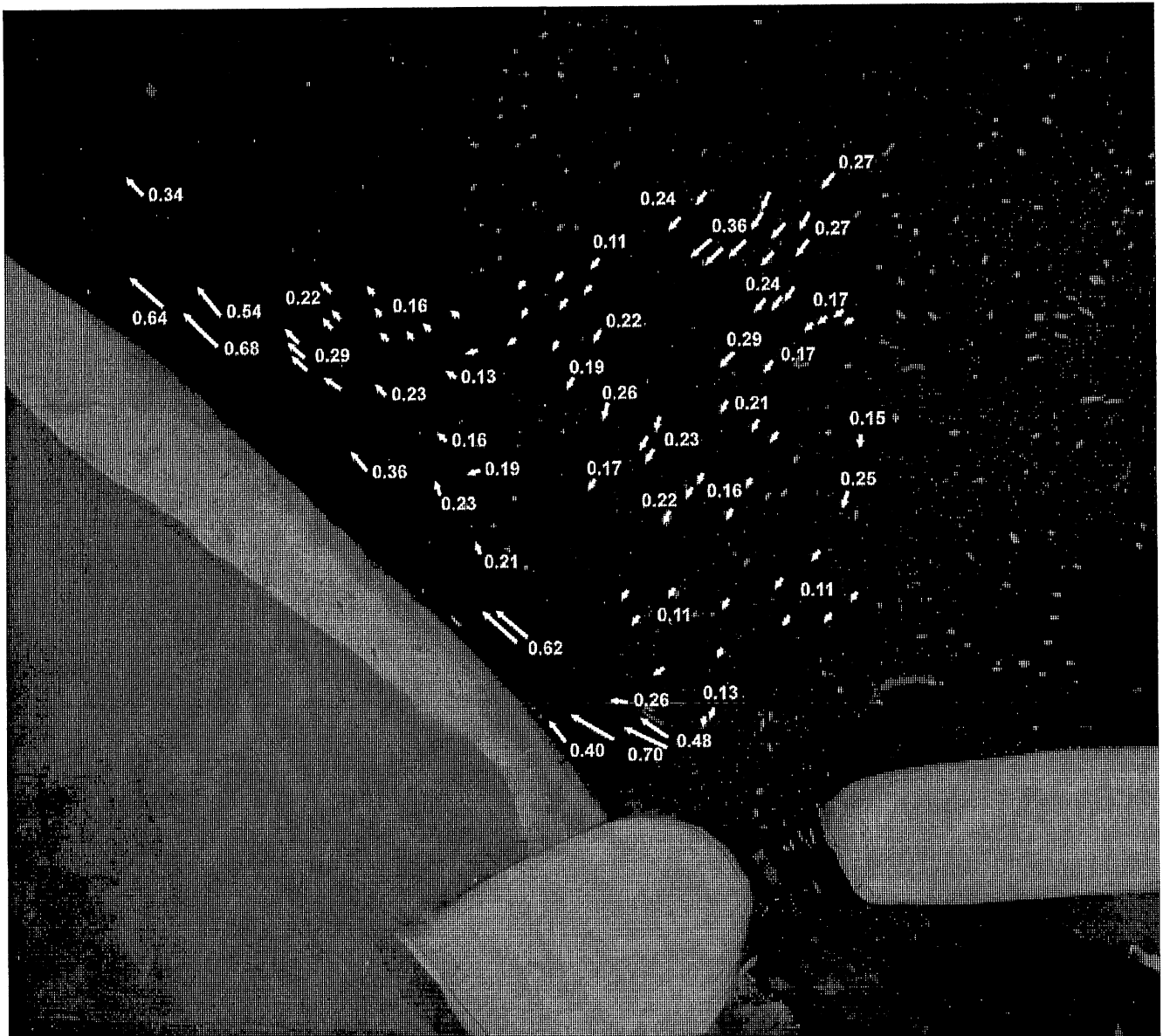


**Figure 23** Surface flow velocities along the east shoreline for a flow of 5285 cfs with spur dike in place.

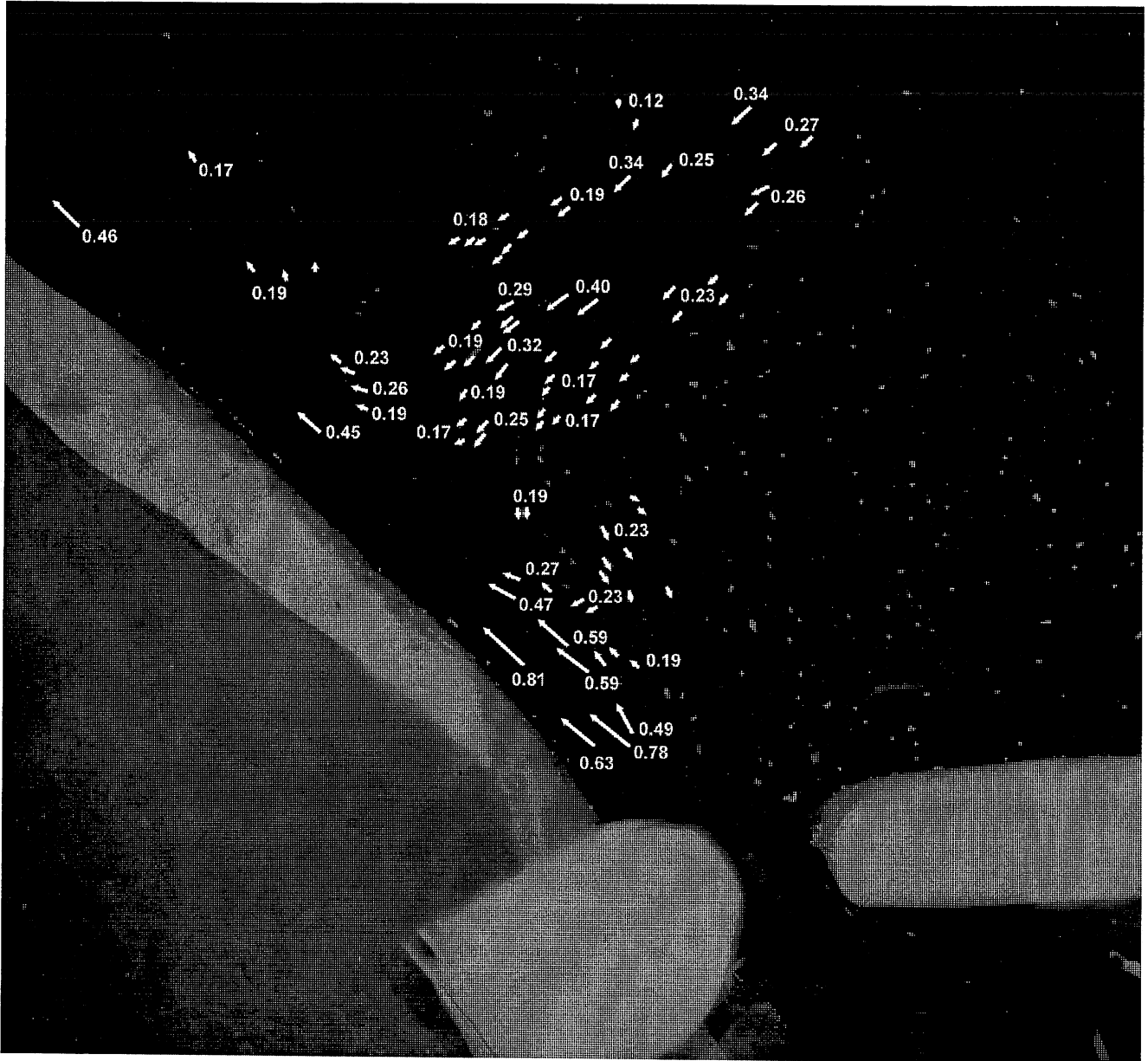


**Figure 24** Surface flow velocities along the east shoreline for a flow of 10,200 cfs with spurdiak in place.



**Figure 25** Surface flow velocities along the east shoreline for a flow of 25,850 cfs with spurdike in place.

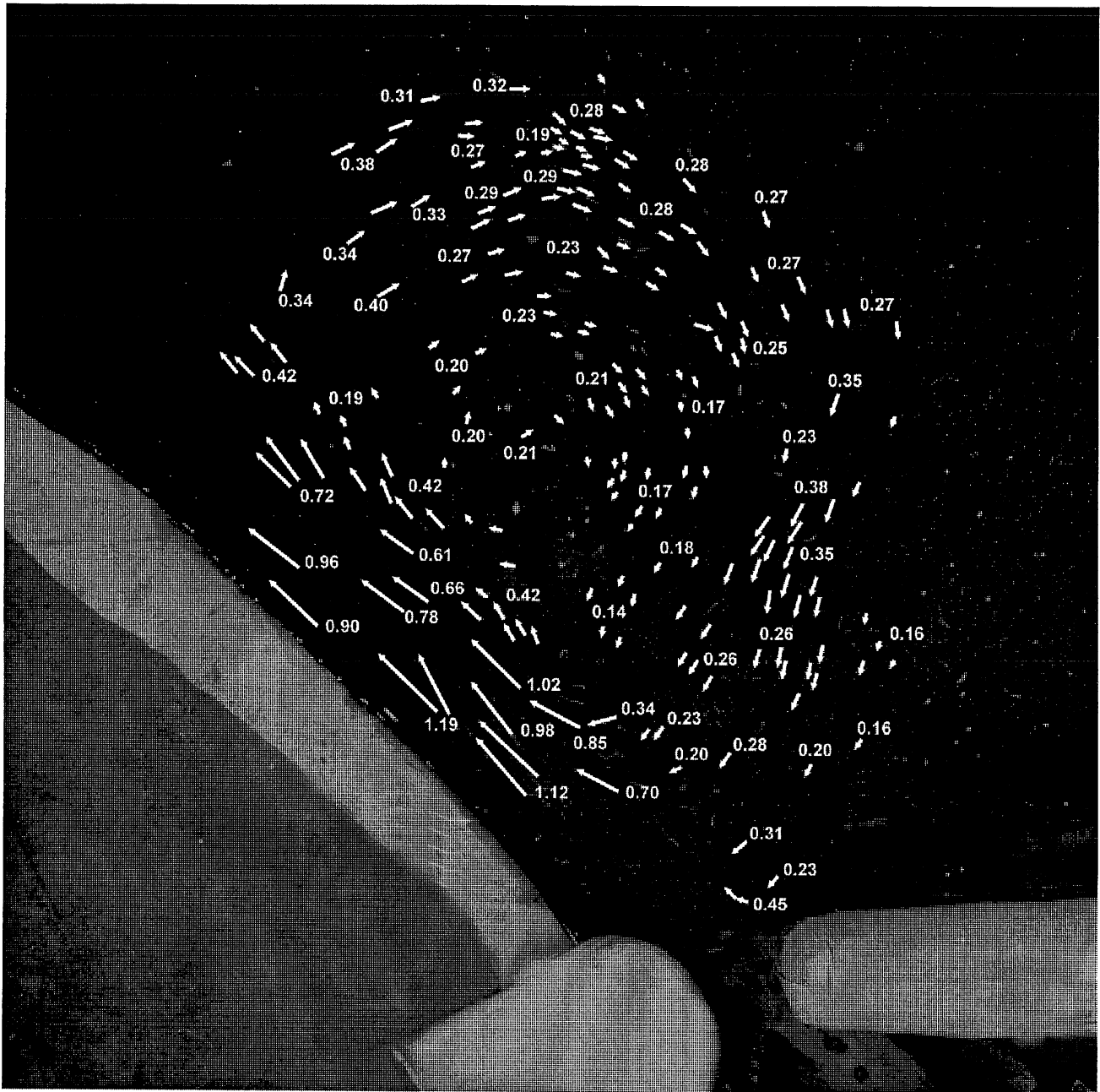


**Figure 26** Surface flow velocities along the east shoreline for a flow of 10,200 cfs with dredging of east channel.

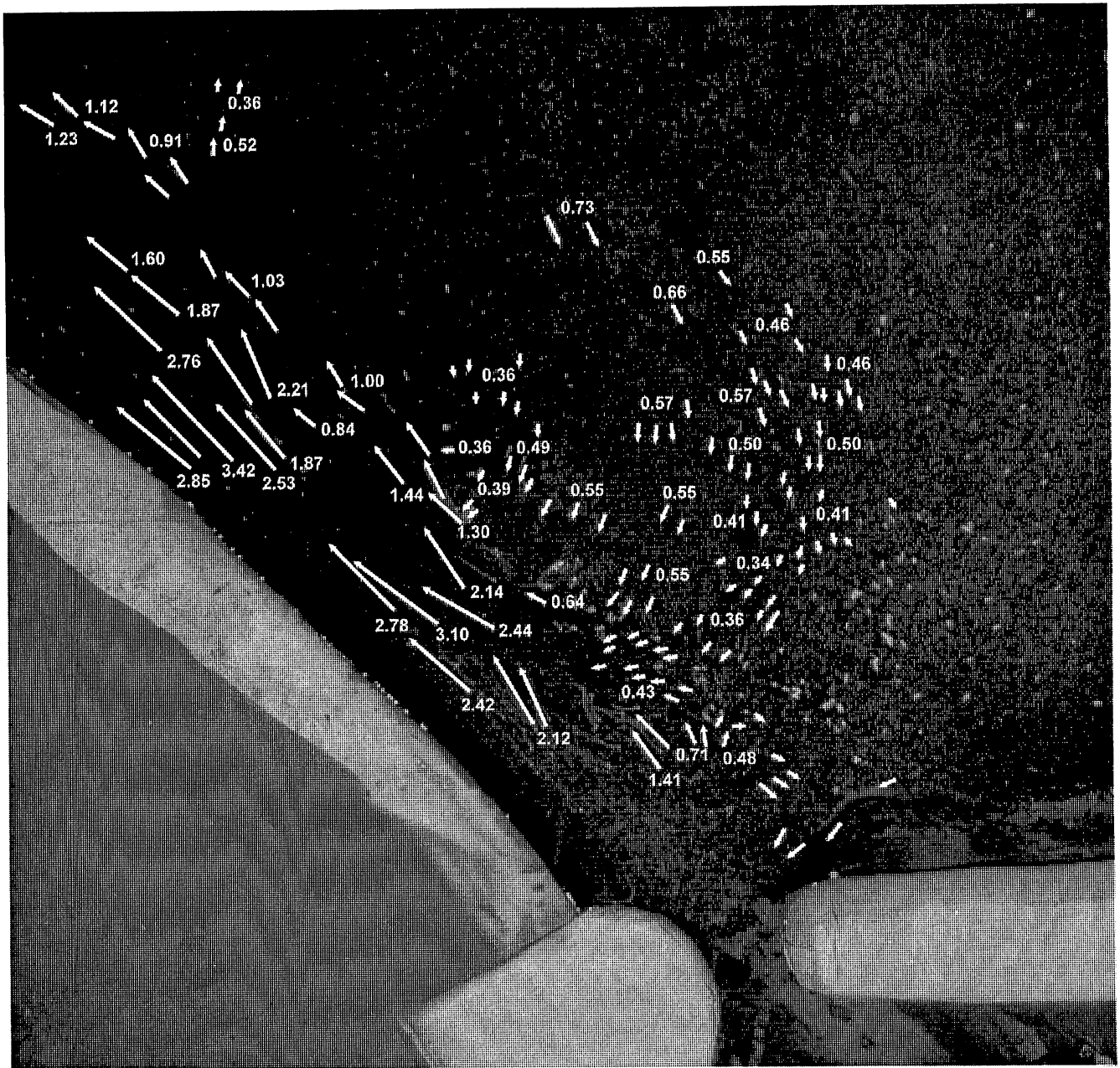


**Figure 27** Surface flow velocities along the east shoreline for a flow of 25,850 cfs with dredging of east channel.

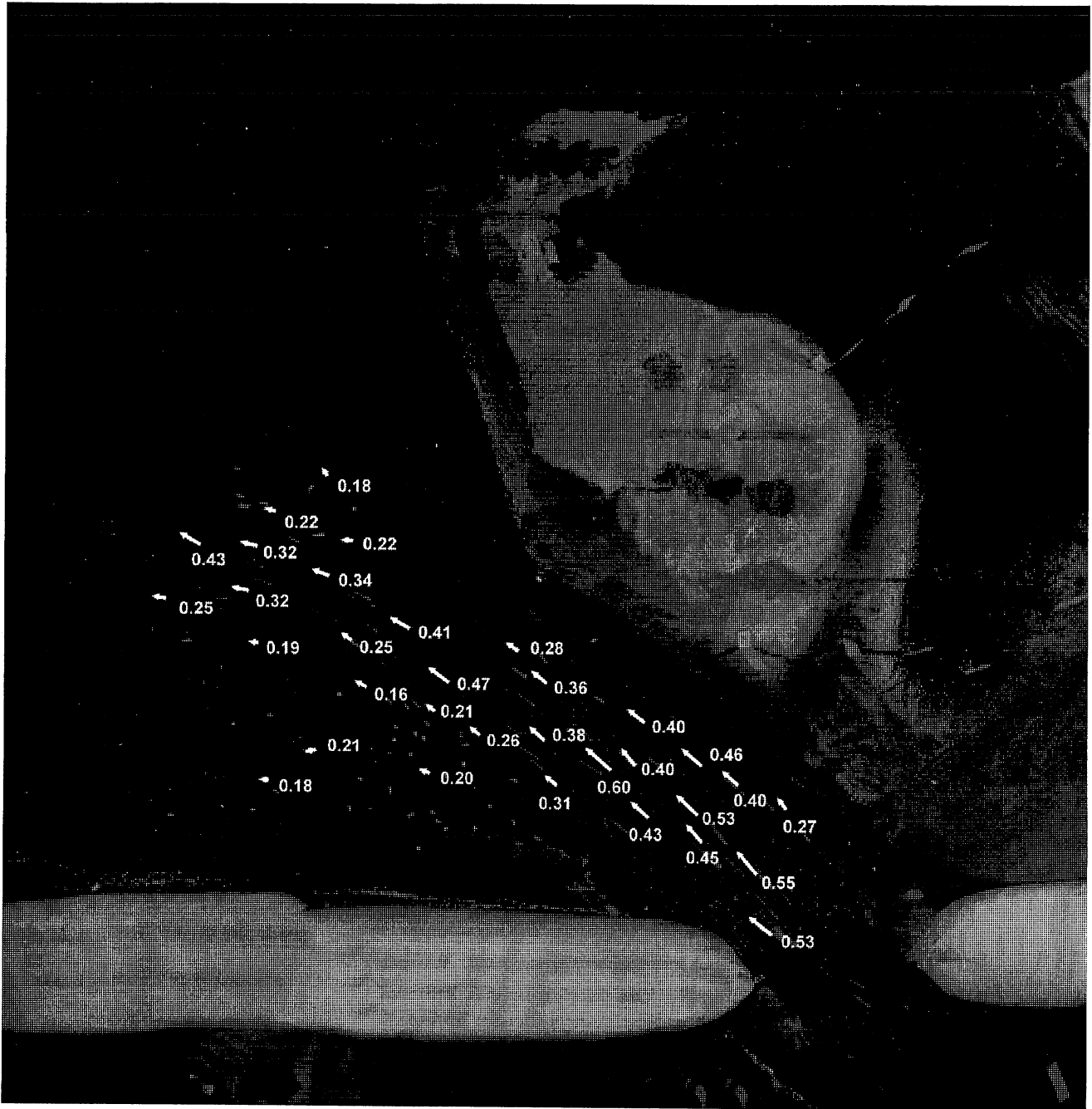


**Figure 28** Surface flow velocities exiting new opening in embankment for a flow of 5285 cfs.

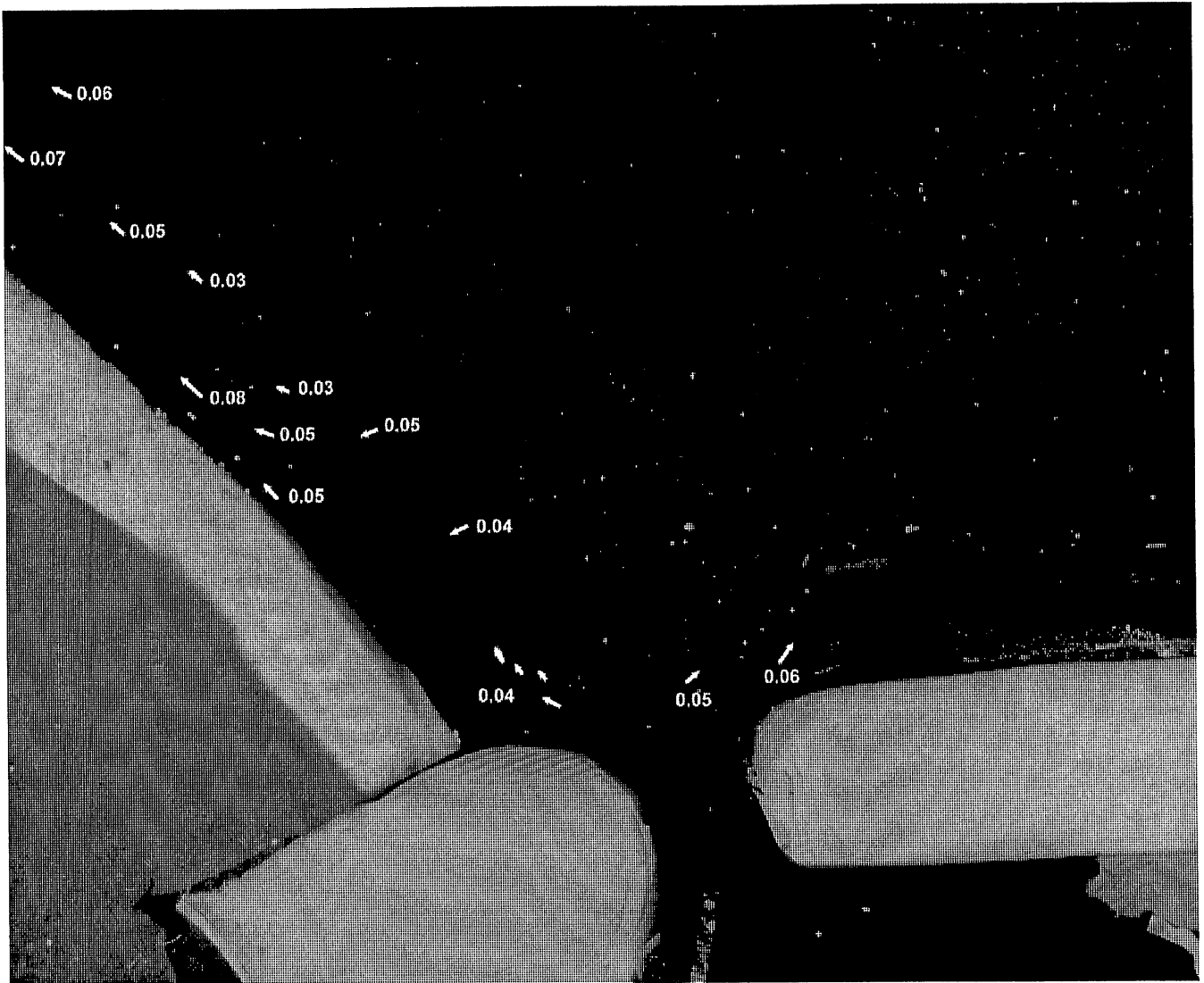


**Figure 29** Surface flow velocities along east shoreline for a flow of 5285 cfs with a new opening in the embankment.

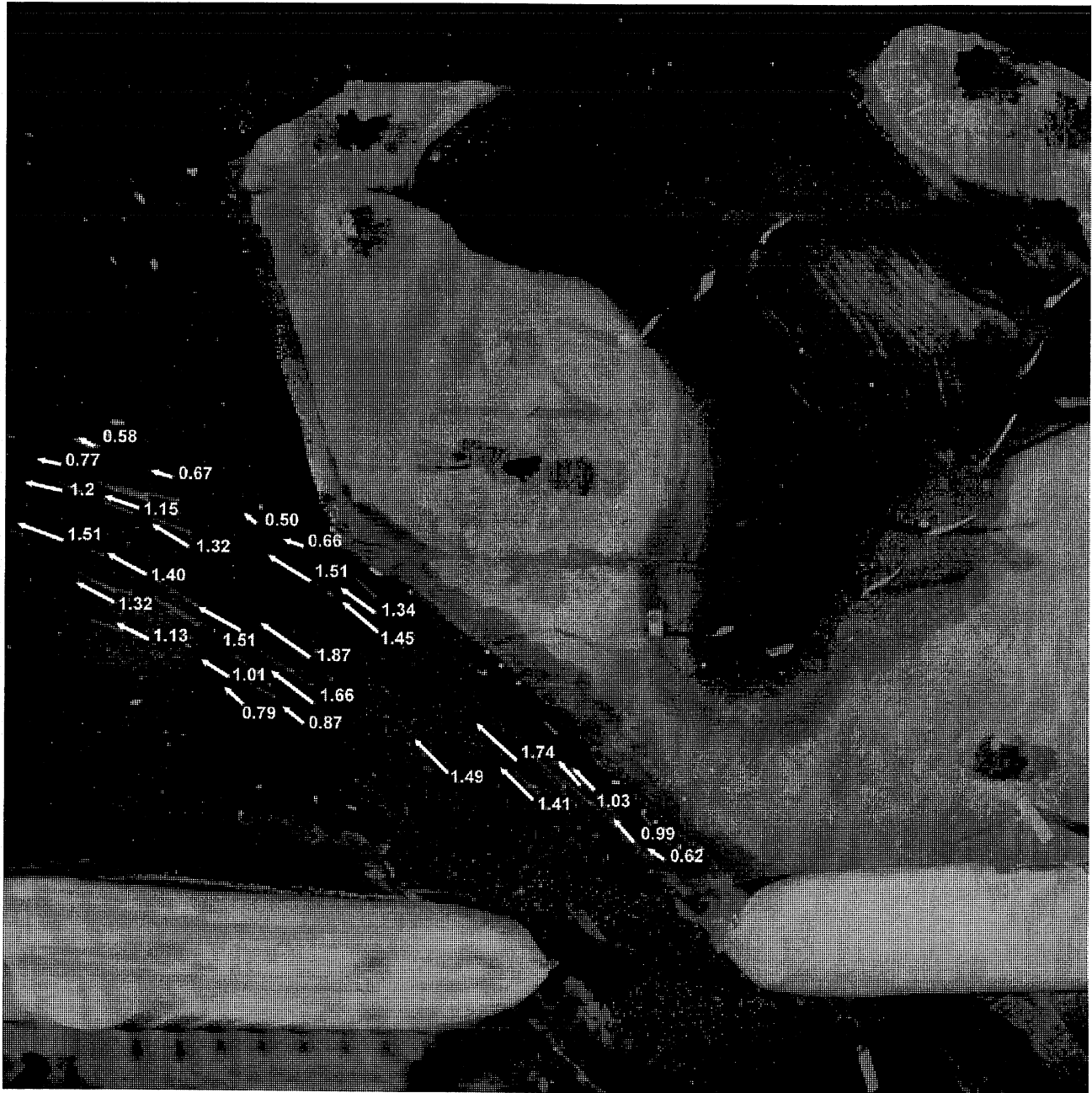


**Figure 30** Surface flow velocities exiting new opening in the embankment for a flow of 10,200 cfs.

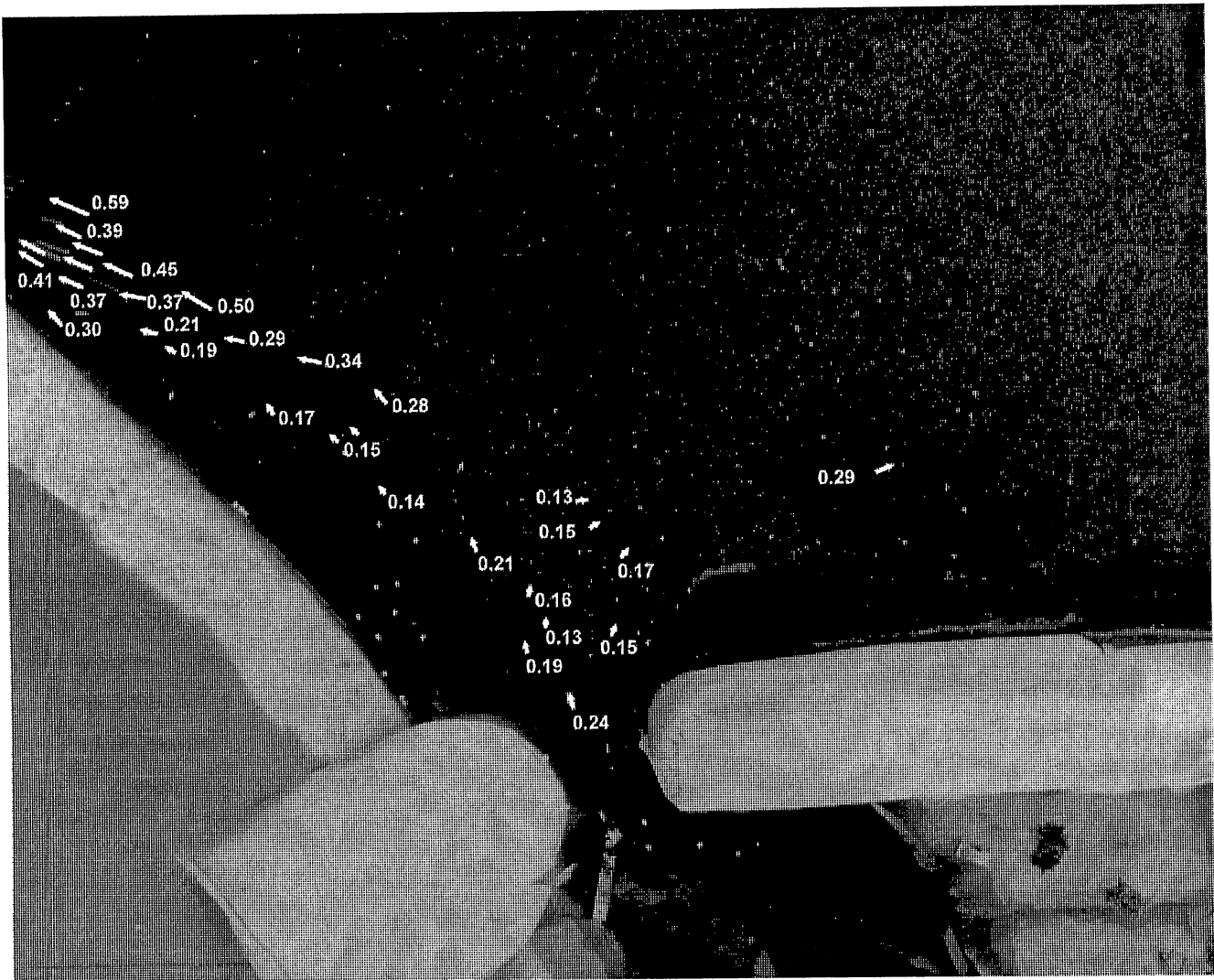


**Figure 31** Surface flow velocities along the east shoreline for a flow of 10,200 cfs with a new opening in the embankment.



**Figure 32** Surface flow velocities exiting the new opening in the embankment for a flow of 25,850 cfs.

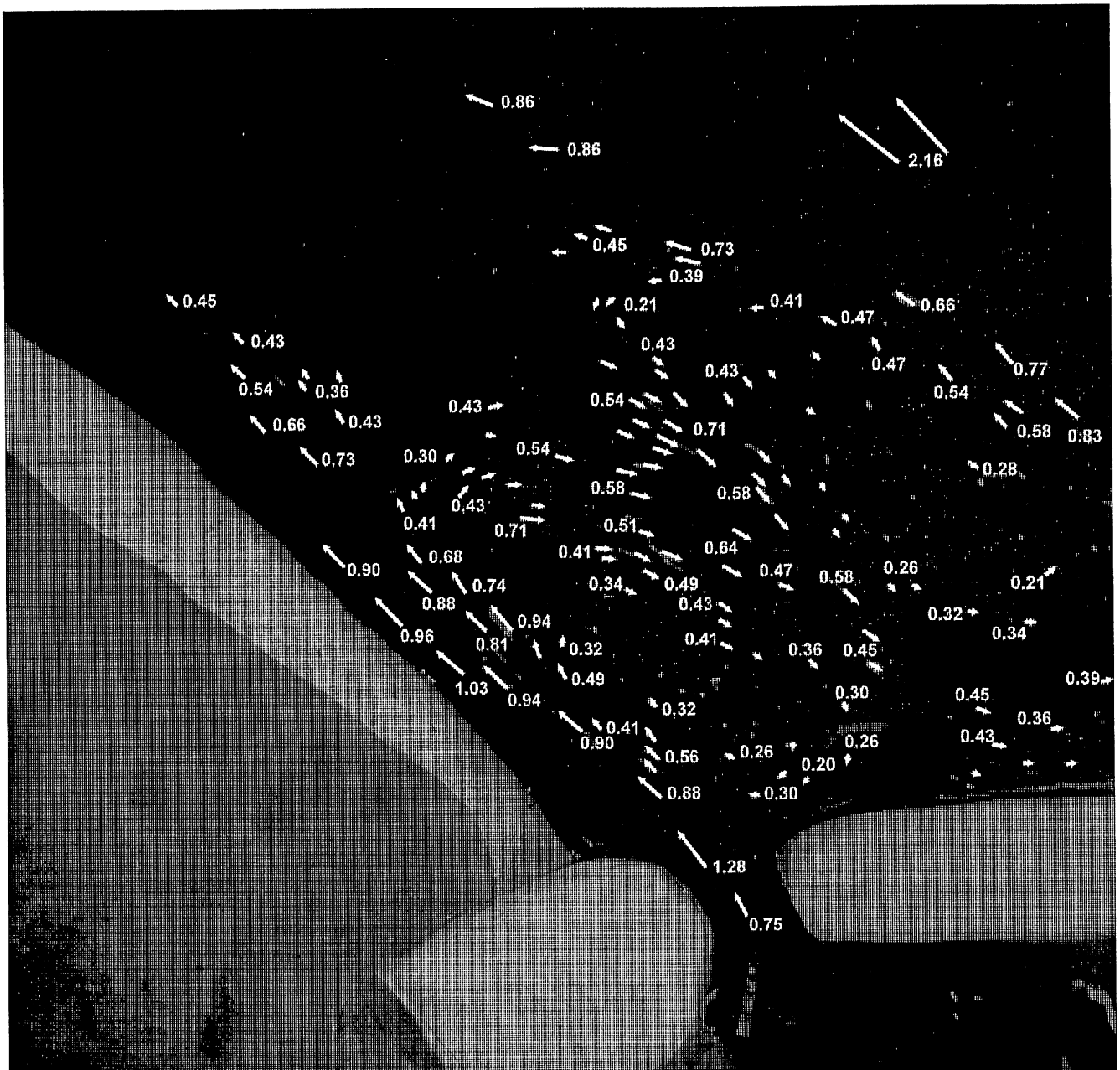


**Figure 33** Surface flow velocities along the east shoreline for a flow of 25,850 cfs with a new opening in the embankment.

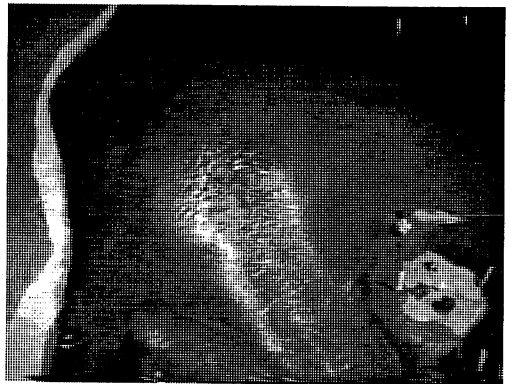
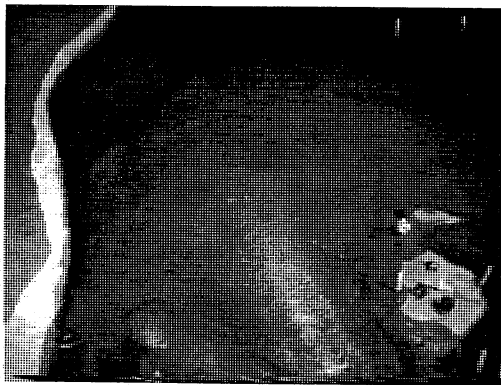
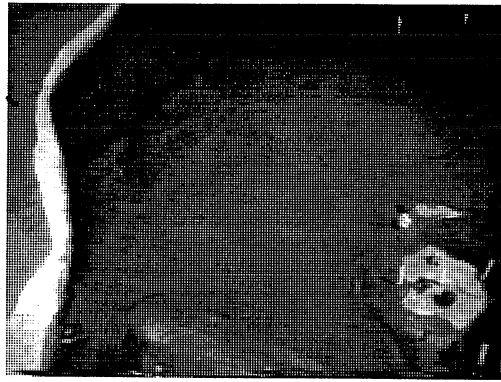


**Fig. 34: Sub-surface sediment deposition without an embankment**



**Fig. 35: Sub-surface sediment deposition with embankment structure in place.**



**Fig. 36: Sub-surface sediment deposition with new opening in embankment.**

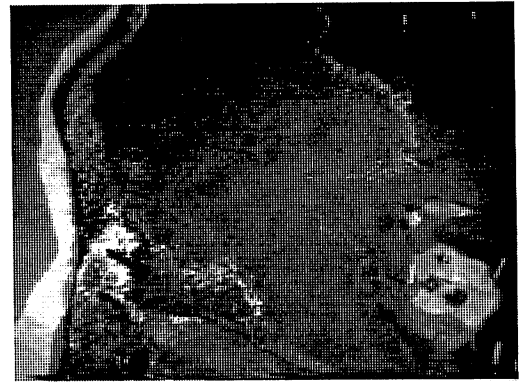
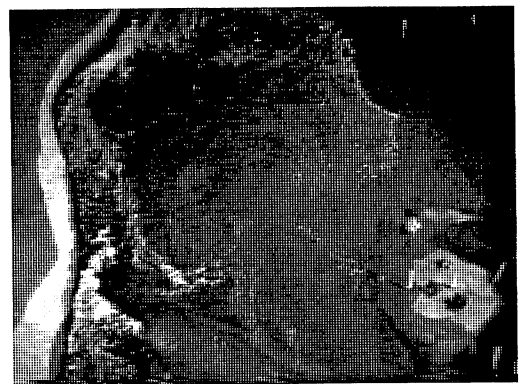
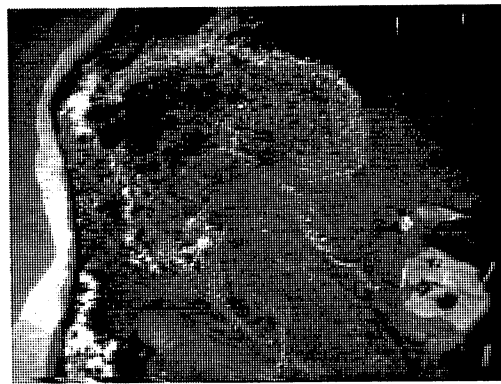


**Fig. 37: Surface flow patterns without embankment structure.**

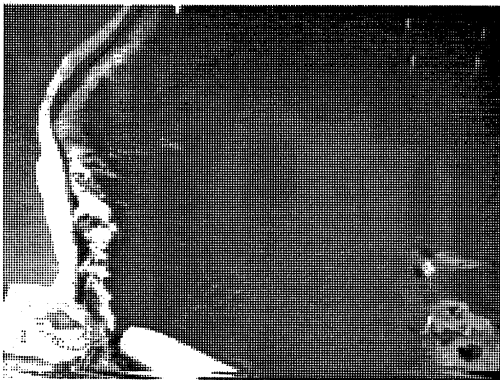
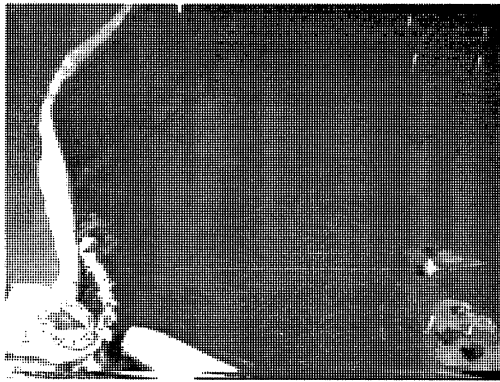


**Fig. 38: Surface flow patterns with embankment structure.**

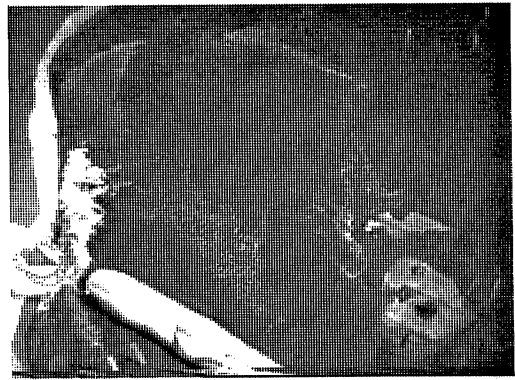
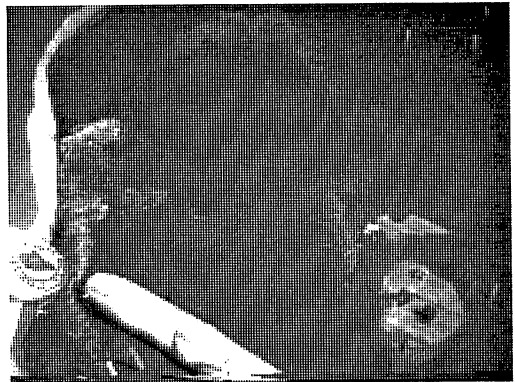
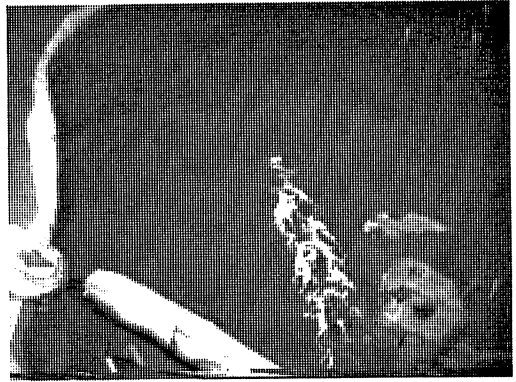


**Fig. 39: Surface flow patterns with new opening in embankment structure.**

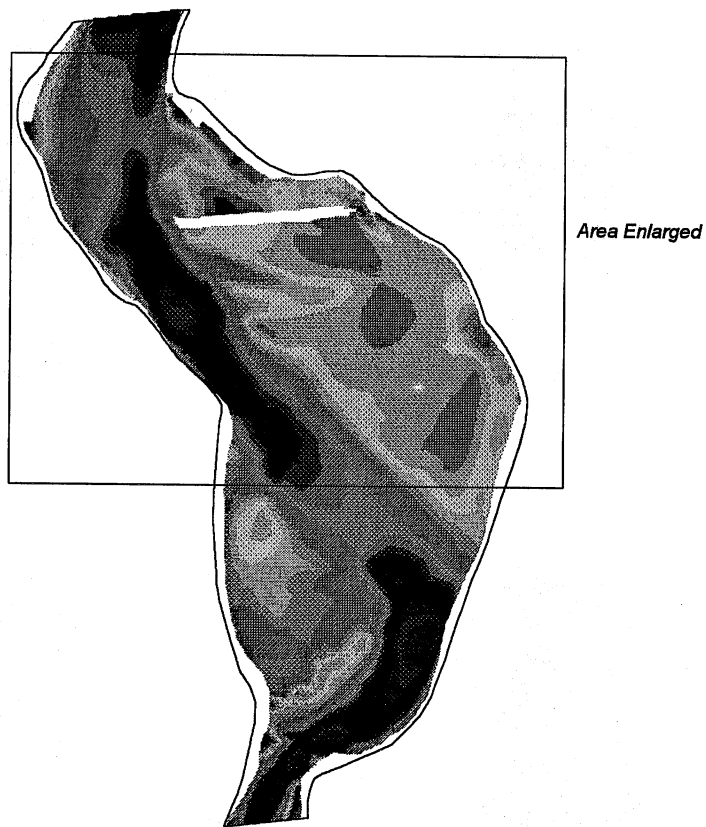
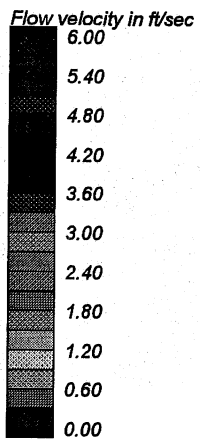


**Figure 40** Velocity contour plot of entire reservoir showing area enlarged in velocity contour plots.



**Figure 41** Velocity contours for a flow of 5285 cfs without the embankment.

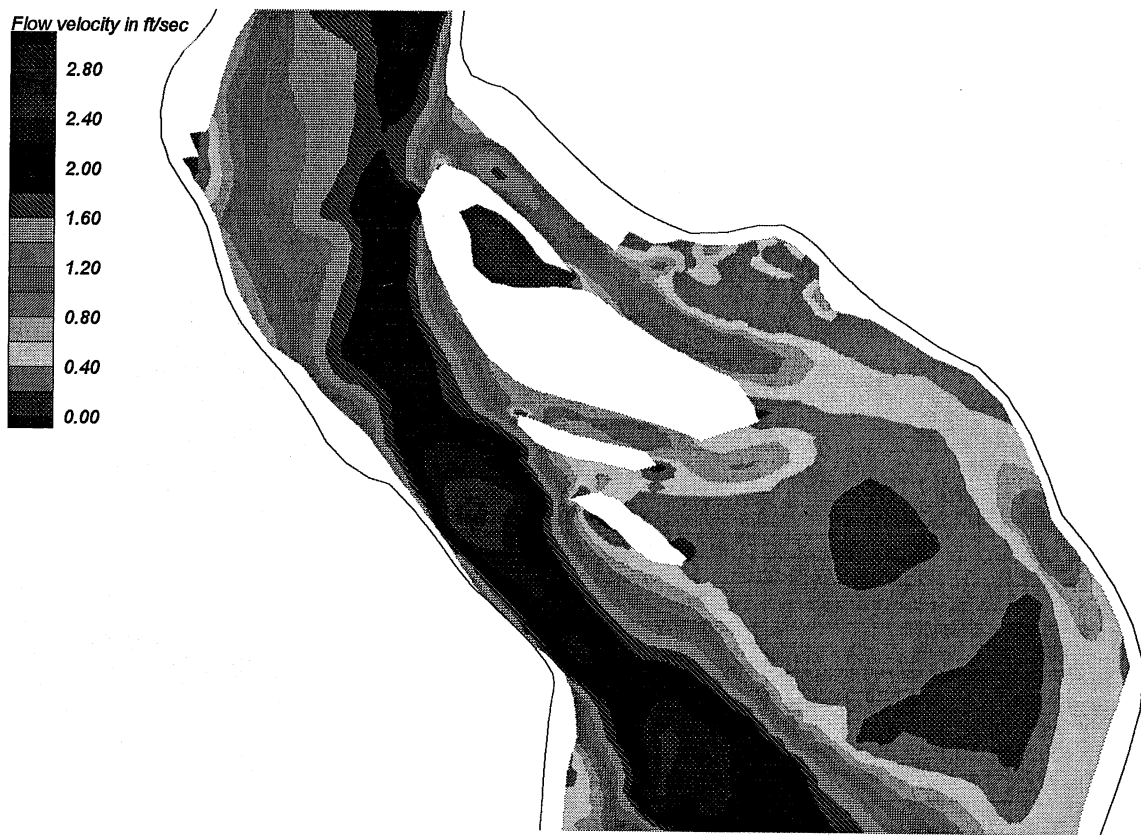


**Figure 42** Velocity contours for a flow of 10,200 cfs without the embankment.

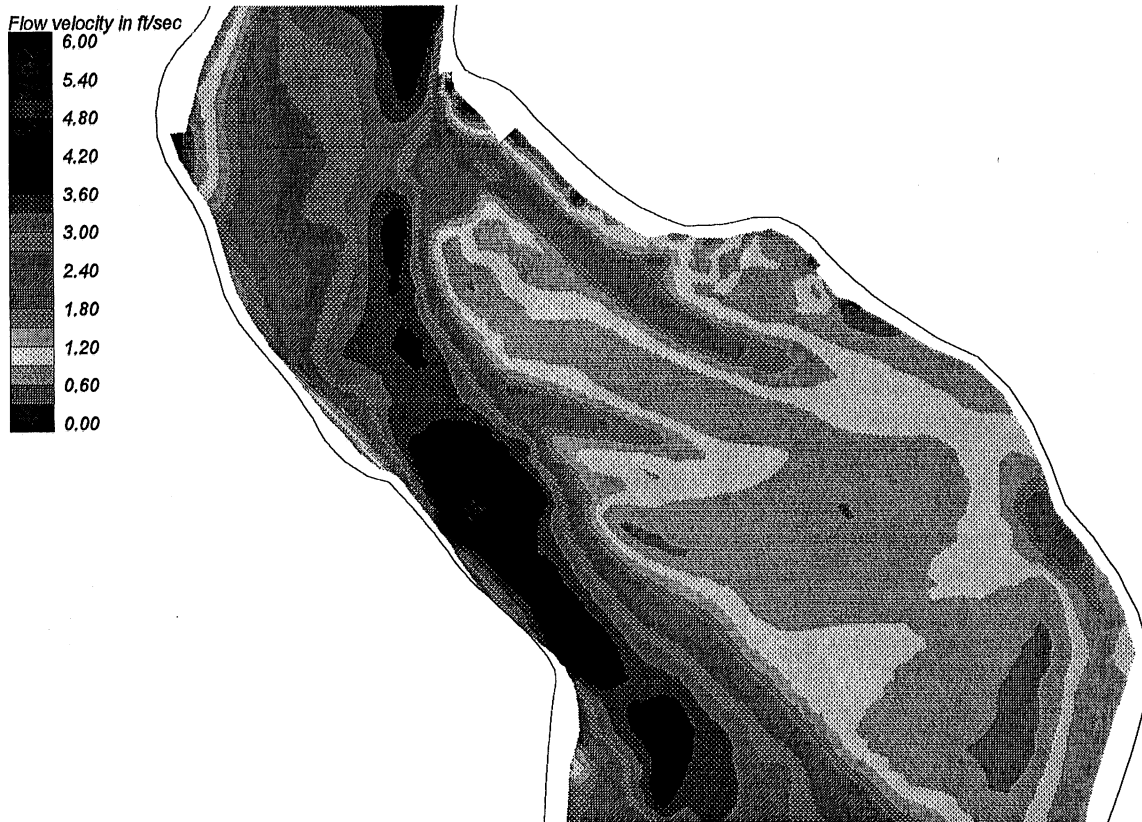


**Figure 43** Velocity contours for a flow of 25,850 cfs without the embankment.

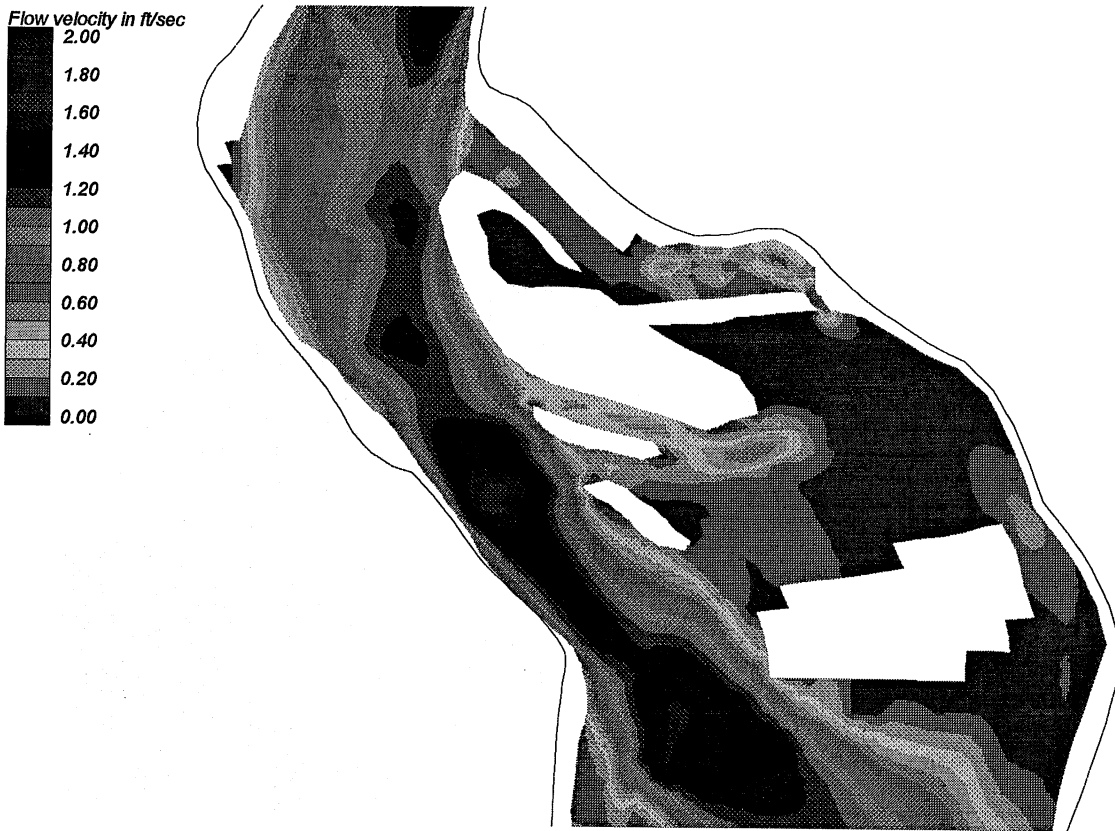


**Figure 44** Velocity contours for a flow of 5285 cfs with the embankment.



**Figure 45** Velocity contours for a flow of 10,200 cfs with the embankment.

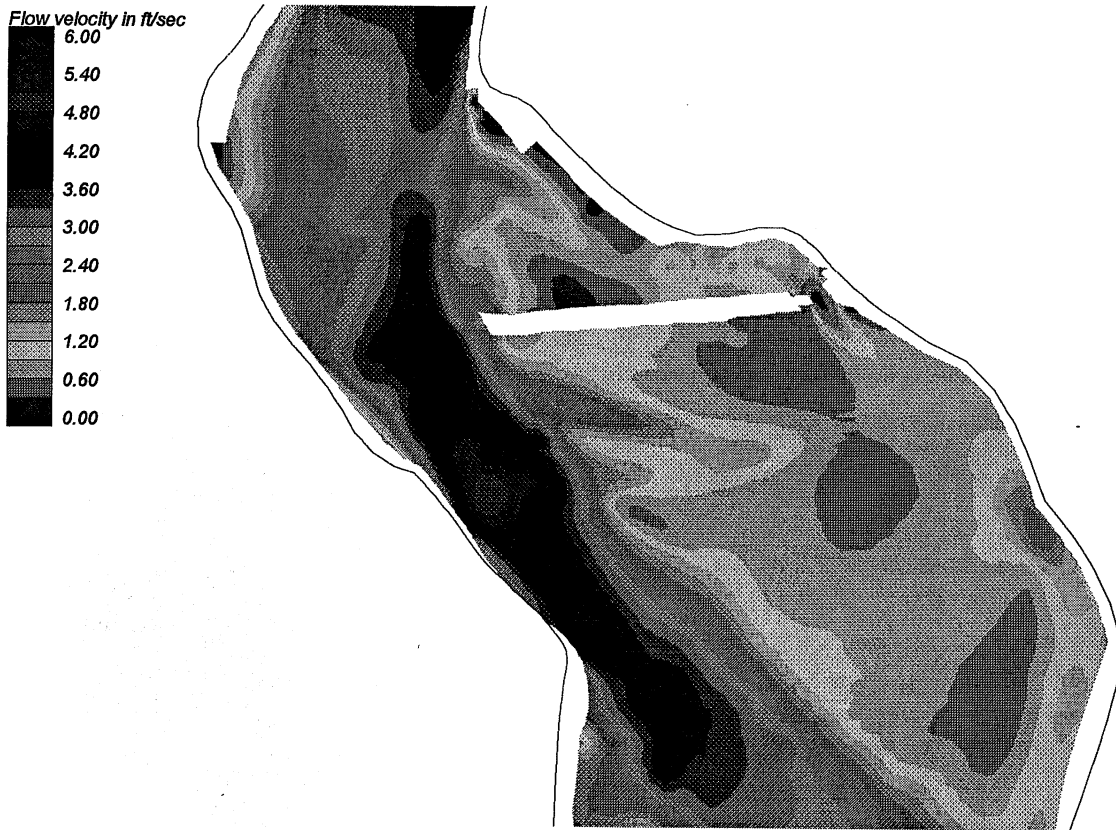


**Figure 46** Velocity contours for a flow of 25,850 cfs with the embankment.

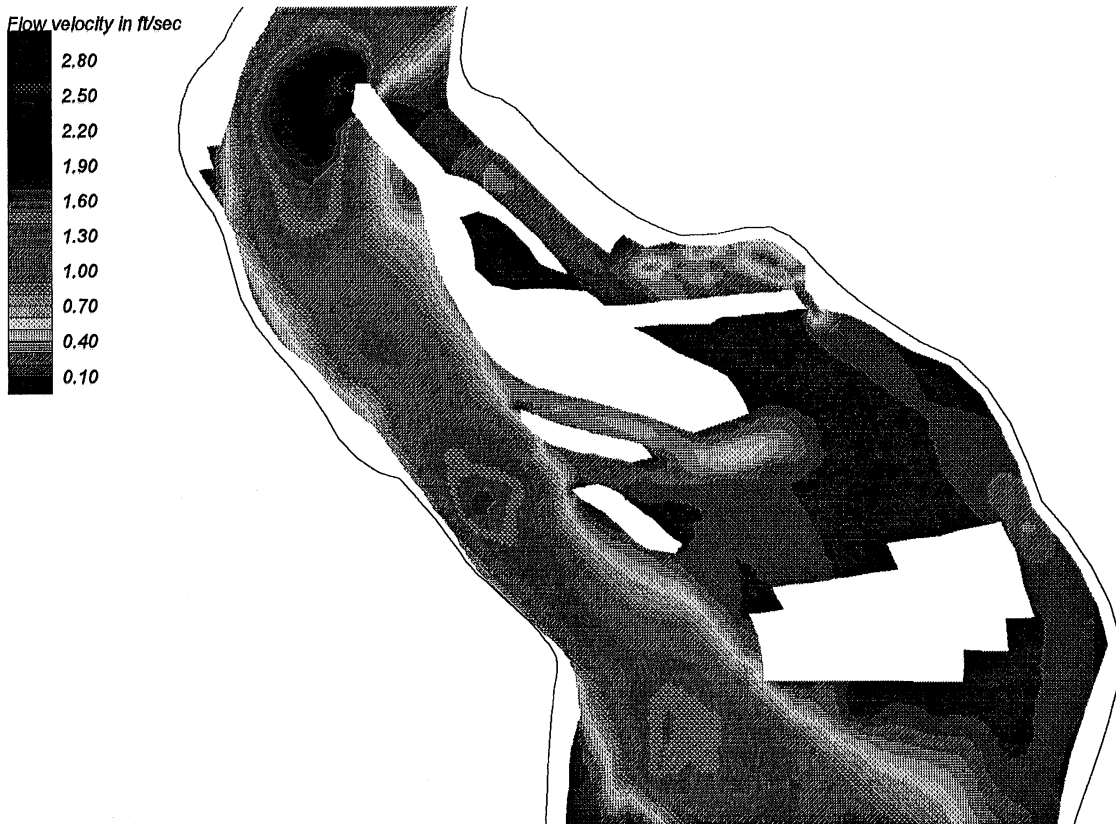


**Figure 47** Velocity contours for a flow of 5285 cfs with the spurdike option.



**Figure 48** Velocity contours for a flow of 10,200 cfs with the spurdike option.

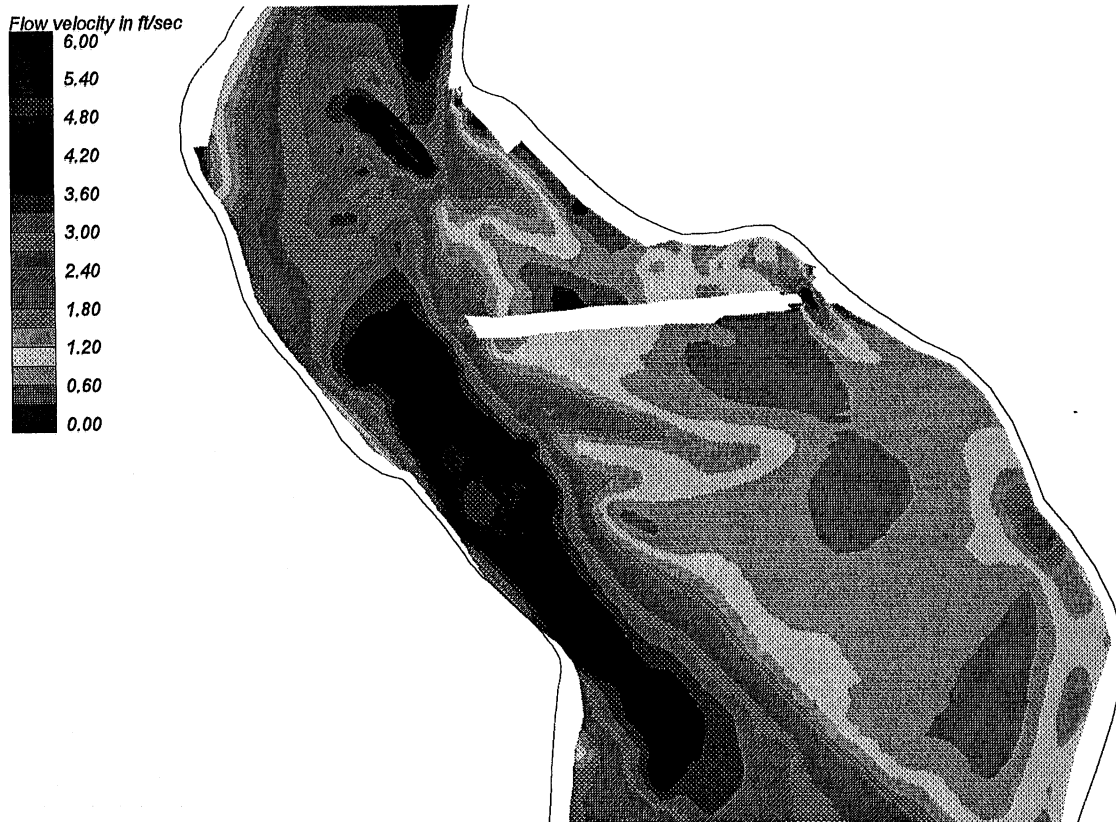


**Figure 49** Velocity contours for a flow of 25,850 cfs with the spurdike option.

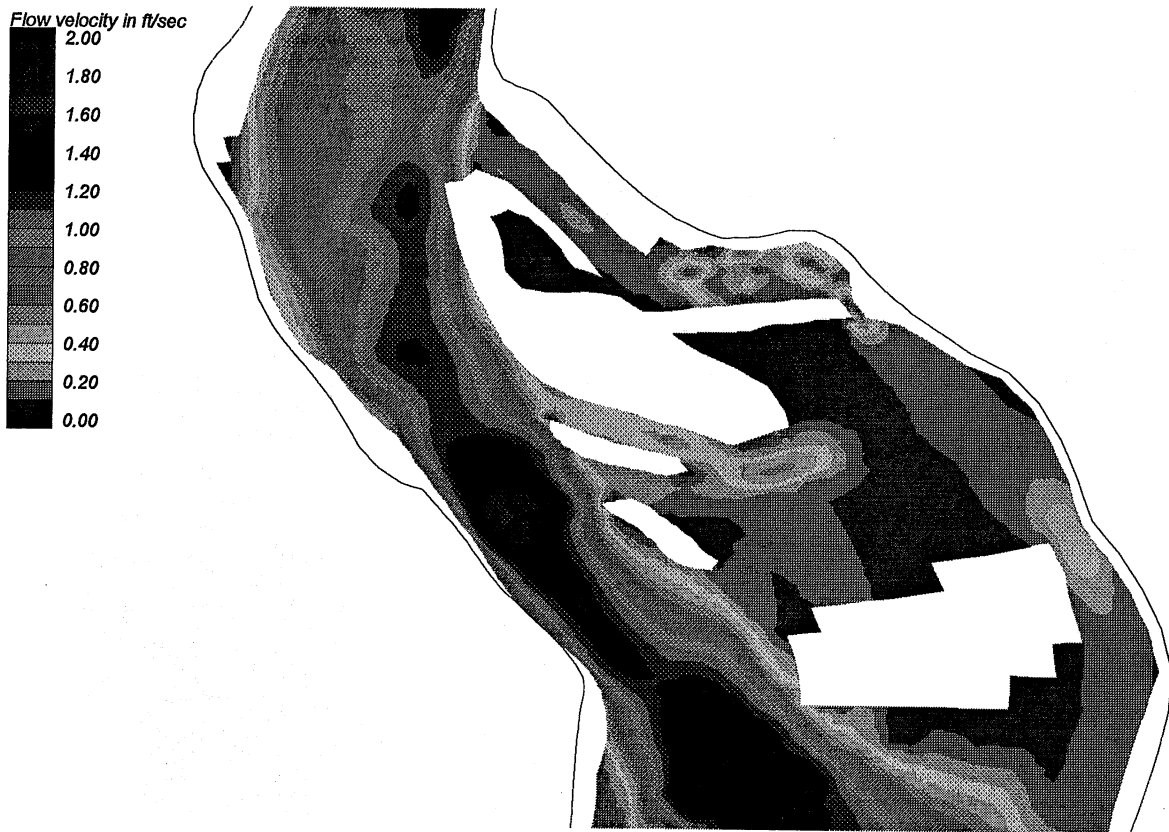


**Figure 50** Velocity contours for a flow of 5285 cfs with 5 ft of dredging in the east channel.



**Figure 51** Velocity contours for a flow of 10,200 cfs with 5 ft of dredging in the east channel.

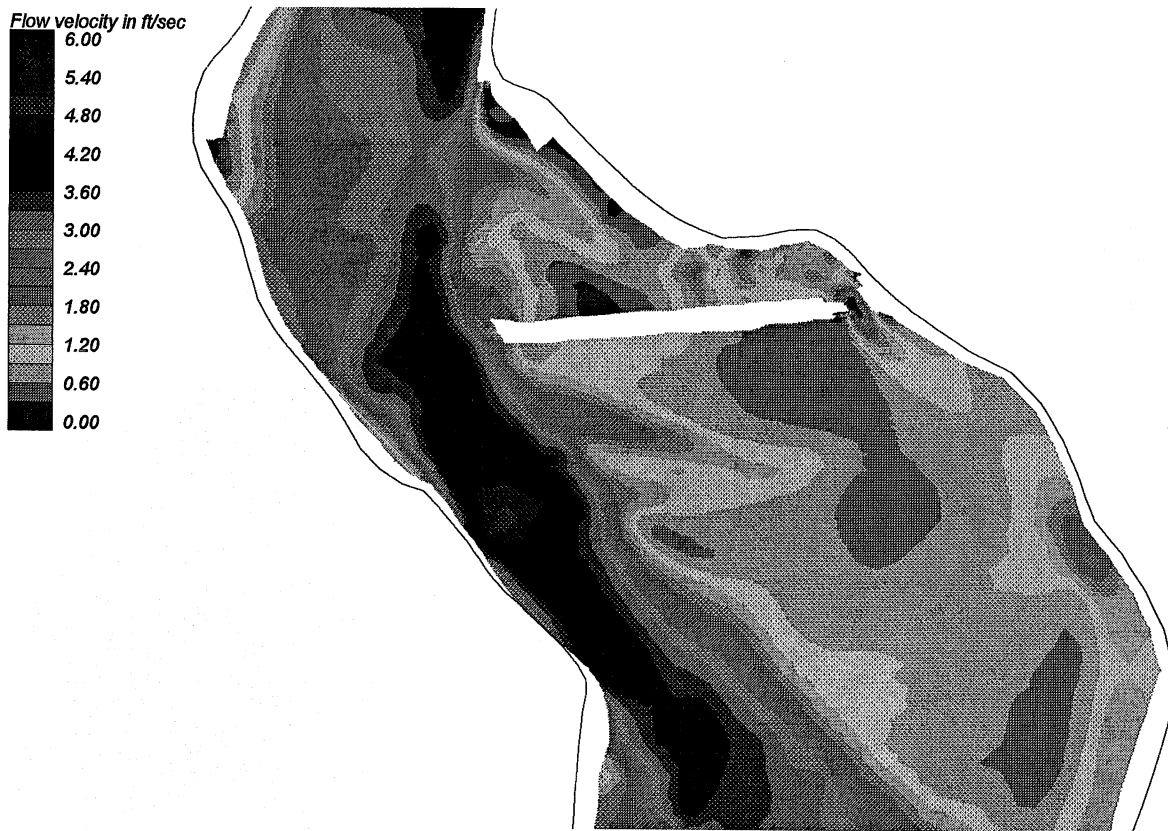


**Figure 52** Velocity contours for a flow of 25,850 cfs with 5 ft of dredging in the east channel.

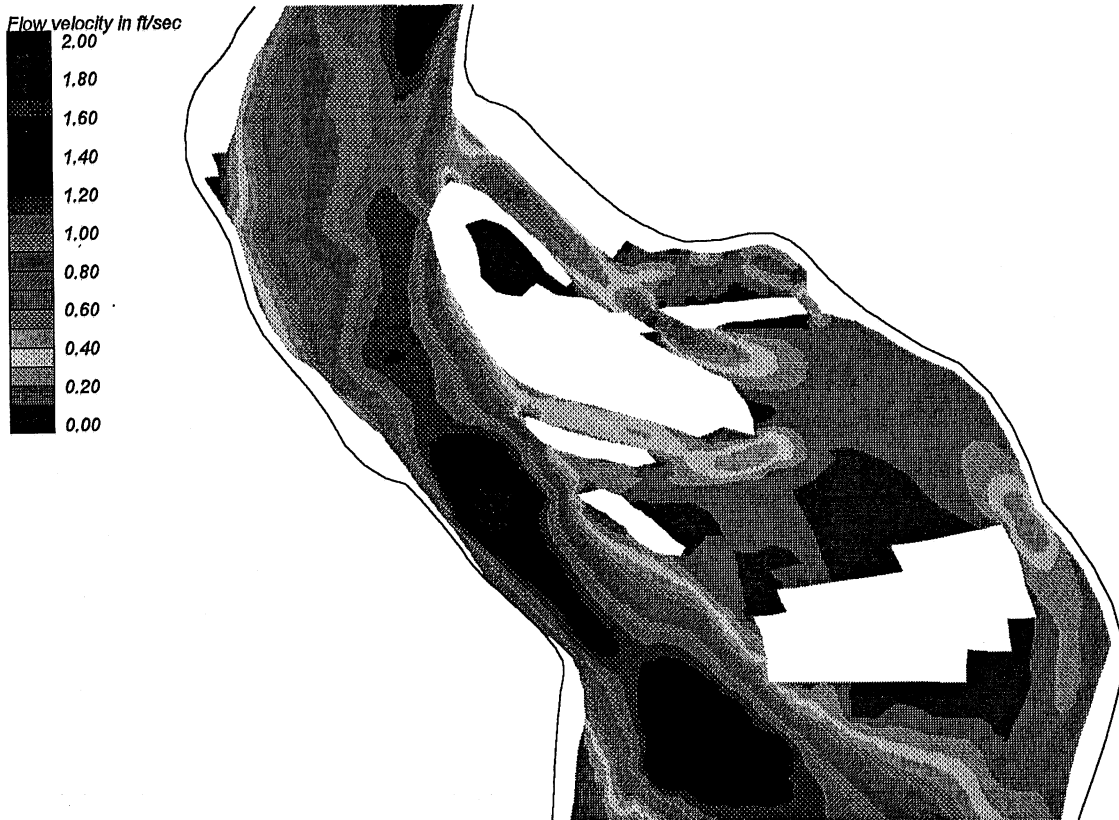


**Figure 53** Velocity contours for a flow of 5285 cfs with the new opening option.



**Figure 54** Velocity contours for a flow of 10,200 cfs with the new opening option.



**Figure 55** Velocity contours for a flow of 25,850 cfs with the new opening option.

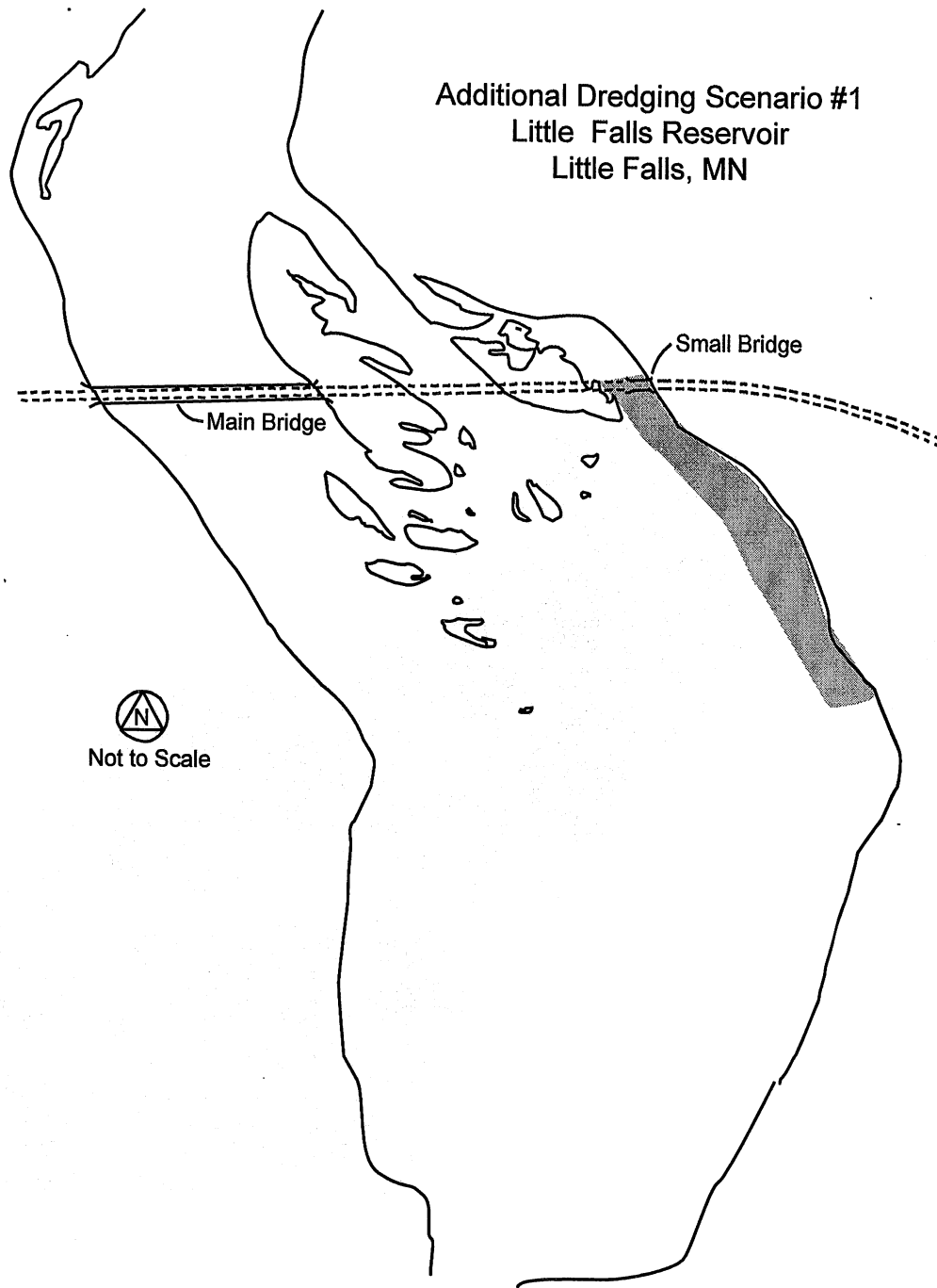


**Figure 56** Additional dredging scenario #1 involving dredging along east shoreline downstream of small bridge.

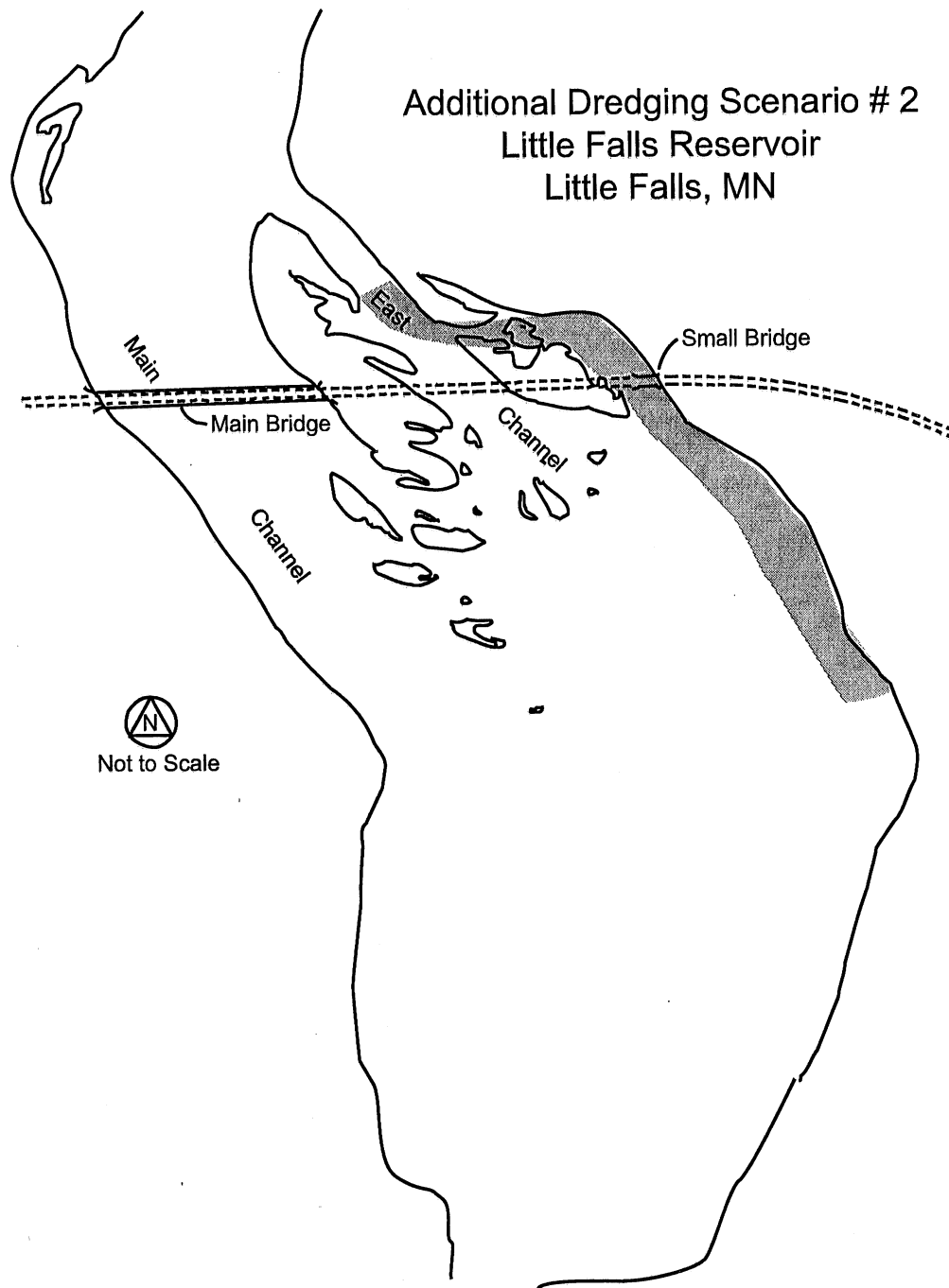


**Figure 57** Additional dredging scenario #2 involving dredging of downstream two-thirds of east channel and along east shoreline downstream of small bridge.

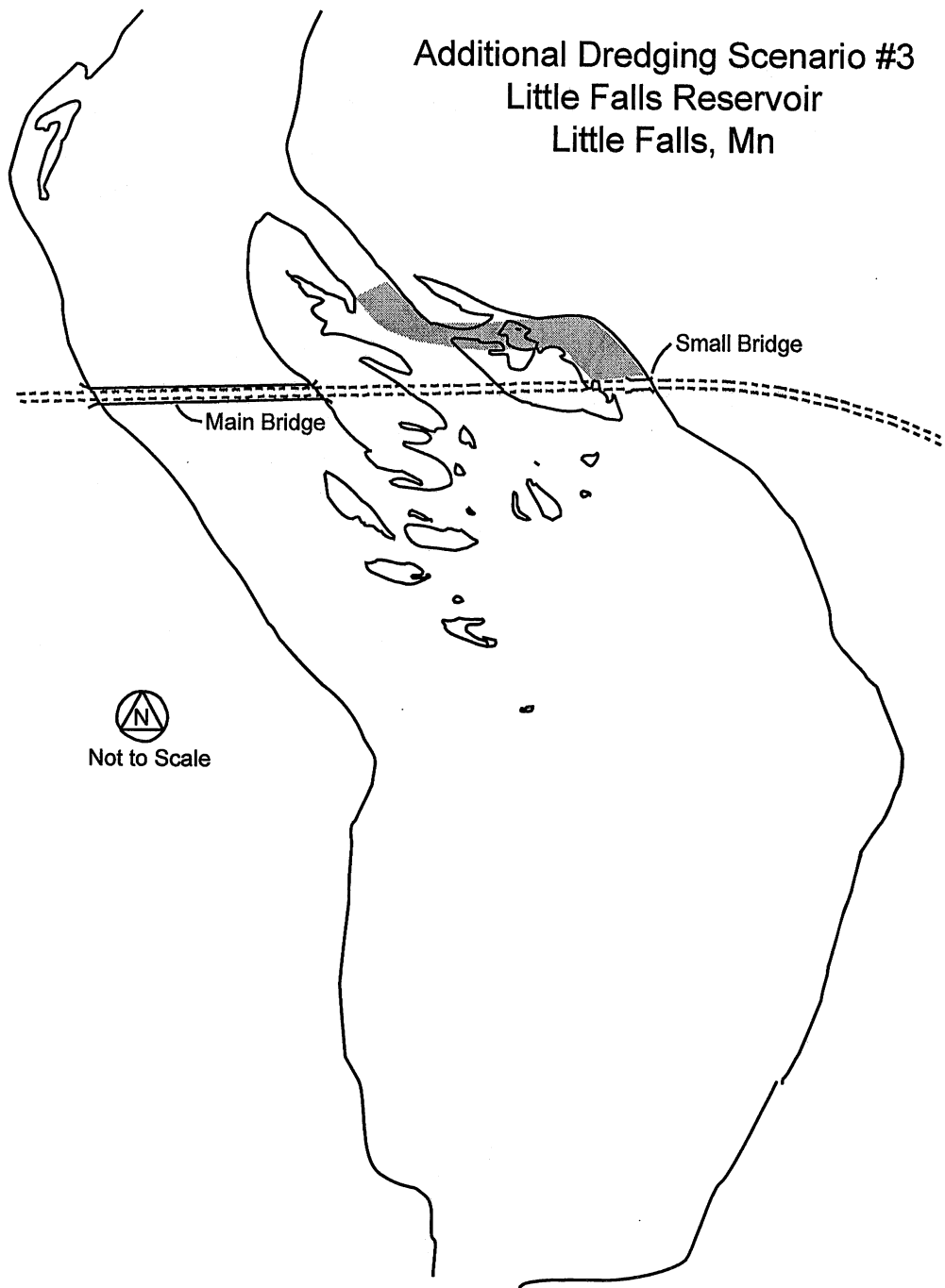


**Figure 58** Additional dredging scenario #3 involving dredging of downstream two-thirds of east channel region.



**Figure 59** Velocity contours for a flow of 5285 cfs with additional dredging scenario #1.

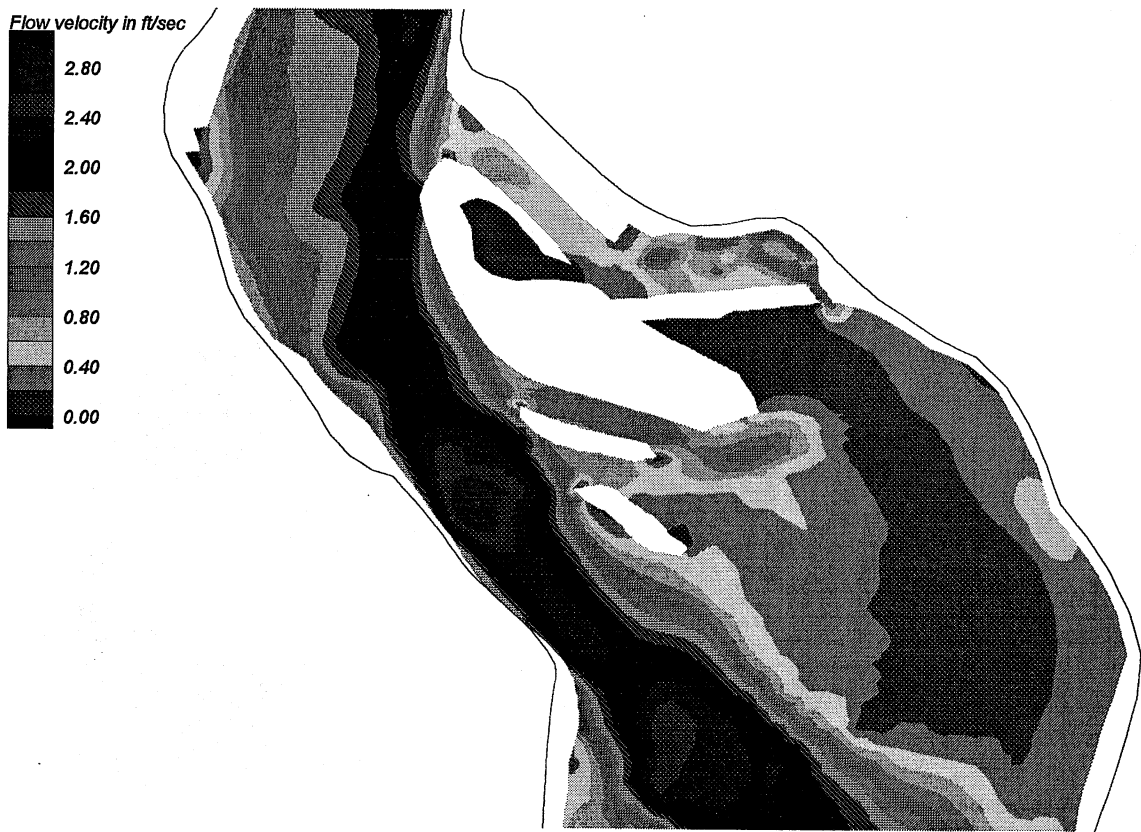


**Figure 60** Velocity contours for a flow of 10,200 cfs with additional dredging scenario #1.

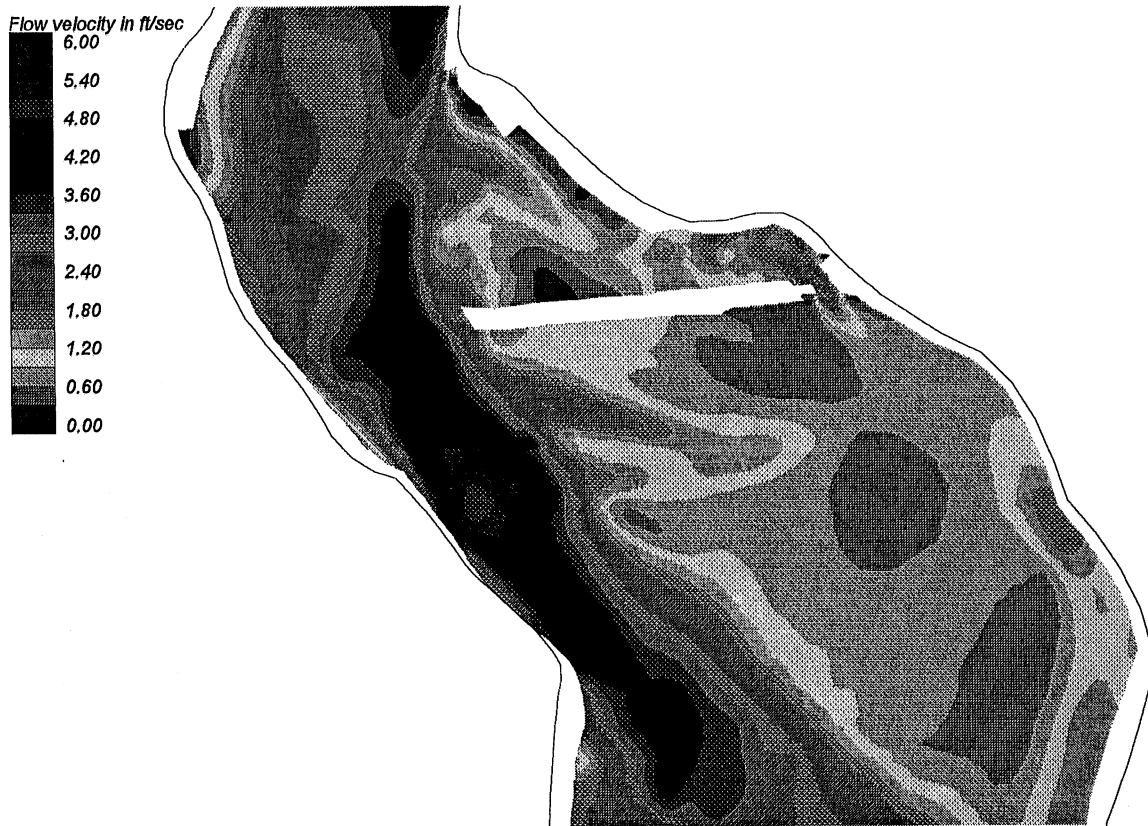


**Figure 61** Velocity contours for a flow of 25,850 cfs with additional dredging scenario #1.

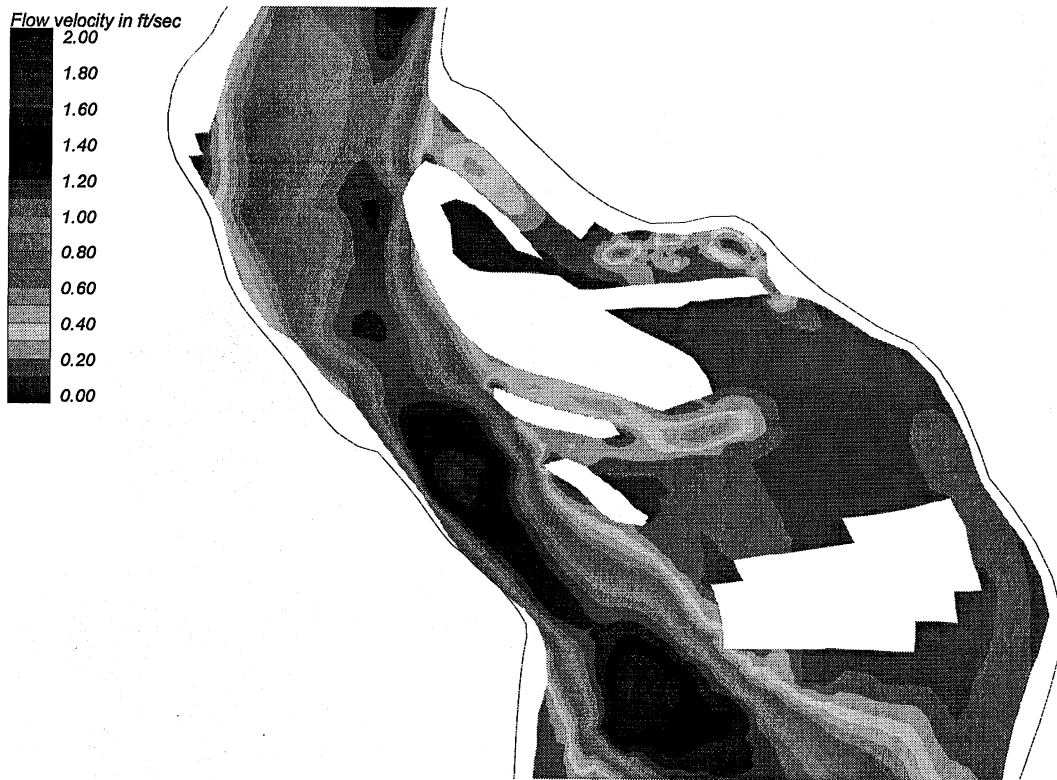


**Figure 62** Velocity contours for a flow of 5285 cfs with additional dredging scenario #2.



**Figure 63** Velocity contours for a flow of 10,200 cfs with additional dredging scenario #2.

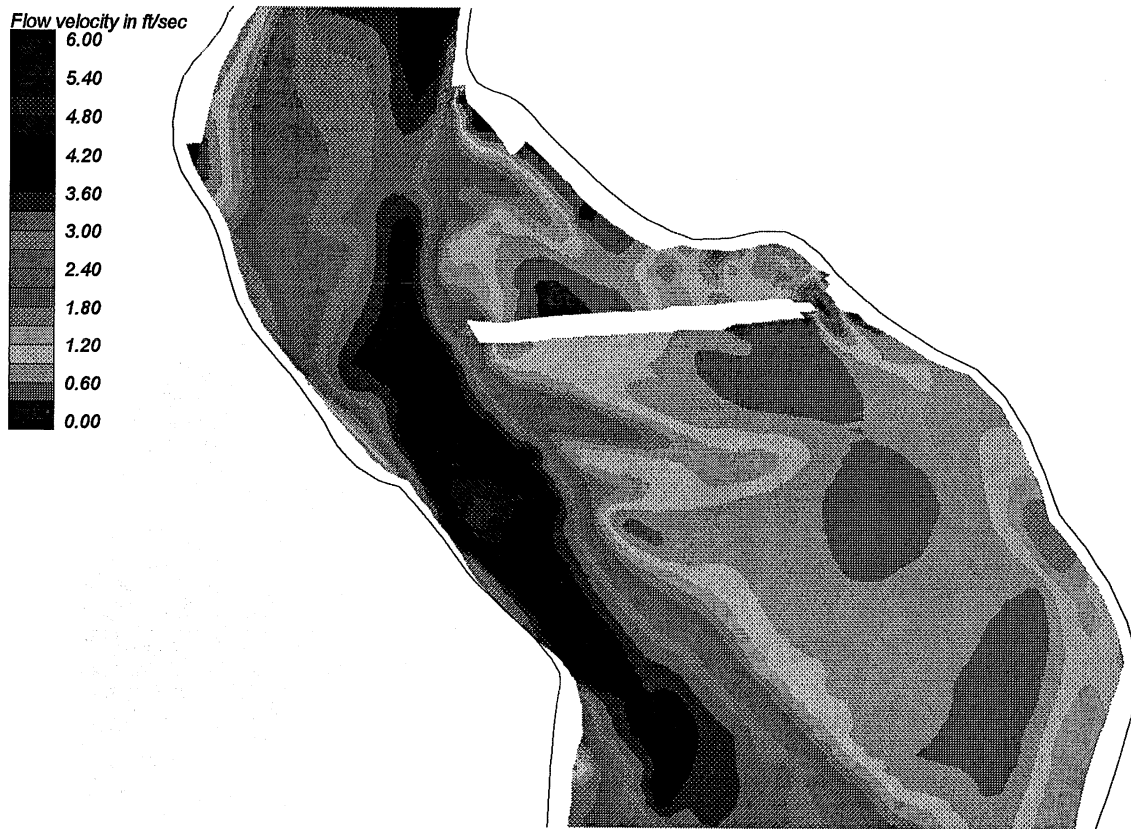


**Figure 64** Velocity contours for a flow of 25,850 cfs with additional dredging scenario #2.



**Figure 65** Velocity contours for a flow of 5285 cfs with additional dredging scenario #3.

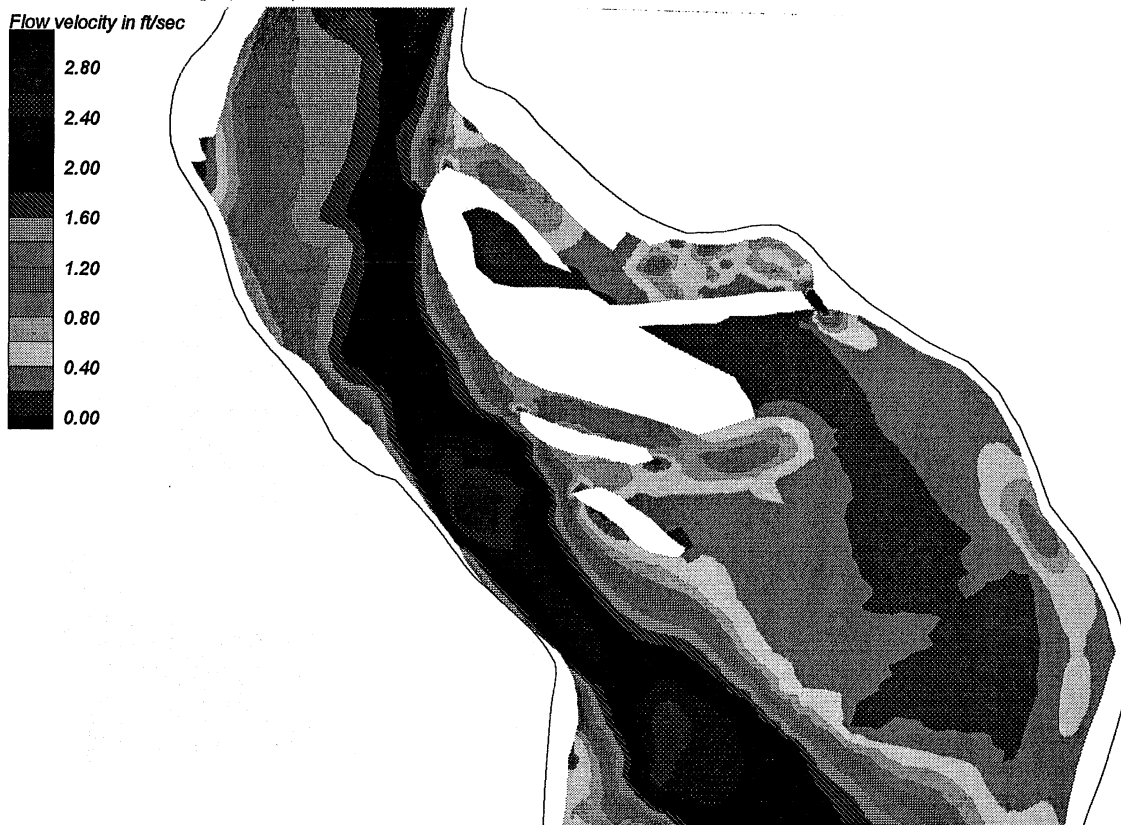


**Figure 66** Velocity contours for a flow of 10,200 cfs with additional dredging scenario #3.

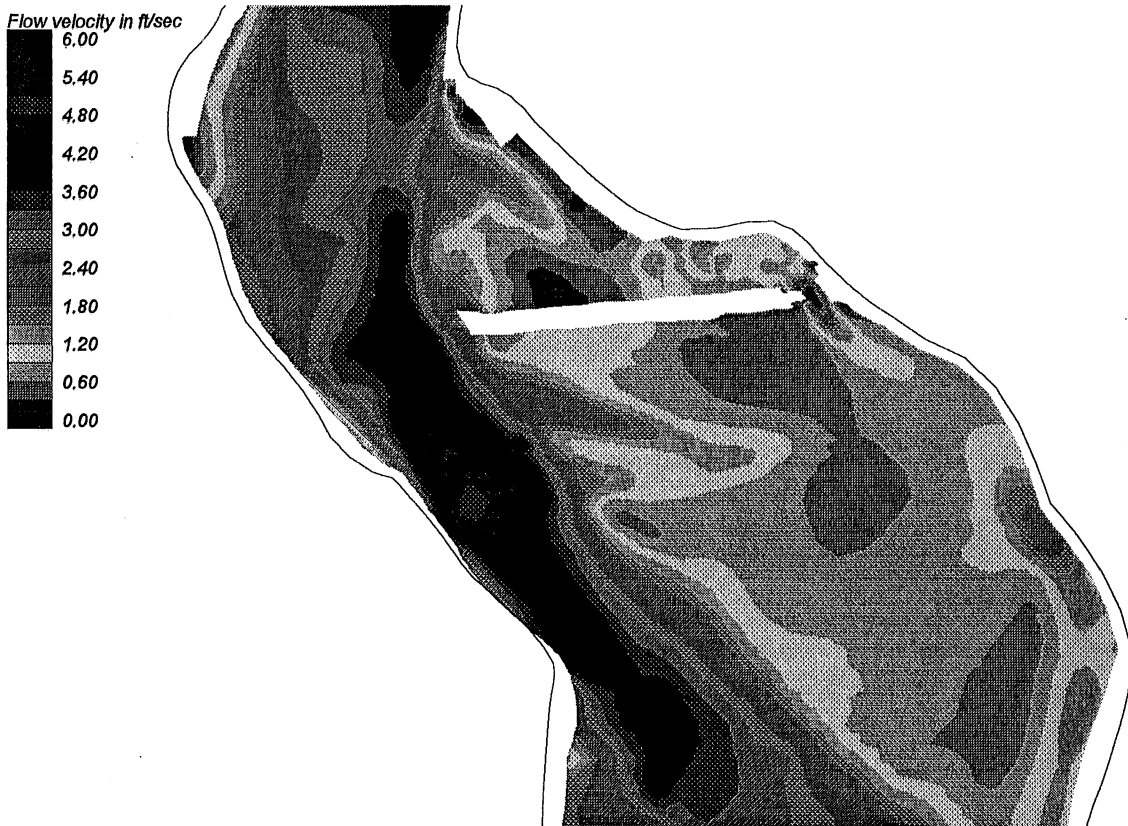


**Figure 67** Velocity contours for a flow of 25,850 cfs with additional dredging scenario #3.



